

Acclimation to Iron Limitation in the Haptophyte
***Coccolithus pelagicus*: A Molecular Investigation**

Christopher Moffat

School of Biological and Environmental Sciences

The University of Stirling

December 2008

ACKNOWLEDGEMENTS

This research was funded by the Natural Environment Research Council.

I would like to thank:

Dr Michael Wyman for his patience, supervision and support.

Dr Rachel Jones, Dr Alan Patterson, Nick Meakin, Sylvia Hodgson, Pauline Monteith and Dr Clare Bird for their encouragement, assistance and general office banter.

My friends and family.

Lastly, I would like to thank the person who has had to tolerate me the most, provide late night lifts and pretend to be interested in iron limitation – Elaine Stewart.

Abstract

Phytoplankton growth is iron limited in at least 20% of the world's oceans. Iron is an important nutrient required to synthesise enzymes necessary for photosynthesis, respiration, and nitrogen assimilation. Due to its low solubility in seawater, iron limitation of phytoplankton production has been the focus of much recent research. These organisms secrete ligands in order to solubilise the available iron, but not all of the iron dissolved in seawater is biologically available. In this study a molecular based approach was employed to investigate the acclimation of the marine haptophyte *Coccolithus pelagicus* to iron limitation.

Using two dimensional electrophoresis, subtractive cDNA hybridisation, and RT real time PCR, changes in the proteome and in gene expression were examined. Iron limited cells were characterised by slower specific growth rates, lower chlorophyll *a* concentrations per unit biomass and less extensive calcification relative to iron replete cells. Addition of iron to iron limited cultures resulted in increased specific growth rates and increased chlorophyll *a* concentration per unit biomass.

A subtracted cDNA library revealed seventeen identifiable sequences of which photosystem I protein E (PsaE), a fucoxanthin binding protein transcript, two chlorophyll binding proteins and a predicted membrane protein were shown to be up-regulated in iron-limited cells to varying extents. Two dimensional SDS PAGE revealed 11 differentially expressed proteins in iron limited cells and 1 highly

expressed protein exclusive to iron replete cells. The potential utility of each of these as biomarkers of iron-limitation/iron sufficiency for natural populations of coccolithophorids like *Coccolithus pelagicus* is discussed.

Declaration

To whom it may concern

This thesis is the sole work of the author. The work reported in this thesis is the result of the author's own research and has not been reported in another thesis. Where material from other sources has been used it has been duly acknowledged in the text and fully listed in the references.

Signed:

Christopher Moffat

School of Biological and Environmental Sciences

The University of Stirling

December 2008

CONTENTS

Acknowledgements.....	i
Abstract.....	ii
Declaration.....	iv
Contents.....	v
List of Figures and Tables.....	viii

Chapter 1 – Introduction

1.1 <i>Phytoplankton.....</i>	1
1.1.1 <i>The coccolihophorids.....</i>	3
1.1.2 <i>The importance of iron in biological systems.....</i>	6
1.1.3 <i>Marine iron limitation.....</i>	7
1.1.4 <i>Iron supply to the ocean.....</i>	8
1.2 <i>Iron uptake by phytoplankton.....</i>	9
1.2.1 <i>The effect of Iron limitation on Nitrogen assimilation.....</i>	13
1.2.2 <i>Effects of iron limitation on photosynthesis and pigment composition.....</i>	15
1.3 <i>Flavodoxin and Ferredoxin as Potential Biomarkers of Iron Limitation.....</i>	19
1.4 <i>Aims of this study.....</i>	22

Chapter 2 – Materials and Methods

2.1 <i>Coccolithus pelagicus – maintenance of stock cultures and experimental cultures.....</i>	23
2.1.1 <i>Determination of chlorophyll a concentrations.....</i>	25
2.1.2 <i>Growth experiments to confirm iron limitation.....</i>	25
2.1.3 <i>Microscopic examination of Coccolithus pelagicus cells.....</i>	26
2.2 <i>RNA extractions.....</i>	26
2.2.1 <i>Buffers and solutions used for RNA extractions and electrophoresis.....</i>	26
2.2.2 <i>Extraction of RNA.....</i>	27
2.2.3 <i>Spectrophotometric determination of RNA concentration.....</i>	29
2.2.4 <i>Electrophoresis of RNA.....</i>	29
2.2.5 <i>Purification of mRNA.....</i>	29
2.3 <i>cDNA subtraction.....</i>	31
2.3.1 <i>Buffers and solutions used for cDNA subtraction.....</i>	34
2.3.2 <i>First-strand cDNA synthesis.....</i>	34
2.3.3 <i>Second-strand cDNA synthesis.....</i>	35
2.3.4 <i>Rsa I digestion.....</i>	37
2.3.5 <i>Adaptor ligation.....</i>	38
2.3.6 <i>Subtractive hybridisation.....</i>	40
2.3.7 <i>PCR amplification of subtracted cDNA samples.....</i>	43
2.3.8 <i>Sequences of Clontech primers and adaptors used in cDNA subtraction.....</i>	46
2.4 <i>Cloning and sequencing of subtracted cDNA sequences.....</i>	46
2.5 <i>Blast analysis, multiple sequence alignments of subtracted cDNA sequences and primer design.....</i>	48
2.5.1 <i>Design of degenerate primers to target flavodoxin and Glyceraldehyde 3-phosphate dehydrogenase (GAPDH).....</i>	51

2.6	<i>Primer optimisation for real-time PCR.....</i>	52
2.6.1	<i>cDNA production for real-time PCR.....</i>	54
2.6.2	<i>Testing primers using cDNA as a template.....</i>	55
2.7	<i>Real time PCR.....</i>	56
2.7.1	<i>Data handling: normalising RT real time PCR results to GAPDH transcript abundance and determining up-regulation of genes in response to iron limitation.....</i>	57
2.8	<i>1-Dimensional and 2-Dimensional SDS-PAGE.....</i>	58
2.8.1	<i>Automated protein spot detection and analysis of 2-D gels.....</i>	61
2.8.2	<i>Mass spectroscopic analysis of iron replete 2D-SDS PAGE spot FeR1.....</i>	62
2.8.3	<i>Western blotting.....</i>	62

Chapter 3 – Growth experiments and proteomic analysis

3.1	<i>Coccolithus pelagicus growth experiments.....</i>	65
3.1.1	<i>Iron addition experiments.....</i>	69
3.1.2	<i>Growth data for cultures used in RNA extractions.....</i>	73
3.2	<i>Microscopic examination of iron replete and iron limited cultures.....</i>	74
3.3	<i>1 Dimensional SDS PAGE analysis of Coccolithus pelagicus proteins.....</i>	79
3.3.1	<i>2 Dimensional SDS PAGE analysis of Coccolithus pelagicus proteins.....</i>	80
3.3.2	<i>Mass spectroscopic analysis of iron replete protein spot FeR1 and western blotting.....</i>	84
3.4	<i>Discussion.....</i>	86

Chapter 4 – Analysis of differentially expressed sequences in the iron replete and iron limited subtracted libraries

4.1	<i>Chapter introduction.....</i>	93
4.1.1	<i>Composition of the subtracted cDNA library.....</i>	93
4.1.2	<i>Blast analysis of the subtracted cDNA library.....</i>	97
4.2	<i>Multiple sequence alignments of fucoxanthin binding protein sequences (FucoBP) detected in the subtracted library.....</i>	102
4.2.1	<i>Multiple sequence alignments for Flavodoxin and GAPDH.....</i>	105
4.3	<i>Discussion.....</i>	107

Chapter 5 – RNA extractions, DNase digests, primer optimisation and real time PCR results

5.1	<i>Chapter introduction.....</i>	113
5.1.1	<i>Examination of extracted DNase treated RNA on agarose gels.....</i>	113
5.2	<i>Thermal gradient PCR primer optimisation.....</i>	114
5.2.1	<i>Testing primers for use in RT real time PCR with cDNA templates.....</i>	120
5.3	<i>RT Real time PCR results.....</i>	123
5.3.1	<i>Analysis of RT real time PCR products on agarose gels.....</i>	127

5.4	<i>Discussion</i>	130
<u>Chapter 6 – Conclusions and future work</u>		
6.1	135
	<u>References</u>	143
	<u>APPENDIX</u>	163

List of Figures and Tables

Chapter 1

Figure 1.1	4
A = Artificially coloured SEM of calcified <i>Emiliana huxleyi</i> cell, www.uga.edu/protozoa/portal/coccolithophores.html (05.08.2009). B = SEM of calcified <i>Coccolithus pelagicus</i> cell, www.botany.unimelb.edu.au/RW/media/5.html (05.08.2009).	

Chapter 2

Figure 2.1	31
Diagram illustrating the principles underlying the Clontech PCR-Select™ cDNA Subtraction Kit (Adapted from the Clontech PCR-Select™ cDNA Subtraction Kit user manual, published 15 September, 1999).	

Chapter 3

Table 3A	67
Mean ± SE (n=3) specific growth rates, generation times and iron limited specific growth rates as a percentage of iron replete rates of <i>Coccolithus pelagicus</i> cultures treated with the iron chelators deferoxamine (DF) and EDTA at various concentrations.	
Table 3B	70
Mean SE ± (n3) specific growth rates, generation times and iron limited growth rates as a percentage of iron replete growth rates of <i>Coccolithus pelagicus</i> cultures used in the iron addition experiment.	
Table 3C	74
Specific growth rates, generation times and iron limited growth rates expressed as a percentage of their respective iron replete control growth rates of replicate cultures of <i>Coccolithus pelagicus</i> used to produce cDNA for RT real time PCR experiments.	

Figure 3.1	66
Growth curves showing mean \pm SE (n=3) increase in biomass of <i>Coccolithus pelagicus</i> cultures grown in the presence of various concentrations of the iron chelators deferoxamine and EDTA as determined by optical density measurements at 750 nm.	
Figure 3.2	68
Mean \pm SE (n=3) change in chlorophyll concentration over time in cultures of <i>Coccolithus pelagicus</i> grown in media containing various concentrations of the iron chelators EDTA and deferoxamine.	
Figure 3.3	68
Temporal change in mean \pm SE (n=3) chlorophyll <i>a</i> concentration per unit biomass in cultures of <i>Coccolithus pelagicus</i> cultures grown under iron replete conditions and in the presence of various concentrations of EDTA or deferoxamine.	
Figure 3.4	69
Growth curves showing mean \pm SE (n=3) increase in biomass of <i>Coccolithus pelagicus</i> cultures grown under iron replete conditions and in the presence of 150 μ M deferoxamine before and after the addition of iron	
Figure 3.5	71
Mean \pm SE (n=3) change in chlorophyll concentration over time in cultures of <i>Coccolithus pelagicus</i> grown under iron replete conditions and in the presence 150 μ M deferoxamine before and after addition of additional iron.	
Figure 3.6	72
Curves showing change in chlorophyll <i>a</i> concentration per unit biomass in cultures of <i>Coccolithus pelagicus</i> cultures grown under iron replete conditions and in the presence of 150 μ M deferoxamine before and after the addition of iron.	
Figure 3.7	73
Growth curves for <i>Coccolithus pelagicus</i> replicate cultures from which RNA was extracted. The growth curves show increase in biomass over time when grown under iron replete conditions and in media containing 150 μ M deferoxamine. The Fe Replete (4) and Fe Limited (4) replicates were inoculated with a different stock from the other replicates shown.	
Figure 3.8	76
Micrograph of iron replete cells of <i>Coccolithus pelagicus</i> at 630 x magnification under a light microscope.	

Figure 3.9	76
Micrograph of iron limited cells of <i>Coccolithus pelagicus</i> at 630 x magnification under a light microscope.	
Figure 3.10	77
Micrograph of an iron replete cell of <i>Coccolithus pelagicus</i> at 630 x magnification under a light microscope.	
Figure 3.11	78
Micrograph of an iron limited cell of <i>Coccolithus pelagicus</i> at 630 x magnification under a light microscope.	
Figure 3.12	79
Coomassie blue stained 1D SDS-PAGE gel showing two proteins detected only in cells of four iron limited <i>Coccolithus pelagicus</i> cultures and one protein detected only in iron replete cultures	
Figure 3.13	81
2D-SDS PAGE gel showing proteins in the cells of an iron replete culture of <i>Coccolithus pelagicus</i> detected by the ImageMaster software.	
Figure 3.14	81
2D-SDS PAGE gel showing proteins in the cells of an iron limited culture of <i>Coccolithus pelagicus</i> detected by the ImageMaster software.	
Figure 3.15	82
2D-SDS PAGE gel showing proteins present in the cells of an iron replete culture of <i>Coccolithus pelagicus</i> with reference proteins annotated (A-J) and differentially expressed proteins annotated (FeR1-FeR4).	
Figure 3.16	83
2D-SDS PAGE gel showing proteins present in the cells of an iron limited culture of <i>Coccolithus pelagicus</i> with reference proteins annotated (A-J) and differentially expressed proteins annotated (1-11).	
Figure 3.17	85
Western blot showing crude cell extracts from iron replete and iron limited <i>Coccolithus pelagicus</i> cells probed with rabbit anti-actin antibody (1:400), (secondary antibody – goat anti-rabbit HRP, 1:10,000). 3 lanes were loaded with 20 µg, 10µg and 5 µg of iron replete crude cell lysate, and another 3 lanes were loaded with 20 µg, 10µg and 5 µg of iron limited crude cell lysate. M = SeeBlue® pre-stained standard protein markers (Invitrogen™).	

Chapter 4

Table 4A	94
-----------------------	----

Table showing the overall sequence composition of the iron limited subtracted library.

Table 4B	95
-----------------------	----

List of the full names of identified sequences in the iron limited subtracted library and the abbreviated names used to refer to them throughout the text and in figures 4.1 and 4.2.

Figure 4.1	96
-------------------------	----

Relative proportion of each RT real time PCR analysed iron limited sequence in the iron limited subtracted cDNA library.

Figure 4.2	96
-------------------------	----

Relative proportion of each RT real time PCR analysed iron limited sequence within the 19% of the sequences in the library that were examined.

Figure 4.3	102
-------------------------	-----

Results from BlastX analysis performed on unique sequences found in the iron limited subtracted library. Each sequence from the library is shown and the EcoR1 restriction sites from the cloning vector and adaptors from the subtraction cloning are highlighted in yellow. The presence of different adaptors on each end of the nucleotide sequence confirms that they are differentially expressed or highly up-regulated sequences.

Figure 4.4	103
-------------------------	-----

Multiple sequence alignment of fucoxanthin binding protein (FucoBP) sequences detected in the iron limited subtracted library showing 5 different nucleotide sequences each highlighted with a different colour. Also shown is the position of the stop codons in each sequence (highlighted in yellow). Sequences highlighted in the same colour are homologous.

Figure 4.5.....105

Multiple peptide sequence alignment for flavodoxin. The binding sites for two alternative degenerate forward primers are highlighted in green and yellow while the binding site for the reverse primer is highlighted in blue. The sequences used in the alignment are from *Emiliana huxleyi*, *Karenia brevis* *Phaeodactylum tricornutum*, *Ostreococcus tauri* and *Thalassiosira pseudonana*.

Figure 4.6.....107

Multiple peptide sequence alignment for GAPDH. The forward and reverse primer binding sites are highlighted in yellow. The organisms from which the sequences were derived are *Phaeodactylum tricornutum*, *Thalassiosira pseudonanna* *Ascophylum nodosum*, *Gonyaulux poledra*, *Emiliana huxleyi*, *Isochrysis galbana* and *Pavlova lutheri*.

Chapter 5

Table 5A..... 115

Figure 5.1..... 114

1.5% agarose gels showing RNA extractions before and after treatment with the Turbo DNA-free kit. In all four gels the lanes were loaded as follows: 1 – *Hind* III λ phage markers, 2 – iron replete RNA before DNase treatment, 3 – iron replete RNA after DNase treatment, 4 – iron limited RNA before DNase treatment, 5 – iron limited RNA after DNase treatment. In each gel showing Fe replete and Fe limited RNA samples prior to and after DNase treatment (A,B,C and D) the contaminating DNA (highest molecular weight band) is greatly reduced or absent in the samples after DNase treatment compared to those samples without DNase treatment.

Figure 5.2..... 116

1% agarose gels showing products from 57°C – 67°C thermal gradient PCR. Gel A = PMP, Gel B = Fuco (3). On both gels: 1 = *Hind* III λ phage markers, 2 = negative controls. The temperature gradient was: 3 = 57°C, 4 = 59 °C, 5 = 62.6 °C, 6 = 64.9 °C, 7 = 66 °C, 8 = 67 °C.

Figure 5.3.....117

1% agarose gels showing products from 60°C – 70°C thermal gradient PCR. Lanes 1 – 6 = Fuco (7), Lanes 7 – 9 and 12 – 14 = Thio, Lanes 15 – 20 = Fuco (6). Lanes 10 and 11 = Hind III λ phage markers. All 3 reactions were run on gradients with the following increments: 60 °C, 62 °C, 64.4 °C, 65.6 °C, 68 °C, 70 °C.

Figure 5.4.....118

1% agarose gels showing products from 60°C – 70°C thermal gradient PCR. A = Cyt bc1, B = Fuco (2), C = Fuco (4), D = UCE, E = Fuco (1), F = Fuco (3) G = Fuco (5). On both gels: 1 = Hind III λ phage markers, 2 = negative controls. The temperature gradient was: 3 = 60 °C, 4 = 62 °C, 5 = 64.4 °C, 6 = 65.6 °C, 7 = 68 °C, 8 = 70 °C.

Figure 5.5.....119

1% agarose gels showing products from 62°C – 72°C thermal gradient PCR. A = PsaE, B = 20s Prot, C = CM4E12, D = Cyt b5, E = Chl LHP. On all of the gels: 1 = Hind III λ phage markers, 2 = negative controls. The temperature gradient was: 3 = 62.9 °C, 4 = 65.2 °C, 5 = 66.4 °C, 6 = 67.6 °C, 7 = 69.9 °C, 8 = 72 °C

Figure 5.6.....120

1% agarose gels showing products from 38°C – 48°C thermal gradient PCR with GAPDH primers. 1 = Hind III λ phage markers, 2 = negative control, 3 = 38C, 4 = 40 °C, 5 = 42.4 °C, 6 = 44.8 °C, 7 = 48 °C.

Figure 5.7.....121

1% agarose gels showing products from PCR reactions with cDNA templates used to optimise primers for real time PCR. The gels were loaded as follows: In all gels M = Hind III λ phage markers. For each target transcript 3 PCRs were run. These 3 reactions were a negative control, the PCR product from iron replete cDNA and the PCR product from iron limited cDNA. In all of the gels every set of 3 lanes were loaded in that sequence from left to right. The gels show the PCR products from the following reactions: A = PsaE, 20s Prot, Cyt b5. B = Chloroplast LHP, CM4E12. C = Thioredoxin, Fucoxanthin BP (2), Fucoxanthin BP (4). D = Fucoxanthin BP (5), Cyt bc1, Fucoxanthin BP (1). E = Fucoxanthin BP (6). F = Fucoxanthin BP (7), PMP. G = DnaJ, UCE. H = Fucoxanthin BP (3). I = Ferredoxin. J = GAPDH.

Figure 5.8	124
Histograms showing mean SE± (n=3) abundance of transcripts in iron limited <i>Coccolithus pelagicus</i> cultures relative to iron replete controls. A value of 1.0 indicates that a transcript is neither up nor down-regulated. A value greater than 1.0 indicates that a transcript is up-regulated in the iron limited cultures.	
Figure 5.9	128
1% agarose gel showing PCR product from RT real time PCR experiment using predicted membrane protein (PMP) primers. 1 - Hind III λ phage markers, 2-7 – Single PCR products of expected size (152 bp).	
Figure 5.10	128
1% agarose gel showing PCR product from RT real time PCR experiment using Ferredoxin primers. 1 - Hind III λ phage markers, 2 – Single PCR product of expected size (103 bp).	
Figure 5.11	129
1% agarose gel showing primer dimers and PCR product from RT real time PCR experiment using GAPDH degenerate primers. 1 - Hind III λ phage markers, 2 + 3 – Single PCR products of expected size.	
Figure 5.12	129
1% agarose gel showing PCR product from RT real time PCR experiment using Chl LHP primers. 1 - Hind III λ phage markers, 2 + 3 – Single PCR products of expected size (198 bp).	

CHAPTER 1: Introduction

1.1 – Phytoplankton

Phytoplankton are free floating photo-autotrophic and mixotrophic micro-organisms that are responsible for the bulk of primary production in the oceans. Phytoplankton photosynthesis accounts for approximately 50% of annual global carbon fixation (Falkowski and Raven 1997). Their taxonomical classification is based on the type of energy storage molecules they produce, their pigment composition, the structure and composition of their cell walls, and their locomotory apparatus and cellular morphology. There are seven major taxonomic groups of phytoplankton. These include two divisions of the kingdom Protozoa: Euglenophyta and Dinophyta (Dinoflagellates), the chlorophyceae and prasinophyceae within the kingdom Plantae, and three divisions of the kingdom Chromista: Cryptophyta, Haptophyta, and the Heterokonts which include the Bacillariophyceae (Diatoms). In addition there are several members of the cyanobacteria, which include the smallest of the phytoplankton (*Synechococcus*, *Prochlorococcus*) and the only members of the phytoplankton capable of fixing atmospheric nitrogen (e.g. *Trichodesmium* spp.). While each of these groups is unique, they all exercise a combined influence over the marine environment and the global climate. Phytoplankton are ubiquitous throughout the oceans, form the base of marine food webs and are responsible for much of the biological drawdown of atmospheric CO₂ and oxygen production on Earth, thereby playing a critical role in the regulation of climate.

As well as exercising a strong influence over climate and being critical to marine nutrient cycling, phytoplankton activities can also have other important ecological and economic implications. Certain species of phytoplankton can form harmful algal blooms (HABs) when conditions favour their growth. These blooms can be hugely problematic to marine organisms and elevated levels of toxins can accumulate higher up the food web. Furthermore, even those species which do not produce toxic compounds can still be problematic, such is the case when large amounts of foam is produced by the mucilage surrounding cells of the coccolithophorid *Phaeocystis globosa* when it blooms (Seuront *et al.*, 2006; Spilmont *et al.*, 2009). The ecological and economic implications of such blooms are clear, in particular within the context of the tourist, fishing, and aquaculture industries. Like many aspects of phytoplankton biology and ecology, the exact conditions and regulatory mechanisms controlling harmful algal blooms are not well understood.

The phytoplankton are an extremely diverse group of organisms and do not represent a monophyletic group, different lineages appear to have evolved independently on several different occasions, each time independently acquiring chloroplasts by endosymbiosis events (Falkowski, 2004; Tomitani, 2006; Simon *et al.*, 2008). This is reflected in the variety of phytoplankton species known. One of the most dominant phytoplankton groups the diatoms, are fundamentally important to the cycling of silica in the marine environment, while the coccolithophorids exercise huge influence over the cycling of carbonate in the ocean.

1.1.1 – *The coccolithophorids*

The coccolithophorids are members of the division Haptophyta, which are distinguished primarily by the possession of a unique organelle: the haptonema which is situated between the two flagella. On a superficial level the haptonema appears to be a flagella-like organelle, however it is structurally different. The haptonema is composed of a different arrangement of microtubules (Manton, 1964; Gregson, 1993) than the typical nine plus two arrangement commonly found in the flagella of eukaryotes. The haptonema can range in length from 160 μm in *Chrysochromulina camella* for example, with the ability to coil and uncoil (Leadbeater & Manton, 1969) or it can also be short and inflexible, minimised to a few microtubules inside the cell or absent in some rare cases. There is not yet a consensus on the function of the haptonema, however it has been suggested that it may serve a role in food gathering and attachment to surfaces (Inouye & Kawachi, 1994). Among the haptophytes the coccolithophorids are arguably the most important members in terms of influence over climate, carbon fixation and certainly calcium carbonate formation. The coccolithophorids produce calcified scales (coccoliths) which surround the cell and form the coccosphere as can be seen in *figure 1.1*. The calcite scales are released upon cell death and transported to the sea floor where they eventually form the major constituent of chalk formations.

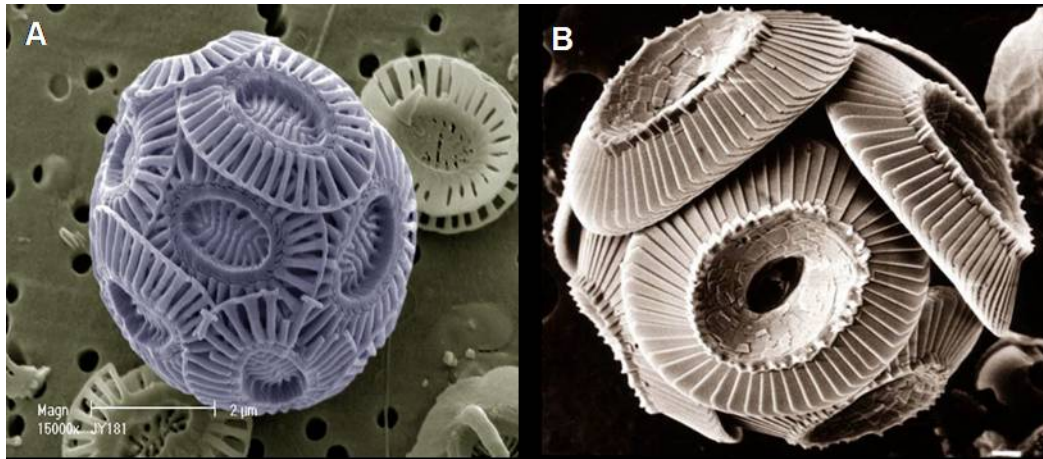


Figure 1.1: A = Artificially coloured SEM of calcified *Emiliana huxleyi* cell, www.uga.edu/protozoa/portal/coccolithophores.html (05.08.2009). B = SEM of calcified *Coccolithus pelagicus* cell, www.botany.unimelb.edu.au/RW/media/5.html (05.08.2009).

Although calcification is such a defining feature of the coccolithophorids there is no obvious reason why they do it. There have been several suggestions: protection from grazing zooplankton, protection from viral infection, and dissipating excess light energy by reflection thereby reducing the risk of photo-damage are a few, however there has been no consensus reached (Harris, 1994; Bratbak *et al.*, 1996; Paasche, 2002). While the purpose of calcification in these organisms is not understood, increasingly, understanding of the control of the rate of calcification and the ratio of calcification to photosynthesis is being improved. Calcification appears to increase under prolonged high light intensities and when phosphorus rather than nitrogen limits growth (Paasche & Brubak, 1994; Riegmann *et al.*, 2000; Zondervan, 2007). Further study also showed that in the model coccolithophorid *Emiliana huxleyi* calcification is closely correlated with the G1 phase of the cell cycle (Marius *et al.*, 2008)

Coccolithophorids are a comparatively recent group of phytoplankton, first appearing in the late Triassic period around 200 Mya, the greatest abundance of these calcareous deposits and the greatest variety of species of coccolithophorids occurred in the Late Cretaceous period (65-95 Ma) (Bown *et al.*, 1992; Young *et al.*, 1994). Data obtained from sediments indicates that coccolith abundance is often correlated with glacial-interglacial transitions over geological timescales, suggesting a predominance of coccolithophorids during interglacial periods (McIntyre *et al.*, 1972). One of the most defining features of the coccolithophorids is the ability to produce calcified plates which cover the cell. Although the coccolithophorids are important primary producers, their drawdown of carbon dioxide due to organic carbon production is partly negated by the release of carbon dioxide during the calcification process. Coccolithophorid primary production therefore represents a smaller sink for carbon dioxide when compared to some non-calcifying primary producers such as diatoms (Robertson *et al.*, 1994). Existing coccolithophorids have the ability to form massive blooms when conditions allow, to the extent that the reflectance of these blooms due to the calcite plates of the coccolithophorid cells can be observed by satellites (Holligan *et al.*, 1983; Balch *et al.*, 1991). These huge blooms have important implications for the global carbon cycle and blooms of *Emiliana* and *Phaeocystis* are involved in the production of dimethyl sulphide (DMS) – a substance involved in cloud formation (Malin *et al.*, 1992).

The formation of coccoliths by the coccolithophorids is hindered by decreasing seawater pH, and ongoing seawater acidification due to elevated atmospheric carbon dioxide levels may change the abundance of calcifiers in the oceans (Riebesell, 2004; Delille, 2005) with as of yet unknown consequences for marine ecosystems.

When the life cycles of some coccolithophorid species were examined it was found that in *Emiliana huxleyi* and *Phaeocystis* spp. there are motile and non-motile phases which possess a haploid and diploid genome respectively (Course *et al.*, 1994; Vaultot *et al.*, 1994; Green *et al.*, 1996). In a study by Rayns (1962) it was found that in *Coccolithus pelagicus* the heterococcolith-bearing phase was diploid while the holococcolith bearing phase was haploid.

1.1.2 – The importance of iron in biological systems

Due to its ability to function in a diverse array of biochemical roles in the cell, iron is required by many biological systems. By virtue of its ability to undergo oxidation-reduction transitions at physiological pH, it is primarily involved in enzymatic redox reactions. Iron can also modify the reactivity of active site residues within an enzyme or serve in a structural role. The photosynthetic and nitrogen assimilatory pathways are critically dependent on iron availability as are many of the enzymes / electron carriers involved in respiration. Paradoxically, however, given its importance in the biochemistry of the cell, the solubility of iron at seawater pH (~8.2) is low. The ferrous (Fe^{2+}) form becomes oxidised to Fe^{3+} and iron is precipitated because the ferric ion (Fe^{3+}) is highly insoluble in aqueous solution under oxic conditions. Consequently, one of the most abundant metals on Earth is relatively unavailable to the organisms occupying the environment that covers most of the planet's surface.

1.1.3 – Marine iron limitation

Understanding the factors that control the size and composition of phytoplankton communities in the marine environment is critical if the contribution that the ocean biota makes to the Earth's climate is to be properly understood. Until the development of sensitive trace metal sampling techniques in the 1980s, the regulation of phytoplankton biomass, species composition and primary production by iron was largely overlooked. As knowledge of the nutrient inventories of the world ocean developed, however, the late John Martin put forward the "iron hypothesis". He suggested that large areas of the ocean where there was high nutrient availability but low chlorophyll concentrations were the result of iron limited surface waters (Martin, 1990), and not a lack of another nutrient such as phosphate or nitrate. Large expanses of the world ocean such as the equatorial Pacific, the high Arctic Pacific, areas of the South Pacific gyre and Southern Ocean have been found to contain concentrations of iron that are low enough to severely limit primary productivity (Behrenfield & Kolber, 1999). In the central and eastern equatorial Pacific Ocean there are sufficient macronutrients in the surface waters to support several doublings of the phytoplankton standing stock (Barber, 1992). It was suggested that a significant influx of iron to these iron limited areas could result in a dramatic increase in phytoplankton biomass. Martin conjectured that the resulting increase in CO₂ fixation could perhaps exert enough influence on the climate to contribute to the onset of an ice age with the previously iron limited areas acting as large carbon sinks (Martin, 1990). Iron fertilisation experiments in high nutrient – low chlorophyll (HNLC) regions, namely in the equatorial Pacific (IRONEX I) (Martin *et al.*, 1994) and IRONEX II (Coale *et al.*, 1996)) and the Southern Ocean (SOIREE and EISENEX 1) (Boyd *et al.*, 2000; Boyd & Law., 2001), have confirmed that increasing

the concentration of iron in surface waters causes a dramatic increase in phytoplankton biomass. In IRONEX I a single enrichment of an experimental patch of the equatorial Pacific Ocean with 4 nM dissolved iron was carried out. A large increase in phytoplankton biomass was observed and yet nitrate drawdown was less than 0.2 μM and the biogeochemical response over the patch was of a lesser magnitude than expected (Martin *et al.*, 1994). IRONEX II was carried out in 1996 to test hypotheses developed from IRONEX I to explain the lack of a biogeochemical response. Secondary limitation due to the depletion of a second nutrient, and iron being quickly lost from the fertilised area were among the hypotheses. In IRONEX II successive iron enrichments were carried out over a longer period of time in order to maintain elevated iron concentrations, while other potentially limiting nutrients and zooplankton grazing were carefully monitored. As with IRONEX I, a large increase in phytoplankton biomass was observed. In the second experiment, however, large quantities of nitrate and CO_2 were drawn down during the development of the bloom (Coale *et al.*, 1996) thus confirming that the phytoplankton were iron limited.

1.1.4 – Iron supply to the ocean

Since there is no marine source of iron, open ocean phytoplankton are dependent upon iron supplied from aeolian dust originating from continental landmasses and deposited in the marine surface layer through wind-driven transport. Estimates of the amounts of iron that are deposited in the oceans as a result of aeolian deposition are varied. In 1991 it was estimated that the total iron flux to the ocean was 3.2×10^{13} g of iron per year, assuming a total iron content in the dust of 3.5% by weight (Duce & Tindale, 1991). In 1994 it was proposed that the estimate of Duce and Tindale (1991) was too high by a factor of five (Rea, 1994). The data gathered by Rea (1994) were based on

analyses of marine sediment cores while the data generated by Duce and Tindale (1991) were the result of a series of field measurements that assumed a dust iron content of 3.5% in the air. Despite uncertainties surrounding the exact amount of iron deposited in the ocean, many studies agree that the largest deposition rates are located adjacent to areas of desert (Duce & Tindale, 1991; Tegen & Fung, 1994, 1995; Mahowald *et al.*, 1999). However, there is uncertainty surrounding the percentage of aeolian iron that is soluble upon entering the ocean water (Moore *et al.*, 2002).

1.2 – Iron uptake by phytoplankton

Iron acquisition strategies vary among phytoplankton. Prokaryotes transport iron via a mechanism which requires the formation of coordination complexes such as siderophores that can be found localised on the cell membrane or freely in the surrounding environment after being secreted (Ratledge *et al.*, 1982; Neilands, 1984). While the secretion of Fe³⁺ - chelating substances into the environment is not unique to prokaryotic phytoplankton, eukaryotic members studied to date appear to favour a ferric-reductase based mechanism such as that found in *Chlamydomonas reinhardtii* (Lynnes *et al.*, 1998) and *Thalassiosira oceanica* (Maldonado & Price, 2001). It has been reported by Anderson and Morel (1980) that iron limited cells of *Thalassiosira weissflogii*, a marine diatom, reduce Fe³⁺ - EDTA complexes to Fe²⁺. Lynnes *et al.* (1998) found that Fe³⁺ reductase activity increased rapidly upon switching cultures of the green alga *Chlamydomonas reinhardtii* grown in Fe sufficient media to media that was free of Fe. Maldonado and Price (2001) reported that in the marine diatom *Thalassiosira oceanica* an Fe limitation-induced cell surface reductase carries out an extracellular reduction step on Fe³⁺ chelated by desferrioxamine B. This occurs prior to uptake of the inorganic iron into the cell and it was suggested that Fe(II) may be re-

oxidised to the ferric form before it is taken into the cell following the reduction step (Maldonado & Price, 2001).

The exact mechanisms by which eukaryotic algae utilise chelator bound iron is unclear but appears to be varied. While Anderson and Morel (1980) reported that iron limited cells of the marine diatom *Thalassiosira weissfloggi* reduce Fe^{3+} - EDTA to Fe^{2+} , Soria-Degg and Hortsman (1995) found that the marine diatom *Phaeodactylum tricornutum* could access both ferrioxamine B and ferrioxamine E-chelated iron as sources of iron. Intriguingly, evidence from this study indicated that the iron bound by each chelator was accessed through different uptake mechanisms. Utilisation of ferrioxamine B bound iron resembles higher-plant strategy I, while utilisation of ferrioxamine E resembles strategy II (Soria-Degg & Hortsman, 1995). All plants with the exception of grasses utilise iron acquisition strategy I which is a reduction based approach which involves acidifying the soil by secreting H^+ from their roots, this has the effect of solubilising iron (Marschner & Romheld, 1994; Schmidt, 2003; Kim & Guerinot, 2007). Strategy II is a chelation based approach in which iron deficiency results in the release of small molecular weight Fe^{3+} binding phytosiderophores from the plant roots, the Fe^{3+} - phytosiderophore complexes are then actively taken up by means of specific transport mechanisms (Marschner & Romheld, 1994; Schmidt, 2003; Kim & Guerinot, 2007). Grasses tend to survive under more drastically iron deficient conditions as the chelation strategy is more effective than the reduction strategy, particularly in well buffered calcareous soils (Mori, 1999). It has been observed that in the green alga *Chlamydomonas reinhardtii* the activity of the ferric-chelate reductase enzyme increases with severity of Fe-limited growth rates (Lynnes *et al.*, 1998; Weger, 1999). The study by Weger (1999) also showed that rates of

cupric reductase enzyme activity increased in parallel with those of ferric-chelate reductase activity as the iron-limited growth became more severe. It was found that addition of 250 μM Cu(II)-citrate to a culture of *Chlamydomonas reinhardtii* that was reducing Fe(III)-EDTA, stimulated cupric reduction while Fe(III)-EDTA reduction was subsequently inhibited (Weger, 1999). Following addition of 250 μM each of Cu(II)-citrate and Fe(III)-EDTA to iron limited cultures of *Chlamydomonas reinhardtii*, only cupric reduction was observed, suggesting that the same enzyme was responsible for the reduction of both Fe(III) and Cu(II) or perhaps that two separate enzymes compete for the same source of reducing power within the cell (Weger, 1999).

Studies on several eukaryotic species have indicated that it is dissolved inorganic iron that is transported by the cell's Fe transporters (Anderson & Morel, 1982; Hudson & Morel, 1990, 1993). As the vast majority of Fe in seawater is complexed by organic chelators (Rue & Bruland, 1995; Wu & Luther, 1995; Witter & Luther, 1998), it is essential that phytoplankton are able to access at least some of these chelated sources of iron. The ferric reductase mechanism to dissociate Fe(III) from organic chelators confers this ability to some eukaryotic phytoplankton that secrete iron chelating substances. A laboratory study by Boye & van den Berg (2000) found that the coccolithophore *Emiliana huxleyi* secreted iron complexing ligands in excess of the concentrations of iron in the culture medium. The same study showed that these ligands are released in response to iron addition rather than when iron levels had declined to limiting concentrations. This response is distinct from siderophore production in prokaryotes. In prokaryotes siderophores are produced during periods

when available iron concentrations are low as opposed to when a fresh input of iron is experienced.

As well as the release of iron chelators by phytoplankton in response to freshly added or low levels of iron, there is a further mechanism by which a variety of iron chelators can enter seawater. Viral lysis (Gobler *et al.*, 1997) and zooplankton grazing (Hutchins & Bruland, 1994) result in the release of intracellular iron chelating compounds such as porphyrins, cytochromes and haem proteins into the external environment. The decomposition of metazoan and protozoan faecal pellets also releases iron ligands into the water column (Strom, 1993; Head & Harris, 1994) adding to the pool of organic iron chelators that keep the nutrient potentially accessible in the euphotic zone of oxic marine environments. Unlike siderophores, however, such iron chelating substances are not secreted deliberately to solubilise iron. Potentially, any micro-organism in the marine environment is able to access this chelated iron. However, it was demonstrated that while *Thalassiosira weissflogii* and *Skeletonema costatum*, two diatom species, could easily utilise porphyrin bound iron (Hutchins *et al.*, 1999), two species of the cyanobacterium *Synechococcus* were relatively less efficient at accessing iron bound to three different porphyrins. By contrast, cyanobacteria can utilise iron bound to siderophores much more efficiently than eukaryotic phytoplankton. The ferric-reductase system (Jones *et al.*, 1987; Weger, 1999; Lynnes *et al.*, 1998; Maldonado & Price, 2001) found in eukaryotes preferentially accesses iron bound by tetra-dentate porphyrin chelators as opposed to the typically hexadentate siderophores secreted by prokaryotes (Hutchins *et al.*, 1999). Hence, the ability of prokaryotes and eukaryotes to access iron bound by

different chelators in iron-limited regions may allow for a degree of ecological niche separation and their co-existence in competition for the same resource.

It has been recently demonstrated that the bloom forming pennate diatoms *Pseudo-nitzschia* and *Fragilariopsis* are able to produce the iron concentrating protein - ferritin (Marchetti *et al.*, 2009). Ferritin has not been reported previously in any other algal species and phylogenetic analysis from the study suggested that this small subset of diatoms obtained the gene by means of lateral transfer. The ability to concentrate iron during times of iron input in chronically iron limited areas of ocean would allow for cell division to continue for a time even after the supply of extra-cellular iron was depleted. It is probable that the ability to utilise ferritin to safely concentrate iron within the cell contributes to the success of certain pennate diatoms in areas of ocean characterised by low iron concentrations and infrequent, intermittent inputs (Marchetti *et al.*, 2009).

1.2.1 – The effect of Iron limitation on Nitrogen assimilation

Two biochemical processes which are highly dependent on iron availability are nitrogen assimilation and photosynthesis. Iron is a vital component in several proteins in the photosynthetic electron transport chain and is a co-factor for both nitrate reductase and nitrite reductase. The nitrate assimilatory pathway is very demanding of the cell's iron supply. Nitrate reductase which reduces nitrate (NO_3^-) to nitrite (NO_2^-) requires two iron atoms (Campbell, 1999), while nitrite reductase requires five iron atoms. By contrast, the use of ammonium (NH_4^+) as a nitrogen source is far less demanding of a cell's Fe supply. NH_4^+ can be incorporated into amino acids directly after uptake by the cell.

It has been hypothesised (Raven *et al.*, 1992) and experimental studies have shown that nitrate assimilation is severely impaired in marine phytoplankton under iron limited conditions (Maldonado & Price, 1996). Raven *et al.* (1992) estimated that phytoplankton growing on nitrate would require 60% more iron than those growing on ammonium. The later study by Maldonado & Price (1996) found that cultures of marine diatoms grown with NO_3^- as a sole nitrogen source required 1.8 times more Fe than those cultures provided with NH_4^+ . However, the study showed that *Thalassiosira oceanica* and *Thalassiosira weissflogii* were able to maintain faster growth rates in NO_3^- supplemented media compared to NH_4^+ under moderate iron limiting conditions that would be expected to impair the growth rate of cells utilising oxidised forms of nitrogen. Despite the fact that Fe was limiting in both the NH_4^+ and NO_3^- cultures, the cells grown on NO_3^- were able to acquire the extra Fe that nitrate reductase and nitrite reductase demand by enhanced Fe uptake which suggests a close relationship between NO_3^- utilisation and Fe acquisition. Under severe Fe limitation, however *T. oceanica* cultures grew faster with NH_4^+ as sole nitrogen source (Maldonado & Price, 1996).

A later study examined the ability of the marine diatom *T. weissflogii* to assimilate NO_3^- under iron replete and iron limited conditions (Milligan & Harrison, 2000). Under iron replete conditions it was found that the rate limiting step in NO_3^- assimilation was the reduction of NO_3^- by nitrate reductase, since the activity of nitrite reductase was fifty times higher than that of nitrate reductase (Milligan & Harrison, 2000). By contrast, during iron limited growth, the activity of nitrite reductase fell dramatically and became rate limiting to NO_3^- assimilation. Despite

this, the activities of both enzymes were maintained at a rate that exceeded nitrogen incorporation rates during the period of iron limited growth. As a consequence of the decreased nitrite reductase activity, nitrite was excreted by cells at a rate of 100 fmol $\text{NO}_2^- \text{ cell}^{-1} \text{ day}^{-1}$ which accounted for approximately 10% of the total incorporated nitrogen (Milligan & Harrison, 2000).

Despite NO_2^- reduction being the rate limiting step in NO_3^- assimilation during severe iron limited growth, the C:N ratios of iron limited cells were found to be similar to iron replete cultures (Milligan & Harrison, 2000). This led Milligan & Harrison (2000) to suggest that the impairment of NO_3^- assimilation during Fe limited growth is not a consequence of an inadequate supply of iron cofactor to the enzymes of the NO_3^- assimilatory pathway, but is brought about by the shortage of photosynthetically derived reductant that is essential if oxidised forms of nitrogen are to be utilised. The same unaltered C:N ratios under Fe limited conditions were observed in the diatom *Chaetoceros muelleri* (Davey & Geider, 2001) and *Scenedesmus quadricauda* (Chlorophyceae) (Rueter & Ades, 1987), leading both groups of investigators to conclude that iron limited phytoplankton are essentially energy limited. It appears that in several species of phytoplankton an inability to process photons due to a shortage of iron results in the shift to NO_2^- reduction as the rate limiting step in NO_3^- assimilation.

1.2.2 – Effects of iron limitation on photosynthesis and pigment composition

An inability to process photons and generate photosynthetically derived reductant indicates that the photosynthetic pathway is impaired by iron limitation. Iron is required by enzymes employed in the production of chlorophyll such as

protochlorophyllide reductase. Thus a shortage of cellular Fe may limit the overall rate of chlorophyll biosynthesis. A reduction in chlorophyll content per cell is not unique to Fe limited cells. It is also observed under conditions of N, S and P limitation and thus may be a general stress response to nutrient depletion. The reduction in chlorophyll *a* content per cell may be compensated for to an extent by an accompanying reduction in cell size as has been found in the Antarctic prymnesiophyte, *Phaeocystis* sp. (van Leeuwe & Stefels, 1998). Van Leeuwe & Stefels (1998) found that in *Phaeocystis* sp. the concentration of accessory light harvesting pigments per cell was similar in both Fe replete and Fe limited cells: however, the ratio of chl *a* : accessory light harvesting pigments was greater in Fe replete cells under both high and low irradiance.

The photosynthetic pathway appears to be the primary target of iron limitation with photosystem I being the most affected component due to the fact that it is highly iron enriched. Photosystem I utilises the iron enriched ferredoxin protein as its terminal electron acceptor under iron replete conditions and several studies have examined the docking and subsequent electron transfer which takes place between photosystem I and ferredoxin (Fischer *et al.*, 1998; Setif *et al.*, 2002; Fromme *et al.*, 2003). It has been demonstrated that the PsaD and PsaE subunits of photosystem I facilitate the docking of ferredoxin and its functional homolog flavodoxin with photosystem I (Rousseau *et al.*, 1993; Fischer *et al.*, 1998; Setif *et al.*, 2002). Photosystem I particles isolated from a *psaE* deleted mutant of *Synechocystis* sp. were shown to be capable of reducing ferredoxin, however they did so at a rate at least 25 times less than the wild type (Rousseau *et al.*, 1993). It is believed that docking of the negatively charged ferredoxin with photosystem I is mediated by electrostatic

interactions with positively charged residues on the PsaE, PsaD and PsaC subunits (Fischer *et al.*, 1998). In iron limited cultures of the diatom *Chaetoceros muelleri* it was found that under light saturated conditions there was a greater decline in photosynthetic oxygen evolution than in mitochondrial oxygen consumption rates in the dark. This suggests that Fe limitation impairs the activity of the photosynthetic electron transport chain to a greater extent than mitochondrial electron transport (Davey & Geider, 2001). The study concluded that the primary target of iron limitation in *Chaetoceros muelleri* was the photosynthetic electron transport chain, resulting in a shortage of reducing power in the cell that leads to limited carbon fixation, reduced nitrogen assimilation and less pigment accumulation. This agrees with the findings of Milligan and Harrison (2000) who proposed that the nearly constant C:N ratios found over a range of iron deprived conditions in *T. weissflogii* was symptomatic of energy limited nitrite reductase activity.

One way in which Fe limitation affects the photosynthetic apparatus is by causing an alteration in the pigment composition of the cell. In the diatom *Phaeodactylum tricornutum* it was observed by Greene *et al.* (1991, 1992) that there was an increase in the ratio of light harvesting pigments to chlorophyll *a* as was found in *Phaeocystis* (van Leeuwe & Stefels, 1998). The study by van Leeuwe & Stefels (1998) found that in *Phaeocystis*, synthesis of the light harvesting pigments 19'-butanoyloxyfucoxanthin and 19'-hexanoyloxyfucoxanthin was induced under iron limitation at the expense of fucoxanthin synthesis which is the main carotenoid present under Fe replete conditions. A later study reported that addition of iron to iron limited *Phaeocystis antarctica* cultures caused a decrease in the ratio of 19'-hexanoyloxyfucoxanthin to chlorophyll *a* and an increase in the ratio of fucoxanthin

to chlorophyll *a* (DiTullio *et al.*, 2007). As Fe limited cells effectively suffer from an excess of absorbed light energy the change in composition of the light harvesting pigments may be a photo-protective response. A switch in the light harvesting pigments from fucoxanthin under iron replete conditions to acyloxyfucoxanthins under iron limited conditions may reduce the efficiency of energy transfer to the photosystems. This would ensure that the redox balance of the photosynthetic electron transport chain is maintained thereby reducing the likelihood of free radical formation (van Leeuwe & Stefels, 1998; DiTullio *et al.*, 2007).

Fucoxanthin is not the only photosynthesis related molecule that changes in abundance under iron limited conditions. A study by Greene *et al.* (1992) reported that the chloroplast proteins *cyt f*, subunit IV – the PQ docking protein in the *cyt b6/f* complex and the photosystem II reaction centre protein D1 of the chlorophyte *Dunaliella tertiolecta* and the marine diatom *Phaeodactylum tricorutum* all increased in abundance over various timescales when iron was added to iron limited cells. Smaller but notable increases in the large subunit of Rubisco and light harvesting proteins (2-fold and 1.5-fold respectively) were also detected. It has been observed that supplementing iron limited cells with iron does not result in an immediate increase in chlorophyll concentrations. Cells recover from chlorosis only after the redox protein flavodoxin has been replaced by its Fe-S containing functional homolog ferredoxin (McKay *et al.*, 1999). This delay in chlorophyll biosynthesis following relief of iron limitation suggests that the cells place a higher priority on repairing components of the photosynthetic electron transport chain to enhance photon processing potential per reaction centre than on returning light harvesting pigments to iron replete levels (McKay *et al.*, 1999). The delay in the accumulation

of light harvesting pigments following addition of iron to iron limited phytoplankton has also been observed in other studies of various phytoplankton species (Greene *et al.*, 1992; Geider & La Roche, 1994; Coale *et al.*, 1996). Such studies agree with the observation that chlorophyll biosynthesis and the repair of components of the electron transport chain are processes that are independent of one another (Guikema, 1987).

1.3 – Flavodoxin and Ferredoxin as Potential Biomarkers of Iron Limitation

If the role of iron in the production ecology of the oceans is to be understood, it is desirable to develop a means of determining the extent of iron limitation in phytoplankton in the field that is ideally quick, relatively simple and reliable. An approach likely to fit these criteria is the use of biomarkers; molecules within phytoplankton cells that would signal that the cell is suffering from a shortage of iron and has become physiologically impaired. An appropriate protein or its mRNA transcript is likely to be the most convenient candidate for a biomarker of iron limitation and much work has been done to investigate the potential of the ferredoxin and flavodoxin proteins as biomarkers of iron limitation (LaRoche *et al.*, 1995; Erdner *et al.*, 1999; McKay *et al.*, 1999). In some species of phytoplankton, iron limited conditions induce the replacement of the iron containing protein, ferredoxin, with a functional homolog flavodoxin that does not require iron. Ferredoxin is an important electron transport protein which is involved in redox reactions in photosynthesis, respiration, nitrogen assimilation and a variety of other cellular activities.

The various means of confirming iron limitation in the field such as mesoscale enrichment experiments and bottle assays are associated with various disadvantages ranging from the risk of contamination with iron to cost and logistical issues. The use

of an iron regulated cellular response as an indicator of iron nutritional status could potentially eliminate these problems. Flavodoxin (LaRoche *et al.*, 1995) and the ratio of ferredoxin:flavodoxin (Doucette *et al.*, 1996) have been proposed as bio-markers of iron nutritional status in marine phytoplankton. A study by Erdner *et al.* (1999) found that flavodoxin induction was a response specific to iron limitation across a range of phytoplankton classes and was insensitive to light stress, phosphate, nitrate, silicate and zinc deficiency. The study suggests that measuring the ratio of ferredoxin to flavodoxin may be a sensitive method of determining the severity of iron stress.

Replacement of ferredoxin with flavodoxin under iron limited conditions is not a universal response. Despite suffering from iron limitation, phytoplankton species across a range of taxonomic groups (dinoflagellates, diatoms and prymnesiophytes) did not produce flavodoxin (Erdner *et al.*, 1999). While most of the non-flavodoxin inducing phytoplankton in the study were of coastal rather than oceanic origin, the majority of the coastal species in the study did produce flavodoxin under iron limitation.

Ferredoxin and flavodoxin can be purified and readily detected by HPLC / Mass spectroscopy although other means of detecting and quantifying these proteins have been examined. An immunological approach was utilised by McKay *et al.* (1999) in an attempt to detect ferredoxin in marine phytoplankton and cyanobacteria. The antibody employed was raised against ferredoxin purified from the marine diatom *Thalassiosira weissflogii*. While the approach was effective at detecting a band with a molecular mass similar to *T. weissflogii* ferredoxin in a variety of other iron replete diatoms and some more phylogenetically distant algae, cross reacting proteins were

not found in *Aureococcus anophagefferens* or the coccolithophore *Emiliana huxleyii*. Suspected ferredoxin bands were observed in extracts of the green algae *Dunaliella tertiolecta* and *Chlamydomonas reinhardtii* but the reactions were weak. The apparent limited range of the reactivity of anti-ferredoxin across a spectrum of phytoplankton classes is likely to result in difficulty in assessing ferredoxin presence and absence in mixed natural samples. This compounded with the observation that a variety of eukaryotic phytoplankton species do not appear to produce flavodoxin in response to iron limitation (Erdner *et al.*, 1999) may have the potential to limit the usefulness of ferredoxin:flavodoxin ratios as biomarkers of iron nutritional status in the field. In the study by Erdner *et al.* (1999) species in which flavodoxin could not be detected originated mainly from coastal areas where they are highly unlikely to encounter the low levels of iron observed in the high nutrient low chlorophyll (HNLC) areas of the open marine environment.

It has been suggested that phytoplankton that are unable to induce flavodoxin in a low iron environment would be uncompetitive in iron limited water and would form a very small fraction of the overall biomass. Ferredoxin:flavodoxin ratios, therefore, might be a useful indicator of iron limitation for the majority of species in an iron limited phytoplankton community. While this may be the case in most instances, it has been reported that a *Synechocystis* PCC 6803 mutant with a disrupted *isiB* gene (encoding flavodoxin) can still grow in conditions that result in flavodoxin expression in the wild type (Kutzki *et al.*, 1998). To compound the potential problems associated with using a ferredoxin : flavodoxin index to assess the extent of iron limitation, it was found that the marine diatoms *Thalassiosira weissflogii* and *Phaeodactylum tricorutum* expressed flavodoxin as an early response to low iron concentrations in

the environment which did not necessarily correspond to the onset of physiological impairment and slower growth rate (McKay *et al.*, 1997).

Given the uncertainties and potential pitfalls of relying on a single biomarker it would be useful to develop alternative biomarkers for iron limitation. Perhaps the most useful of these might be other proteins associated with photosynthetic electron transport, the main target for iron limitation, that are common to flavodoxin and non-flavodoxin producing phytoplankton species.

1.4 – Aims of this study

This investigation aims to study the acclimation of *Coccolithus pelagicus* to iron limitation by utilising molecular techniques such as subtractive cDNA hybridisation, reverse transcription (RT) real time PCR and two dimensional SDS PAGE to probe gene expression changes and changes in the proteome occurring between iron replete and iron limited cells. A secondary objective of this study is to use the aforementioned techniques to attempt to identify potential biomarkers of iron limitation in *C. pelagicus*.

CHAPTER 2: Materials and Methods

2.1 – Cocolithus pelagicus – maintenance of stock cultures and experimental cultures

Stock and experimental cultures were maintained in an illuminated orbital incubator at 18°C at an incident irradiance of 25 $\mu\text{mol photons m}^{-2} \text{s}^{-1}$ under a 16:8 h light:dark cycle. Cultures were grown in a defined artificial seawater medium supplemented with 1 x Guillard's f/2 enrichment solution (Guillard and Ryther 1962) minus silicate.

Artificial seawater (ASW):

NaCl	25 gL^{-1}
MgSO ₄	3.5 gL^{-1}
MgCl ₂	2.0 gL^{-1}
CaCl ₂	0.5 gL^{-1}
KCl	0.5 gL^{-1}
Tris HCl	0.5 gL^{-1}
Tris Base	0.5 gL^{-1}

50 x Guillard's f/2 enrichment solution (Sigma)

NaNO ₃	44.15 mM
NaH ₂ PO ₄	1.81 mM
FeCl ₃ .6H ₂ O	0.5 mM
Na ₂ EDTA.2H ₂ O	0.5 mM
CuSO ₄ .5H ₂ O	2 μM
Na ₂ MoO ₄ .2H ₂ O	1.5 μM

ZnSO ₄ .7H ₂ O	4 μM
CoCl ₂ .6H ₂ O	2.25 μM
MnCl ₂ .4H ₂ O	45 μM
Vitamin B ₁₂	5 nM
Biotin	100 nM
Thiamine.HCl	15 μM

Experimental *Coccolithus pelagicus* cultures were grown in 250 ml glass conical flasks containing 100 mL of artificial seawater (ASW) (pH 8.0) supplemented with 2 mL of 50 x F/2 Guillard's marine enrichment solution and varying concentrations of EDTA or deferoxamine. All glassware was pre-washed in 0.1 M HCl for 1 hour and then rinsed thoroughly with MillQ grade de-ionised H₂O prior to use. ASW was sterilised by autoclaving at 121⁰C for 20 minutes and left for 24 hours at room temperature to allow gas equilibration. 50 x F/2 Guillard's marine enrichment solution, EDTA and deferoxamine were added to ASW after autoclaving and gas equilibration. The medium was then left overnight to allow for Fe chelation. No EDTA or deferoxamine was added to the iron replete control cultures. During initial growth experiments a range of concentrations of EDTA (400 nM – 2 mM) and deferoxamine (400 nM – 200 μM) were used to determine the concentration of each chelator that would reduce the growth of cultures by 40-50% relative to that of the control cultures containing no chelator. Increase in biomass was determined by measuring optical density measurements at 750 nm every 24 hours.

2.1.2 – Determination of chlorophyll a concentrations

Chlorophyll *a* concentrations were determined by centrifuging 1 mL of culture at 13,000 rpm for 5 minutes and then re-suspending the cell pellet in 1 ml of 90% methanol. The methanol – cell pellet re-suspension was left in the dark for 1 hour. The sample was then centrifuged at 13,000 rpm for 5 minutes and 0.8 ml of the supernatant was recovered. The absorbance of the supernatant at 665 nm was determined and chlorophyll *a* concentrations were estimated using the extinction coefficient: chlorophyll *a* ($\mu\text{g/ml}$) = $13.9 \times A_{665\text{nm}}$.

2.1.3. – Growth experiments to confirm iron limitation

Experimental cultures containing EDTA or deferoxamine that were in the exponential growth phase at growth rates that were approximately 40-50% lower than that of the corresponding control cultures were used to inoculate fresh 100 ml cultures. ASW was prepared exactly as described in section 2.1 and supplemented with F/2 Guillard's marine enrichment solution to serve as iron replete cultures. The same culture was also used to inoculate 100 ml of ASW supplemented with F/2 Guillard's marine enrichment solution and containing an additional 200 nM FeCl_3 and either 1.25 mM EDTA or 150 μM deferoxamine. Growth rates were determined by measuring optical density at 750 nm every 24 hours. Cultures were grown at 18⁰C on a continuous cycle of 16 hours light, 8 hours dark. All glassware used in the growth experiments was washed in 0.1 M HCl for 1 hour and then rinsed thoroughly with Milli-Q grade H₂O prior to use.

*2.1.4 – Microscopic examination of *Coccolithus pelagicus* cells*

10 μl of culture was placed on a glass slide and examined under a light microscope equipped with a CCD camera. The cells were examined at 630 x magnification.

Counts of flagellated / non-flagellated cells were performed at 630 x magnification. Fresh culture was placed on the microscope slide every 2.5 minutes to avoid any artefacts due to heating by the light source and counts were resumed.

2.2 – RNA extractions

All glassware and equipment used in the extraction and handling of RNA was sterile and where possible was washed with diethylpyrocarbonate (DEPC) treated MilliQ grade distilled water. Where possible all reagents (i.e. those not containing Tris.HCl or known to be RNase-free) involved in RNA extraction protocols were treated with DEPC.

DEPC treatment was performed by adding DEPC to solutions at a concentration of $1\mu\text{l ml}^{-1}$. The solution was then shaken vigorously and left in a fume cupboard overnight with the lid left loose. The solution was then autoclaved in order to sterilise it and to evaporate any residual ethanol formed from the breakdown of DEPC.

2.2.1- Buffers and solutions used for RNA extractions and electrophoresis

- DEPC ($1\mu\text{L ml}^{-1}$) treated distilled water.
- 10 x TAE buffer (400 mM Tris-Acetate, 10 mM EDTA)

- Agarose gels were made by dissolving 1% (w:v) agarose in 1 x TAE buffer and ethidium bromide was added to a concentration of 0.002%. All apparatus used in the preparation of gels was soaked in 0.1 M NaOH for 1 hour and then rinsed extensively with DEPC treated distilled water prior to use.
- TE buffer (10 mM Tris-HCl pH 8, 1 mM EDTA)

2.2.2 – Extraction of RNA

RNA was extracted from cultures in exponential growth phase. Cells from 30 ml of each culture were harvested by centrifugation and either processed immediately or stored in RNAlater™ (Ambion) at -20°C until RNA was extracted. Cells were centrifuged at 8,000 x g at 18°C in a bench top centrifuge for 3 minutes and then re-suspended in 5 ml of RNAlater™ (Ambion). The optical density of the harvested cultures at 750 nm were as follows: Fe replete (1, 2 & 3) = 0.327, Fe replete (4) = 0.396, 150 μM DF (1) = 0.185, 150 μM DF (2) = 0.206, 150 μM DF (3) = 0.203, 150 μM DF (4) = 0.175.

RNA extractions were performed using the RNAqueous™ kit from Ambion®. Cells stored in RNAlater™ (Ambion) were centrifuged at 15,000 x g for 5 minutes in order to pellet the cells. The supernatant was discarded and the cell pellet was quickly re-suspended in 300–700 μl of RNAqueous™ lysis/binding buffer. The solution was gently pipetted up and down several times in order to facilitate lysis of the cells. Once lysis had occurred (as indicated by the increased viscosity of the solution and the absence of any solid material), an equal volume of 64% ethanol was added and the tube was gently inverted several times in order to mix the contents. A filter cartridge /

collection tube (provided with the kit) was assembled and the lysate / ethanol mixture was applied to the filter cartridge. The filter cartridge / collection tube assembly was centrifuged at RCF 15,000 x g in a bench top centrifuge at room temperature for 1 minute to draw the lysate / ethanol solution through the filter. The flow-through was discarded and the collection tube was re-used in the following washing steps. 700 µl aliquots of any remaining lysate / ethanol mixture were loaded onto the filter and the process of drawing the mixture through the filter was repeated in exactly the same manner as previously described. Once the entire sample had been drawn through the filter, 700 µl of Wash Solution #1 (supplied with the kit) was applied to the filter cartridge and drawn through the filter by centrifugation at RCF 15,000 x g in a bench top centrifuge at room temperature for 1 minute. The flow-through was discarded and the filter was washed twice with 500 µl Wash Solution #2/3 (supplied with the kit) using the same procedure as the previous wash step. After the second 500 µl wash, the wash solution was discarded and the filter cartridge assembly was centrifuged briefly (10-30 seconds) to draw through any remaining Wash Solution #2/3. The filter cartridge was then placed inside a fresh collection tube and 40-50 µl of preheated Elution Solution (75°C) (supplied with the kit) was added to the filter. The filter cartridge assembly was centrifuged at RCF 15,000 x g for 30 seconds at room temperature. A second aliquot (10-20 µl) of 75°C Elution Solution was added to the filter and centrifuged again using the same conditions. Eluted RNA that was not used immediately was kept at -20°C for short term storage and at -70°C for long term storage.

2.2.3– Spectrophotometric determination of RNA concentration

A dilution of RNA (1:500 – 1:200) was made in DEPC treated MQ and the absorbance was read at 260 nm and 280 nm. RNA concentrations were calculated based on an absorbance of 1.0 being equal to 40 $\mu\text{g ml}^{-1}$ RNA. The DEPC treated MQ used to dilute the RNA samples was used to blank the spectrophotometer at each wavelength. The quartz cuvettes used were soaked in concentrated HCl / methanol (50:50) and then rinsed with DEPC treated MQ before use.

2.2.4 – Electrophoresis of RNA

All glassware and apparatus used in the preparation and running of RNA agarose gels were soaked in 0.1 M NaOH for 1 hour and then rinsed extensively with DEPC treated MQ. RNA was run on 1% agarose gels amended to 0.002% ethidium bromide (room temperature) at 150 V for 10 – 15 minutes and then at 100 V for a further 15 minutes. Samples were run alongside 10 μl of Hind III λ phage digest markers.

2.2.5 – Purification of mRNA

mRNA was purified from total cellular RNA samples using the Dynabeads[®] mRNA purification kit from DYNAL BIOTECH[®].

Assuming that mRNA accounts for between 1 – 5% of total cellular RNA, 100 μg of RNA should contain between 1.0 – 5.0 μg of mRNA. Total cellular RNA samples were diluted with DEPC treated MQ to 100 μg in a total volume of 100 μl . RNA samples were heated at 65°C for 2 minutes and then placed on ice. 200 μl (1 mg) of

Dynabeads Oligo (dT)₂₅ were washed once in 100 µl of binding buffer (20 mM Tris-HCl (pH 7.5), 1.0 M LiCl, 2mM EDTA) (supplied with the kit). The Dynabeads Oligo (dT)₂₅ were placed on a magnet to separate them from the solution and after 30 seconds the supernatant was removed. The Dynabeads Oligo (dT)₂₅ were then re-suspended in 100 µl of binding buffer. The Dynabeads Oligo (dT)₂₅ were added to RNA samples and mixed thoroughly by pipetting before being allowed to anneal to polyadenylated mRNAs for 5 minutes at room temperature (RT). A magnet was used to remove the Dynabeads Oligo (dT)₂₅ - mRNA from solution and the supernatant was removed and discarded before the Dynabeads Oligo (dT)₂₅ were washed twice with 200 µl of Washing Buffer B (provided with kit) (10 mM Tris-HCl (pH 7.5), 0.15 M LiCl, 1 mM EDTA). The Dynabeads Oligo (dT)₂₅ were re-suspended in 10 µl 10 mM Tris-HCl pH 7.5 and then heated to 75°C for 2 minutes. The 1.5 ml eppendorf tube containing the Dynabeads Oligo (dT)₂₅ and mRNA in 10 mM Tris-HCl was then placed against a magnet and the supernatant (mRNA) was transferred to a fresh, RNase free tube. The mRNA was used immediately to produce a subtracted cDNA library.

2.3 – cDNA subtraction

In the proceeding section an overview of the cDNA subtraction process is presented before the protocol for the technique is detailed.

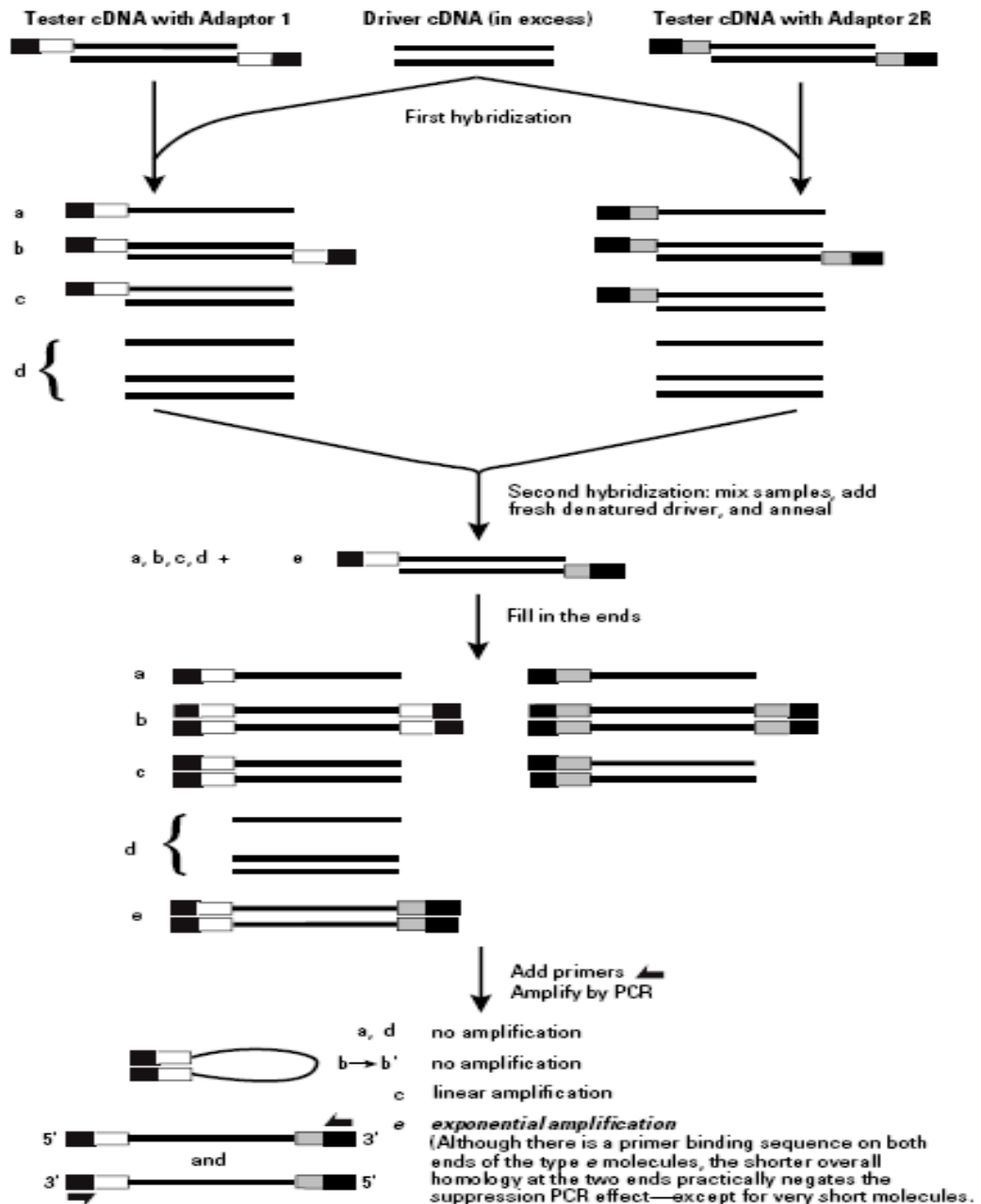


Figure 2.1: Diagram illustrating the principles underlying the Clontech PCR-Select™ cDNA Subtraction Kit (Adapted from the Clontech PCR-Select™ cDNA Subtraction Kit user manual, published 15 September, 1999).

In the first stage of the cDNA subtraction process both populations of mRNA to be subtracted are converted into double stranded cDNA. The cDNA that contains specific differentially expressed transcripts is referred to as “tester” cDNA and the reference cDNA is referred to as “driver” cDNA.

Both the tester and driver cDNAs are digested by Rsa I and after digestion the tester cDNA is subdivided into two portions, and each is ligated with a different cDNA adaptor. The adaptors are de-phosphorylated so that additional adaptors cannot be ligated to the 5' end of the initial adaptor that is attached to the cDNA. The two adaptors contain stretches of identical sequence to allow annealing of the PCR primer once the recessed ends have been filled in. No adaptors are ligated to the driver cDNAs.

After the adaptor ligations two hybridisations are performed in which each sample of tester cDNA is mixed with an excess of driver cDNA. The samples are denatured by heating and allowed to anneal. This generates the type a, b, c, and d molecules in each sample (see *figure 2.1*). The single stranded type *a* molecules are significantly enriched for differentially expressed sequences, as the cDNAs that are not differentially expressed form type *c* molecules with the driver (see *figure 2.1*).

In the second hybridisation step, the two primary hybridisation samples are mixed together but are not denatured. Now, only the remaining equalised and subtracted single stranded tester cDNA molecules are capable of re-associating and forming new type *e* hybrids (see *figure 2.1*). These type *e* hybrids are double stranded cDNA molecules with ends which correspond to the sequences of adaptors 1 and 2R (see *section 2.3.8*). Thus the type *e* molecules are the only combination which can undergo exponential amplification during PCR as the PCR primers target the sequences on the

two adaptors. In order to further enrich fraction *e* for differentially expressed transcripts freshly denatured driver cDNA is added again (without denaturing the subtraction mix) and the molecules are allowed to hybridise. After DNA polymerase has filled in the ends of the type *e* molecules they will have different annealing sites for the nested primers on their 5' and 3' ends. These type *e* molecules represent differentially expressed sequences.

PCR is carried out on the entire mix to overwhelmingly enrich the sample for differentially expressed sequences. During PCR, the type *a* and *d* molecules are missing primer annealing sites, and thus cannot be amplified. Due to the suppression PCR effect, most type *b* molecules form a pan-like structure (see *figure 2.1*) that prevents their exponential amplification. The type *c* molecules have only one primer annealing site and thus amplification is only linear. Only the type *e* molecules, which have two different adaptors and therefore forward and reverse priming sites, are capable of undergoing exponential amplification. These amplified sequences are the equalised, differentially expressed transcripts.

In order to further reduce any background PCR products and to further enrich for differentially expressed sequences a secondary, nested PCR amplification is performed. Upon completion of this nested PCR the amplified sequences can be cloned into a vector and sequenced or can be utilised in a variety of other downstream applications such as hybridisation probing DNA libraries.

cDNA subtraction was carried out using the PCR-select™ cDNA subtraction kit from Clontech Laboratories. Both the forward and reverse subtractions were carried out in accordance with the protocol provided in the PCR-select™ cDNA subtraction kit user manual. The protocol is detailed here.

2.3.1 – Buffers and solutions used for cDNA subtraction

The following solutions were used in the cDNA subtractive hybridisation procedure but were not provided with the Clontech PCR-Select™ cDNA Subtraction kit. All other solutions, buffers or enzymes used in the cDNA subtractive hybridisation procedure were provided with the Clontech PCR-Select™ cDNA Subtraction kit.

Aqua phenol (pH 8.0) (QBioGene)

80% Ethanol

95% Ethanol

Phenol (pH 8.0) : chloroform : isoamyl alcohol (25 : 24 : 1 v/v)

Chloroform : Isoamyl alcohol (24 : 1 v/v)

2.3.2 – First-strand cDNA synthesis

The following components were added to a sterile PCR tube:

<u>Reaction component</u>	<u>Per reaction</u>
mRNA	2 - 4 μ l
cDNA synthesis primer (10 μ M)	1 μ l

2 μ l (containing 2 μ g of mRNA) of the control mRNA (human skeletal muscle mRNA provided with the kit) and approximately 1 μ g of experimental mRNA (mRNA extracted from Fe replete and Fe limited cultures) were used in the reverse transcription reactions. dH₂O was added to each reaction so that the final volume in each tube was 5 μ l. In total there were 3 reactions set up – a control reaction with skeletal muscle mRNA, and two reactions to produce the cDNA for the forward and reverse subtractions. The contents of the PCR tubes were mixed gently by flicking the tubes and then centrifuged for 10 seconds in a microcentrifuge prior to incubation

at 70°C for 2 minutes in a thermal cycler. Following incubation the reactions were cooled on ice for 2 minutes and then centrifuged briefly.

To each reaction the following components were added:

	<u>Per reaction</u>
5X First-strand buffer	2 µl
dNTP mix (10 mM each)	1 µl
Sterile H ₂ O	1 µl
AMV Reverse transcriptase (20 units / µl)	1 µl

The reactions were mixed gently by vortexing and then centrifuged briefly. The reactions were then incubated at 42°C for 1.5 hours in a thermal cycler with the cycler lid temperature set to 105°C to prevent any evaporation of the reaction mix. After the incubation the reactions were placed on ice immediately in order to terminate first strand cDNA synthesis.

2.3.3 – Second-strand cDNA synthesis

To each of the first-strand cDNA synthesis reactions from section 2.3.2 (containing 10 µl) the following components were added:

	<u>per reaction</u>
Sterile H ₂ O	48.4 µl
5X Second-strand buffer	16.0 µl
dNTP mix (10 mM each)	1.6 µl
20X Second-strand enzyme cocktail	4.0 µl

The contents of each reaction were mixed gently by flicking the tube and spinning briefly in a microcentrifuge. The reactions were incubated at 16°C for 2 hours in a thermal cycler. After the incubation 2 µl (6 U) of T4 DNA polymerase was added to each reaction and the contents were mixed gently. The reactions were then incubated at 16°C for a further 30 minutes in a thermal cycler. To terminate the reactions 4 µl of 20X EDTA / Glycogen mix was added to each tube.

100 µl of phenol (pH 8.0) : chloroform : isoamyl alcohol (25 : 24 : 1 v/v) was added to each reaction. The reactions were then vortexed and centrifuged at 14,000 rpm at room temperature. The top aqueous layer from each tube was collected and placed in sterile 0.5 ml microcentrifuge tubes. 100 µl of chloroform : isoamyl alcohol (24 : 1 v/v) was added to each of the 0.5 ml tubes and the previous vortexing and centrifugation steps were repeated in order to separate the phases. Following centrifugation, the top aqueous phases were collected and placed in sterile 0.5 ml microcentrifuge tubes. 40 µl of 4M NH₄OAc and 300 µl of 95% ethanol was added to each 0.5 ml tube before vortexing and then centrifugation at 14,000 rpm for 20 minutes at room temperature. The supernatant was carefully removed from each 0.5 ml tube and the cDNA pellet was overlaid with 500 µl of 80% ethanol. Each tube was centrifuged at 14,000 rpm for 10 minutes at room temperature. The supernatant was removed taking care not to disturb the pellet and the tubes were left with the caps open at room temperature for 30 minutes to allow for evaporation of any residual ethanol. Each pellet was dissolved in 50 µl of sterile H₂O and 6 µl from each reaction was transferred to a fresh PCR tube and stored at -20°C until it was needed to be run alongside *Rsa* I digested cDNA.

2.3.4 – *Rsa I* digestion

The remaining cDNA samples produced as described in sections 2.3.2 and 2.3.3 were digested with the restriction endonuclease *Rsa I*. The restriction digest was carried out by combining the following components in PCR tubes for each cDNA sample (3 in total – Skeletal muscle control, iron replete cDNA and iron limited cDNA):

	<u>per reaction</u>
ds cDNA	43.5 µl
10X <i>Rsa I</i> restriction buffer	5.0 µl
<i>Rsa I</i> (10 U / µl)	1.5 µl

The reactions were mixed by vortexing and were then centrifuged briefly. The reactions were then incubated at 37°C for 1.5 hours in a thermal cycler. After the incubation 5 µl of each restriction digest was set aside on ice to be run on a 1% agarose gel alongside the un-digested cDNA set aside in section 2.3.3 in order to observe whether the restriction digest had been successful. 2.5 µl of 20X EDTA / glycogen mix was added to each restriction digest to terminate the reaction. Digested cDNA was purified by means of phenol (pH 8.0) : chloroform : isoamyl alcohol (25 : 24 : 1 v/v) purification followed by a further chloroform : isoamyl alcohol (24 : 1 v/v) step before the cDNA was precipitated by adding 25 µl of 4M NH₄OAc and 187.5 µl of 95% ethanol to each tube. Each tube was centrifuged at 14,000 rpm for 10 minutes at room temperature in order to pellet the cDNA. The supernatant was carefully removed and each pellet was overlaid with 200 µl of 80% ethanol. The tubes were centrifuged at 14,000 rpm for 5 minutes and the supernatants were removed. The

cDNA pellets were allowed to dry at room temperature for 30 minutes before they were each dissolved in 5.5 μ l of sterile H₂O and stored overnight at -20°C.

The *Rsa* I digested and un-digested cDNA samples were run out on 1% agarose gels alongside *Hind* III digested λ phage markers. The cDNA was visualised on a UV trans illuminator and the success of the *Rsa* I restriction digest was confirmed by a shift in the mean molecular weight of the digested cDNA smear compared to the un-digested cDNA.

2.3.5 – Adaptor ligation

Blunt ended adaptors were ligated to diluted samples of the cDNAs produced as part of the subtractive hybridisation procedure. Each tester cDNA sample (3 samples) was split into two tubes and a different adaptor was ligated to each. After adaptor ligation there were 3 tubes for each of the original *Rsa* I digested cDNA samples. The skeletal muscle tester control was labelled “1” and thus sample 1 with adaptor 1 ligated cDNA was labelled 1-1 while adaptor 2R ligated cDNA was labelled 1-2 and a tube containing a mixture of both adaptor ligated cDNA populations was labelled 1C. The tubes containing the equivalent iron replete and iron limited adaptor ligated cDNAs were labelled 2-1, 2-2, 2C, 3-1, 3-2 and 3C respectively.

1 μ l of each *Rsa* I digested cDNA sample was diluted with 5 μ l of sterile H₂O and the remaining cDNA was stored at -20°C to be used later as driver cDNA. Control skeletal muscle tester cDNA was prepared by diluting *Hae* III digested Φ X174 DNA (Sigma-Aldrich) to a final concentration of 150 ng / ml with sterile H₂O and then mixing 5 μ l of this with 1 μ l of the *Rsa* I digested control skeletal muscle cDNA. This control skeletal muscle tester cDNA contained approximately 0.2% *Hae* III digested Φ X174 DNA (Sigma-Aldrich), each fragment of which corresponded to

approximately 0.02% of the total cDNA. It is these fragments which should be subtracted by the end of the skeletal muscle control subtraction.

Adaptor ligated tester cDNA was prepared as follows:

A ligation master mix was prepared by mixing the following components together in a PCR tube. Enough master mix was prepared for all ligations plus one additional reaction.

	<u>Per reaction</u>
Sterile H ₂ O	3 µl
5X Ligation buffer	2 µl
T4 DNA Ligase 400 U / µl)	1 µl

For each experimental tester cDNA (iron replete and limited samples) and for the control skeletal muscle tester cDNA, the following reagents were combined in the order shown:

	<u>Tube number</u>	
	1	2
	<u>Tester 1-1*</u>	<u>Tester 1-2*</u>
Diluted tester cDNA	2 µl	2 µl
Adaptor 1 (10 µM)	2 µl	-----
Adaptor 2R (10 µM)	-----	2 µl
Ligation master mix	6 µl	6 µl
Final volume	10 µl	10 µl

- The same setup was used for testers 2-1, 2-2, 3-1 and 3-2.

In a fresh PCR tube 2 μ l of tester 1-1 was mixed with 2 μ l of tester 1-2 and after the completion of the ligation reaction this served as an un-subtracted tester control, it was labelled 1C. The same was done for the other two cDNA samples 2 and 3 (iron replete and iron limited cDNAs) and they were labelled 2C and 3C respectively. All 9 of the ligation reactions were centrifuged briefly and then incubated at 16°C overnight in a thermal cycler. After the overnight incubation 1 μ l of EDTA / glycogen mix was added to each tube to terminate the ligation reactions. The reactions were then heated to 72°C for 5 minutes in a thermal cycler in order to inactivate the ligase. The tubes were then centrifuged briefly and 1 μ l from each un-subtracted tester control reaction (1C, 2C and 3C) was diluted in 1 ml of sterile H₂O. These three diluted samples were stored at -20°C until required later for PCR. All other ligations were used immediately in the next stage of the subtractive hybridisation procedure or stored at -20°C.

2.3.6 – Subtractive hybridisation

In the first hybridisation step an excess of driver (without adaptors) cDNA was mixed with tester cDNA (adaptor ligated) and the samples were heat denatured together and then allowed to anneal. Non-target cDNAs common to the driver and tester cDNA form hybrids under these conditions and the remaining single stranded cDNAs are enriched for differentially expressed sequences. The first hybridisation was carried out as follows:

The following components were set up in PCR tubes for each of the subtractions.

	<u>Hybridisation sample</u>	
	1	2
	<u>Tester 1-1*</u>	<u>Tester 1-2*</u>
Rsa I digested driver cDNA	1.5 µl	1.5 µl
Adaptor 1 ligated tester (1-1)*	1.5 µl	-----
Adaptor 2R ligated tester (1-2)*	-----	1.5 µl
4X Hybridisation buffer	1.0 µl	1.0 µl
Final volume	4.0 µl	4.0 µl

* The same setup was used for samples 2-1, 2-2, 3-1 and 3-2.

The samples were incubated at 98°C for 1.5 minutes and were then left to hybridise for 12 hours at 68°C in a thermal cycler.

A second hybridisation was performed. For each subtraction the two samples from the first hybridisation were mixed together but not denatured. Fresh denatured driver cDNA was then added to further enrich for differentially expressed sequences. By the end of the second hybridisation the subtracted cDNA population should contain hybrid molecules with two different adaptors on each end. Therefore, these differentially expressed sequences are the only ones which should amplify exponentially during PCR where the two different adaptors are used as priming sites.

For each subtraction the following reagents were added into a sterile tube:

	<u>Per reaction</u>
Driver cDNA	1 μ l
4X Hybridisation buffer	1 μ l
Sterile H ₂ O	2 μ l

For each subtraction 1 μ l of this mixture was placed in a PCR tube and heated at 98°C for 1.5 minutes. For each subtraction the appropriate tube of freshly denatured driver was removed from the thermal cycler and was mixed simultaneously with its two corresponding hybridisation samples by setting a micropipettor to 15 μ l and then taking up one of the hybridisation samples and freshly denatured driver into the same pipette tip with an gap of air separating them and then adding both into the other hybridisation sample still in a PCR tube. By doing this the two hybridisation samples 1-1 and 1-2 (or 2-1 & 2-2 or 3-1 & 3-2) were mixed only in the presence of freshly denatured driver cDNA. Each of the 3 hybridisations were mixed gently by pipetting and then centrifuged briefly before being incubated at 68°C overnight in a thermal cycler. After the overnight incubation the hybridisations were transferred to 0.5 ml tubes and 200 μ l of dilution buffer was added to each. Each sample was mixed by gently flicking the tubes and then heated at 68°C for 7 minutes in a heat block. The hybridisations were then stored at -20°C.

2.3.7 – PCR amplification of subtracted cDNA samples

Seven PCR reactions were carried out. (1) The forward subtracted experimental cDNA, (2) the un-subtracted tester control (tube 2C – see section 2.3.5), (3) the reverse subtracted experimental cDNA, (4) the un-subtracted tester control for the control subtraction (tube 3C – see section 2.3.5), (5) the subtracted control skeletal muscle cDNA, (6) the un-subtracted tester control for the control subtraction (tube 1C – see section 2.4.5) and (7) the PCR control subtracted cDNA (provided with the Clontech PCR-Select™ cDNA Subtraction Kit).

During PCR, differentially expressed cDNAs were selectively amplified over primary and nested PCRs. A brief incubation at 75°C was necessary prior to commencing PCR in order to fill in the sections of missing ends complementary to the adaptors in order to produce the binding sites for the primers. Only cDNAs with a different adaptor on each strand should be amplified exponentially thus enriching the PCR for subtracted cDNA sequences. A second amplification using nested PCR was carried out in order to reduce the background cDNAs and further enrich the sample for subtracted sequences.

PCR templates were prepared on ice by aliquoting 1 µl of each diluted subtracted cDNA sample (from section 2.3.6) and the corresponding diluted un-subtracted tester control (from section 2.3.5) into an appropriately labelled PCR tube. 1 µl of the control subtracted cDNA (provided with the Clontech PCR-Select™ cDNA Subtraction Kit) was aliquoted into an appropriately labelled tube. A master mix was prepared as follows:

	<u>Per reaction</u>
Sterile H ₂ O	19.5 µl
10X PCR reaction buffer*	2.5 µl
dNTP mix (10 mM)*	0.5 µl
PCR primer 1 (10 µM)	1.0 µl
50X Advantage cDNA polymerase mix*	0.5 µl
<hr/>	
Total volume:	24 µl
<hr/>	

* These reagents were provided in a separate kit – Clontech Advantage™ cDNA Polymerase Mix.

The master mix was mixed by vortexing and was then centrifuged briefly in a microcentrifuge. 24 µl master mix was added to each of the PCR templates prepared previously and kept on ice. Each reaction was then incubated at 75°C for 5 minutes in a thermal cycler and then the following PCR cycling parameters were begun:

27 cycles:

94°C	30 seconds
66°C	30 seconds
72°C	1.5 minutes

After completion of thermal cycling 8 µl of each reaction was run on a 2% agarose gel amended to 0.002% ethidium bromide and visualised with a UV trans illuminator.

3 µl of each primary PCR product mixture was diluted in 27 µl of sterile H₂O and the remaining primary PCR products were stored at -20°C. 1µl of each diluted primary PCR product mixture was aliquoted into an appropriately labelled PCR tube. Master mix was prepared for the secondary PCR reactions as follows:

	<u>Per reaction</u>
Sterile H ₂ O	18.5 µl
10X PCR reaction buffer*	2.5 µl
Nested PCR primer 1 (10 µM)	1.0 µl
Nested PCR primer 2R (10 µM)	1.0 µl
dNTP mix (10 mM)*	0.5 µl
50X Advantage cDNA Polymerase Mix*	0.5 µl
<hr/>	
Final volume:	24.0 µl
<hr/>	

* These reagents are provided in a separate kit – Clontech Advantage™ cDNA Polymerase Mix.

The secondary PCR master mix was mixed by vortexing and was then briefly centrifuged. 24 µl of secondary PCR master mix was added to each of the secondary PCR templates prepared previously and the following thermal cycling parameters were commenced immediately:

12 cycles:

94°C	30 seconds
68°C	30 seconds
72°C	1.5 minutes

8 µl of the secondary PCR products were then run on a 2% agarose gel amended to 0.002% ethidium bromide and visualised with a UV trans illuminator and the remaining PCR products were stored at -20°C.

2.3.8 – Sequences of Clontech primers and adaptors used in cDNA subtraction

cDNA synthesis primer:

TTTTGTACAAGCTT₃₀N₁N

Adaptor 1:

CTAATACGACTCACTATAGGGCTCGAGCGGCCCGCCCGGGCAGGT

Adaptor 2R:

CTAATACGACTCACTATAGGGCAGCGTGGTCGCGGCCGAGGT

PCR primer 1:

CTAATACGACTCACTATAGGGC

Nested primer 1:

TCGAGCGGCCCGCCCGGGCAGGT

Nested primer 2R:

AGCGTGGTCGCGGCCGAGGT

2.4. – Cloning and sequencing of subtracted cDNA sequences

The TOPO TA cloning kit from Invitrogen™ was used to ligate cDNA fragments from both the forward and reverse subtracted libraries into pCR®II-TOPO®. The ligated plasmids were then used to transform chemically competent and electro-competent TOP10 One Shot® *E.coli* cells. Transformants were selected at 37°C for 16 hours on LB agar spread plates containing 100 µg ml⁻¹ ampicillin and 40 µl of a 40 mg ml⁻¹ X-GAL stock spread evenly across the plate. The LB plates contained the following – tryptone 10 g L⁻¹, NaCl 10 g L⁻¹, Yeast extract 5 g L⁻¹, Bacto agar 15 g L⁻¹. The LB agar was autoclaved and, once cool enough to handle, approximately 25 ml was used to pour each agar plate. After 16 hours of growth the plates containing the *E.coli* transformants were stored at 4°C overnight.

As many successfully transformed recombinant colonies as possible were picked using sterile pipette tips and each was grown in 250 μl of terrific broth (Yeast extract 24 g L^{-1} , Bacto Tryptone 12 g L^{-1} , K_2HPO_4 12.5 g L^{-1} , KH_2PO_4 g L^{-1}) in 96 well sequencing plates provided with the Edge BioSystems™ SeqPrep™ 96 Plasmid Prep Kit. The terrific broth contained 100 $\mu\text{g ml}^{-1}$ ampicillin. The 96 well plates containing the picked colonies were incubated at 37°C and shaken at 200 rpm for 16 hours prior to plasmid purification.

After the 16 hour incubation the 96 well plates were centrifuged at 2,500 rpm for 3 minutes. The supernatant was decanted by inverting the plate and blotting it on a paper towel. Cells were resuspended in the remaining terrific broth (approximately 5-15 μl) by covering the plate with an adhesive sealer and vortexing while ensuring not to cause any splashing from the wells. 100 μl of lysis solution / enzyme mix (provided with the kit) was added to each well and plates were shaken gently at room temperature for 2 minutes. The plates were then allowed to incubate on the bench top at room temperature for 3 minutes. The lysate in the wells was removed by inverting the plates and decanting the liquid. 100 μl of wash solution (provided with the kit) was added to each well and the plates were shaken gently on the bench top. The wash solution was removed by inverting the plates and decanting the liquid. The contents of the wells were washed twice with 100 μl of 70% isopropanol. During each 70% isopropanol wash step the plates were shaken gently on the bench top for 1 minute. On each occasion the 70% isopropanol was removed by inverting the plates. The plates were then inverted onto a paper towel and centrifuged at 2000 rpm for 1 minute in order to remove any residual isopropanol. The plates were left at room temperature for at least 2 hours to ensure that all isopropanol had evaporated before 40 μl of dH_2O was added to each well. The plates were shaken gently for 2 minutes on the bench top

and then allowed to sit for 10 minutes at room temperature before they were covered with an adhesive sealer and stored at -20°C.

The plasmids were sequenced at the NERC Molecular Genetic Facility at Edinburgh University by means of automated sequencing (ABI 3730 capillary sequencer).

2.5 – Blast analysis, multiple sequence alignments of subtracted cDNA sequences and primer design.

The Fe replete and Fe limited sequences obtained from the forward and reverse subtracted libraries were subjected to BLAST analysis using the BLAST tool facilities available at the NCBI website (www.ncbi.nlm.nih.gov).

Sequences from the Fe limited subtracted library which returned a strong hit when subjected to BLAST analysis (Blastn or BlastX) were selected and primers were designed to amplify those cDNA sequences of interest. The primers were designed using the Primer3 software available at the Primer3 website (<http://frodo.wi.mit.edu/>). In total 17 sets of primers were designed in order to target each sequence of interest.

The primers were as follows:

20s Proteasome subunit (20S Prot)

Forward: TGTCTATGAACAGCCGATGC

Reverse: GGGCTGCGTCTCATAACAGAT

Cytochrome b5 like heme / steroid binding domain containing Protein (Cyt b5):

Forward: ATAAAACCCGTGCCACTCAG

Reverse: ACCGACGAACTCAAGCTGTT

Cytochrome bc1 complex, subunit 7 (Cyt bc1):

Forward: GGCAGCGTCCTTTACTTGAG

Reverse: TACGAGGACTCCTTGGTGA

DnaJ protein (DnaJ):

Forward: CGGTCTTGTAGCCCTTCTTG

Reverse: GTGTCGTGAAGGACGGAAAC

Chloroplast light harvesting protein isoform 8 (CM4E12):

Forward: GCCAGCTGATGTTTTCCATT

Reverse: CCTGGAAGAAGAAGCCAGTG

Predicted membrane protein (PMP):

Forward: GCGAGAGAAATGGAGGTCAG

Reverse: GAAAAGGTCCCCAAAGATCC

PsaE:

Forward: AGGTACCCTGTTGTGGTTCG

Reverse: GCCTGAATATTTTGCAGGTCA

Thioredoxin (Thio):

Forward: CTGTCCAGGTGCCATCAGTA

Reverse: ATTTCAATTTTGGCGAAACG

Ubiquitin conjugating enzyme (UCE):

Forward: GTGCCGTCTGGGTAGATGTT

Reverse: GCTTCGCCTTATGAGTGACC

Chloroplast light harvesting protein isoform 2 (Chl LHP):

Forward: ACTCGAGGCCAGCTGTCAA

Reverse: ACAAGAACCTGGCAACGAAG

Seven different fucoxanthin binding protein sequences were detected including five of which that were exclusive to the iron limited subtracted library. Two forward primers and seven reverse primers were designed to target each of the fucoxanthin binding protein sequences.

Fucoxanthin binding protein (FucoBP) forward primers

1. ACATCATCAACGACCTGCTG
2. ACAT(C/T)ATCAACGACCTGCTC

Fucoxanthin binding protein (FucoBP) reverse primers:

1. CGTGCACCTTCTAACAGACG
2. CGTCCAACACATGCACAGTA
3. GCCAGTTTAGGGCGTAATCA
4. GGCAGTTAGCGAGACCAAAG
5. CTAACGGCGTGCGTAGAAT
6. TGTTTTTAGAAAAGGCATGGAAA
7. GCCCCGCAATAGTAAAAGAA

2.5.1 – Design of degenerate primers to target ferredoxin, flavodoxin and Glyceraldehyde 3-phosphate dehydrogenase (GAPDH)

Degenerate primers were designed based on conserved sequence motifs identified from multiple sequence alignments to target flavodoxin. Two alternative forward primers and one reverse primer were designed for flavodoxin. Ferredoxin primers were designed based on conserved regions of nucleotide sequence between part of a ferredoxin transcript identified in the iron replete subtracted library from *Coccolithus pelagicus* and the ferredoxin sequence of *Pavlova lutheri*. Degenerate primers were also designed for the housekeeping gene, glyceraldehyde 3-phosphate dehydrogenase (GAPDH) to be used as a reference to normalise real time PCR results between iron replete and iron limited cDNA templates. Primers were designed from multiple sequence alignments of sequences from a range of phytoplankton taxa. The multiple sequence alignments were produced using the CLUSTALX multiple sequence alignment software.

Sequences returning the same hits when subjected to BLAST analysis were aligned using the CLUSTALX multiple sequence alignment software to ensure that the sequences were identical and that the primers designed would recognize all of the cDNA fragments which return the same BLAST results. The primer sequences for Ferredoxin, Flavodoxin and GAPDH were as follows:

Ferredoxin:

Forward: TACGCGGTCACCCTCGTCAC

Reverse: ACGGCAGGTCCAGGCCCTC

Flavodoxin:

Forward 1:

GGNAAYACNGARACNGTNGC

Forward 2:

CCNACNTGGMAYACNGGNGC

Reverse:

CCRAANAYNGCNACYTTYTTNCC

GAPDH:

Forward:

TAYGTNTGYGARWSNACNGGN

Reverse:

NGTNGGNACNCKRAANGCCAT

2.6 – Primer optimisation for real-time PCR

Primers were optimised using a gradient thermal cycler (Biometra T-Gradient – Thistle Scientific). The templates used for optimisation were 1:10 dilutions of the original plasmids containing the target cDNA fragment as an insert. All PCR reactions contained 2.5 mM MgCl₂ and 2X ReddyMix™ available from Thermo Scientific was used as master mix. All thermal gradient PCR reactions were run alongside negative controls. PCR products were run out on 1.0% agarose gels containing 0.002% ethidium bromide and viewed with a UV trans illuminator. The PCR reactions and cycling conditions for the thermal gradient PCR primer optimisations were as follows:

PCR Reaction:

Sterile H ₂ O	10 µl (11 µl in negative control reactions)
MgCl ₂ (25mM)	1 µl
Forward primer	0.25 µl (100 pmol µl ⁻¹ stock)
Reverse primer	0.25 µl (100 pmol µl ⁻¹ stock)
Template	1 µl
ReddyMix (1.5mM MgCl ₂)	12.5 µl

Cycling Parameters:

95°C	2 minutes
<hr/>	
<i>26 CYCLES:</i>	
94°C	30 seconds
Thermal gradient	30 seconds
72°C	1 minute
<hr/>	
72°C	10minutes

The optimum annealing temperature determined for each target transcript was as follows:

38°C = GAPDH

62°C = Fucoxanthin BP (6), Predicted membrane protein, Fucoxanthin BP (3).

65°C = Thioredoxin, Fucoxanthin BP (7), DnaJ, Fucoxanthin BP (2), Fucoxanthin BP (4), Ubiquitin conjugating enzyme, Fucoxanthin BP (5), Ferredoxin.

67°C = psaE, Chl LHP, 20S proteasome subunit, Cyt b5, CM4E12, Cyt bc1, Fucoxanthin BP (1) + (3).

2.6.1 – cDNA production for real-time PCR

RNA extractions were carried out on Fe replete and Fe limited cultures of *Coccolithus pelagicus*. The RNA extractions were carried out using the RNAqueous[®] kit employing exactly the same method as described in section 2.2.2 and nucleic acid concentrations were estimated using the spectrophotometric method described in section 2.2.3.

The extracted RNA was treated with the TURBO DNA-free[™] kit from Applied Biosystems in order to remove any genomic DNA that was carried over from the RNA extraction process. Each treatment was carried out in 50 μ l volumes with 1 μ l of Turbo DNase enzyme (2U of enzyme) at 37°C for 30 minutes. Samples of the untreated RNA and the treated RNA were run out on a 1% agarose gel in order to confirm that any genomic DNA was no longer visible on a gel and that the RNA had not been degraded during the DNase treatment. The concentration of RNA after DNase treatment was determined spectrophotometrically.

Approximately 1 μ g of RNA was used in each reverse transcription reaction. The QuantiTect[®] Reverse Transcription kit available from Qiagen was used to produce cDNA for use as template in real time PCR reactions. A genomic DNA elimination reaction was carried out, the reaction contained the following components:

gDNA wipeout buffer, 7x:	4 μ l
Template RNA:	approximately 2 μ g (variable volume)
RNase-free water:	variable
TOTAL VOLUME:	28 μ l

The genomic DNA elimination reaction was incubated in a heat block at 42°C for 2 minutes and was then placed immediately on ice. A reverse transcription master mix was prepared on ice. The reverse transcription master mix was comprised as follows:

Quantiscript Reverse Transcriptase	2 µl
Quantiscript RT Buffer, 5x	8 µl
RT Primer Mix	2 µl

12 µl of reverse transcription master mix was added to the 28 µl genomic DNA elimination reaction containing the template RNA. This reaction was incubated for 30 minutes at 42°C in a thermal cycler. Parallel reactions for each template were carried out omitting Quantiscript reverse transcriptase as a control for any residual DNA contamination. After the 30 minute incubation the reaction was heated to 95°C for 3 minutes in a thermal cycler to inactivate the Quantiscript reverse transcriptase. The reactions were then either used immediately as template in real time PCR reactions or stored at -20°C. If it was necessary reactions were scaled up linearly to a maximum reaction volume of 100 µl.

2.6.2 – Testing primers using cDNA as a template

In order to assess the effectiveness of the primers detailed in sections 2.5 and 2.5.1 PCRs were carried out using cDNA as template to check for non-specific products since the optimum primer annealing temperatures were determined using plasmids with the target insert as templates. The only possible non-specific products using plasmid DNA would have been from complementary sequences within the vector whereas the complexity of the cDNA was far greater. PCR reactions were run using

exactly the same reaction conditions as described in section 2.6 with the exception that two reactions were run for each primer set, one using iron replete cDNA as template and another using iron limited cDNA as template. The optimum annealing temperatures determined as described in section 2.6 were used and all reactions were run alongside negative controls containing no template. The products from the reactions were run out on 1% agarose gels and PCR products were visualised under UV radiation.

2.7 – Real time PCR

The cDNA produced as described in section 2.6.1 was used as a template in real time PCR reactions utilising the primers detailed in sections 2.5 and 2.5.1 in order to quantitate the relative abundances of the transcripts detected in the iron limited subtracted library. The cycler used for real time PCR was the Stratagene Mx3000P real time thermal cycler. PCR tube strips with optical caps were used in all real time PCR reactions. The PCR reaction composition and thermal cycling parameters were as follows:

PCR components:

Sterile H ₂ O	10 µl (11 µl in negative control reactions)
Forward primer	0.25 µl (100 pmol µl ⁻¹ stock)
Reverse primer	0.25 µl (100 pmol µl ⁻¹ stock)
Template	1 µl
Master mix*	12.5 µl

*The master mix used for RT real time PCR was Brilliant[®] SYBR Green QPCR Master Mix (Stratagene) containing a final concentration of 2.5 mM MgCl₂.

95°C	10 minutes
<i>40 cycles:</i>	
94°C	30 seconds
Appropriate annealing temperature (see below)	30 seconds
72°C	1 minute

The instrument was set to detect fluorescence at the end of the extension step at 72°C. Dissociation curves were plotted using fluorescence measurements at 1°C intervals over a temperature range from 55 °C to 95°C.

Annealing temperatures used for each target transcript were as follows:

38°C = GAPDH

62°C = Fucoxanthin BP (6), Predicted membrane protein, Fucoxanthin BP (3).

65°C = Thioredoxin, Fucoxanthin BP (7), DnaJ, Fucoxanthin BP (2), Fucoxanthin BP (4), Ubiquitin conjugating enzyme, Fucoxanthin BP (5), Ferredoxin.

67°C = PsaE, 20s proteasome subunit, Cyt b5, CM4E12, Cyt bc1, Fucoxanthin BP (1) + (3).

2.7.1 – Data handling: normalising RT real time PCR results to GAPDH transcript abundance and determining up-regulation of genes in response to iron limitation.

The relative abundance of mRNAs represented in the iron replete and iron limited cDNA samples was normalised to the transcript abundance of the housekeeping gene glyceraldehyde 3-phosphate dehydrogenase (GAPDH) in each reaction and the extent

to which the target transcript was up-regulated in the iron limited cDNA samples was calculated. The equation used was:

$$2^{(\text{Ct Fe Limited cDNA} - \text{Ct GAPDH})} / 2^{(\text{Ct Fe Replete cDNA} - \text{Ct GAPDH})}$$

(Wyman & Bird, 2007)

In the equation Ct Fe Limited cDNA and Ct Fe Replete cDNA are the threshold cycles for the target transcript in the iron limited and iron replete samples respectively and Ct GAPDH is the threshold cycle of the corresponding GAPDH transcripts in the iron limited and iron replete cDNA samples. For experiments run in triplicate the threshold cycle values for each sample were averaged and the mean value obtained was used in the equation. All GAPDH real time PCR experiments were run in triplicate.

2.8 – 1-Dimensional and 2-Dimensional SDS-PAGE

Cells were pelleted by centrifugation at 8,000 x g for 3 minutes in a bench-top centrifuge. The pellets were washed with a sucrose solution (250 mM sucrose, 10 mM Tris pH 8.0) by re-suspending the cells in the sucrose solution and repeating the centrifugation step. Cells were re-suspended in 100 µl of lysis buffer (0.1 M Tris-HCl, pH 7.4, 1 mM EDTA, 8 M Urea, 0.05 M dithiothreitol (DTT), 10% glycerol, 5% NP-40, 2% IPG buffer of appropriate pH) and incubated at room temperature for 1 hour. Non-soluble cellular debris was removed from the lysate by centrifugation at 15,000 x g for 5 minutes. Protein was purified from the lysate using the 2D-Clean up kit (Amersham) according to the manufacturer's instructions. Purified protein was re-suspended in an appropriate volume of rehydration buffer (8 M urea, 2% NP-40, 60

mM dithiothreitol (DTT), 0.5% IPG buffer of appropriate pH) and protein concentrations were determined using the 2D Quant Kit (Amersham) according to the manufacturer's instructions. Samples were adjusted to the same protein concentrations and bromophenol blue was added to a concentration of 0.002%. The protein sample was applied to the immobilised pH gradient (IPG) strip by means of re-hydration loading. The IPG strip was laid in a channel in a re-swelling tray containing the protein sample in re-hydration buffer. The strip and protein sample were sealed off from the air with dry strip cover fluid (Amersham) and left overnight at room temperature. Immobilised protein gradient (IPG) strips are strips of acrylamide containing either a linear or non-linear pH gradient mounted on a plastic backing. They provide a less laborious and more reproducible means of running 2D SDS-PAGE.

The volume of re-hydration buffer used to re-suspend the protein sample varied depending on the length of IPG strip that was to be used for isoelectric focussing. Two different IPG strips were used in this investigation and the lengths of the strips and the sample volumes were:

<u>IPG strip length</u>	<u>Volume of re-hydration buffer applied</u>
7 cm strip (pH 3-10)	125 μ l
13 cm strip (pH 4-7)	250 μ l

All isoelectric focussing was carried out at 20°C with a maximum current of 50 μ A per IPG strip. The voltage parameters used varied depending on the length of the IPG strip being used. The voltage parameters for each IPG strip length were as follows:

7 cm pH 3-10 IPG strips

<u>Voltage mode</u>	<u>Voltage (V)</u>	<u>Time</u>	<u>KVh</u>
Step and hold	300	30 minutes	0.2
Gradient	1000	30 minutes	0.3
Gradient	5000	1 hr 20 mins	4.0
Step and hold	5000	25 minutes	2.0
Total		2 hr 45 mins	6.5

13 cm pH 4-7 IPG strips

<u>Voltage mode</u>	<u>Voltage (V)</u>	<u>Time</u>	<u>KVh</u>
Step and hold	500	1 hr	0.5
Gradient	1000	1 hr	0.8
Gradient	8000	2 hr 30 mins	11.3
Step and hold	8000	55 minutes	7.4
Total		5 hr 25 mins	20.0

After isoelectric focussing IPG strips were equilibrated for second dimension SDS-PAGE by incubation at room temperature for 15 minutes in 10 ml SDS equilibration buffer (75 mM Tris-HCl, pH 8.8, 6 M Urea, 30% glycerol, 2% SDS, bromophenol blue 0.002%, 10 mg ml⁻¹ DTT). A second equilibration was then performed using 10 ml of an equilibration buffer containing iodoacetamide instead of DTT - (75 mM Tris-HCl, pH 8.8, 6 M Urea, 30% glycerol, 2% SDS, bromophenol blue 0.002%, 25 mg ml⁻¹ iodoacetamide). The second equilibration was also for 15 minutes at room temperature. For both equilibrations the IPG strips were placed in sterile tubes containing the appropriate equilibration buffer and then placed on a rocking platform for the duration of the incubation.

Equilibrated IPG strips were run out on 12% Tris-Glycine polyacrylamide gels alongside Mark 12[™] unstained protein standards. The IPG strips were placed directly on top of the resolving gel and sealed in place using a 2% agarose stacking gel.

For 1-D SDS-PAGE a 4% acrylamide stacking gel was used made as follows:

Sterile H ₂ O	3.05 ml
0.5 Tris HCl, pH 6.8	1.25 ml
10% SDS	50 µl
30 % acrylamide	650 µl
10% Ammonium persulphate	25 µl
TEMED	5 µl

The 12% Tris-Glycine polyacrylamide running gels used for 1-D SDS-PAGE and second dimension electrophoresis of 2-D gels contained the following:

Sterile H ₂ O	3.35 ml
1.5 M Tris HCl, pH 8.0	2.5 ml
10% SDS	100 µl
30 % acrylamide	4.0 ml
10% Ammonium persulphate	50 µl
TEMED	5 µl

SDS-PAGE electrophoresis was carried out at a constant voltage of 100 V at 4°C in a cold room. The gels were then stained using the Colloidal Blue Staining Kit (Invitrogen™) according to the manufacturer's instructions. Glass containers used to stain gels were cleaned with de-con in sterile H₂O and then with ethanol before staining. The gel staining containers were covered with cling film and then placed on bench top rocking platforms in order to facilitate the staining. After 6 hours staining gels were de-stained overnight in sterile H₂O.

2.8.1 – Automated protein spot detection and analysis of 2-D gels.

The gels were scanned and analysis of 2-D gels was carried out using the ImageMaster 2D Platinum Software (version 5.0). Protein spots were detected automatically on 2-D gels by the ImageMaster software using the following settings:

Saliency	1.0
Minimum area	5.0
Smooth	2.0

The spot detection was scrutinised by eye and the molecular weight marker proteins were deleted from the detected spots as well as any detected regions that were clearly not protein spots such as dark areas of the dye front or specks of dust that had not been eliminated by the minimum area filter.

Reference spots were selected by eye to align the iron replete and iron limited gels in order to guide the software to highlight differentially expressed proteins. Spot pairs identified by the software were confirmed by eye and differentially expressed proteins on both the iron replete and iron limited gel were annotated using the ImageMaster software.

2.8.2 – Mass spectroscopic analysis of iron replete 2D-SDS PAGE spot FeR1

The prominent spot FeR1 in the iron replete 2D-SDS gel (*figure 3.15*) was excised using a micropipette with a sterile 200 µl tip. The excised protein was then stored in a sterile 1.5 ml tube at -20°C until it was sent for mass spectroscopic and bioinformatic analysis at the Fingerprints proteomics facility, Post-genomics and Molecular Interactions Centre, University of Dundee.

2.8.3 – Western blotting

Cells were harvested from *Coccolithus pelagicus* cultures in exponential growth phase and lysed by immersion in 500 µl of SDS loading buffer (250 mM Tris-HCl pH 6.8, 2% SDS, 10% glycerol, 20 mM dithiothreitol, 0.01% bromophenol blue). The samples were incubated at 90°C for 1 minute in a water bath. Protein concentrations were determined using the 2D Quant Kit (Amersham) according to the manufacturer's

instructions. The SDS gel was run at room temperature, 150 V constant voltage for 90 minutes. Seeblue® (Invitrogen) standard markers were loaded on the gel.

The separated proteins were electroblotted for 2 hours onto a PVDF membrane using PVDF transfer buffer (25 mM Tris base pH 7.4, 192 mM glycine, 10% methanol) at room temperature, 65 V (constant voltage). The SDS gel was stained with Coomassie blue to ensure that the proteins had been transferred to the PVDF membrane and were no longer present in the gel.

The blot was blocked with blocking buffer (5% goat serum albumin (Sigma), 0.1% Tween 20, 10 mM Tris base pH 7.4, 0.9% NaCl) at room temperature for 1.5 hours with constant agitation. The blot was then incubated with a 1:400 dilution of rabbit anti-actin antibody (Sigma) in blocking buffer. The primary antibody incubation was conducted for 16 hours at 4°C with constant agitation. After the primary incubation three 5 minute washes were performed at room temperature using wash buffer (10 mM Tris base pH 7.4, 0.9% NaCl, 0.1% Tween 20) with constant agitation.

The blot was incubated with the secondary antibody (HRP-conjugated goat anti-rabbit) diluted to 1:10,000 in blocking buffer. The incubations were performed at room temperature for 30 minutes with constant agitation. After the secondary antibody incubation the blot was washed four times with wash buffer each time for 5 minutes with constant agitation. A final 5 minute wash in distilled water was performed in order to remove any residual Tween 20 prior to chemiluminescent detection.

The SuperSignal® West Pico Chemiluminescent Substrate (Pierce) was used to detect antibody binding according to the manufacturer's instructions. Optimum exposure times were determined empirically and found to be 30 seconds.

Chapter 3 – Growth experiments and proteomic analysis

3.1 – *Coccolithus pelagicus* growth experiments

The iron chelating compounds EDTA and deferoxamine were assessed for their ability to induce iron limitation in cultures of *Coccolithus pelagicus*. The extent to which each chelator produced iron limited conditions in cultures was dependent on the concentration of the chelator. It was found that much greater concentrations of the divalent cation chelator EDTA were required to produce an iron limited response compared to deferoxamine which binds ferric iron exclusively. The effects of various concentrations of each chelator on growth rates and chlorophyll *a* concentration per unit biomass, and the response of iron limited cultures to the addition of iron are presented. Apparent morphological changes associated with both iron replete cells and iron limited cells are also presented alongside the growth data. The effectiveness of the chelators at artificially inducing iron limitation in *Coccolithus pelagicus* cultures and the possible disadvantages of using such a system are discussed. SDS-PAGE data and two-dimensional SDS-PAGE gels are presented as evidence that the proteome of iron limited cells is different from that of their iron replete counterparts indicating that there are changes occurring at the molecular level which coincide with iron limitation-induced slower growth rates. Data resulting from attempts to identify a differentially expressed protein by means of mass spectroscopy and western blotting are also presented.

The growth of *Coccolithus pelagicus* in triplicate cultures in artificial sea water (ASW) containing various concentrations of iron chelators was monitored using optical density measurements at 750 nm. In conjunction with these growth

measurements chlorophyll *a* concentrations were used as a proxy indicator for iron limitation under the conditions employed. Growth as determined by measuring the culture optical density at 750 nm and following a series of preliminary experiments using chelators at a wide range of concentrations growth was deemed to be moderately iron limited if the growth was 80% of the rate of the control and more severely iron limited if the growth was 60% or less than that of the control cultures. This was achieved at additional EDTA concentrations in the range 1.5 – 2 mM and deferoxamine concentrations in the range 150 – 200 μ M (Figure 3.1, Table 3A).

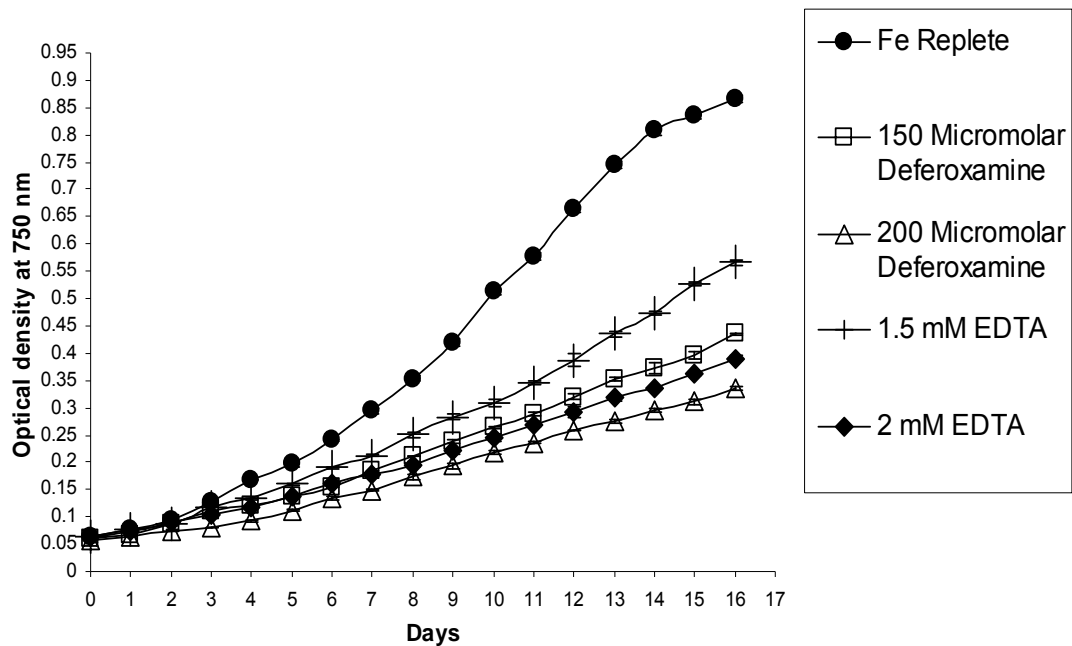


Figure 3.1: Growth curves showing mean \pm SE (n=3) increase in biomass of *Coccothius pelagicus* cultures grown in the presence of various concentrations of the iron chelators deferoxamine and EDTA as determined by optical density measurements at 750 nm.

<i>Culture</i>	<i>Mean(n=3) Specific Growth Rate (μ) (per day)</i>	<i>Generation Time (G) (Days)</i>	<i>μ expressed as a % of the iron replete μ</i>
Fe Replete	0.165 (SE \pm = 0.001)	4.2	100%
150 Micromolar DF	0.107 (SE \pm =0.0021)	6.48	64.5%
200 Micromolar DF	0.110 (SE \pm = 0.0014)	6.3	66.7%
1.5 mM EDTA	0.118 (SE \pm = 0.00054)	5.87	71.5%
2 mM EDTA	0.097 (SE \pm = 0.0012)	7.14	58.8%

Table 3A: Mean \pm SE (n=3) specific growth rates, generation times and iron limited specific growth rates as a percentage of iron replete rates of *Coccolithus pelagicus* cultures treated with the iron chelators deferoxamine (DF) and EDTA at various concentrations. The data to calculate specific growth rates was taken from the growth curves shown in *figure 3.1*.

While both EDTA and deferoxamine were able to reduce the growth rate of cultures compared to the iron replete control cultures, EDTA was required at far higher concentrations than deferoxamine to achieve a similar degree of growth inhibition. Even at millimolar concentrations of EDTA (i.e. ten times that of deferoxamine) the EDTA grown cultures still displayed specific growth rates similar to those cultures grown in the presence of much lower concentrations of deferoxamine.

In iron limited cultures the increase in chlorophyll concentrations over time was less than the rates observed in the iron replete cultures. As with the optical density at 750 nm, chlorophyll concentrations were inversely related to the concentration of iron chelator (deferoxamine or EDTA) in the growth medium.

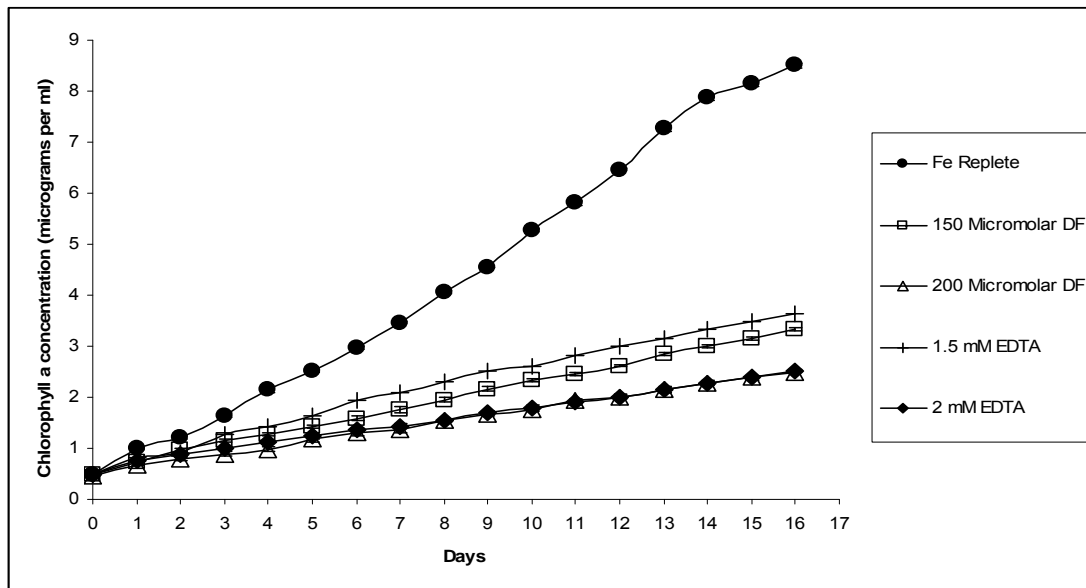


Figure 3.2: Mean \pm SE (n=3) change in chlorophyll concentration over time in cultures of *Coccolithus pelagicus* grown in media containing various concentrations of the iron chelators EDTA and deferoxamine.

Chlorophyll concentrations per unit biomass were lower in iron limited cultures than in iron replete cultures indicating that the amount of the pigment in iron limited cells is reduced relative to iron replete cells (Figure 3.3).

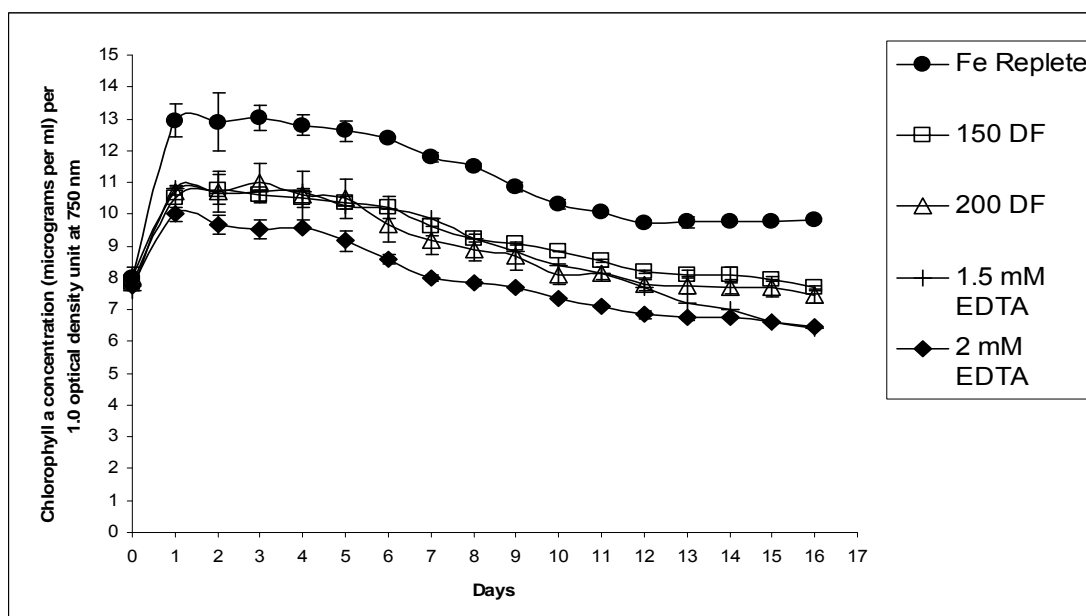


Figure 3.3: Temporal change in mean \pm SE (n=3) chlorophyll a concentration per unit biomass in cultures of *Coccolithus pelagicus* grown under iron replete conditions and in the presence of various concentrations of EDTA or deferoxamine.

3.1.1 – Iron addition experiments

In order to confirm that *Coccolithus pelagicus* cultures grown in the presence of deferoxamine were iron limited, growth experiments in which 100 nM FeCl₃ was added to iron limited cultures were carried out to observe the response to a fresh input of iron. Iron was added after optical density and chlorophyll *a* measurements had been taken on the seventh day of growth. The growth data obtained in the iron addition experiments are shown below in *figure 3.4*.

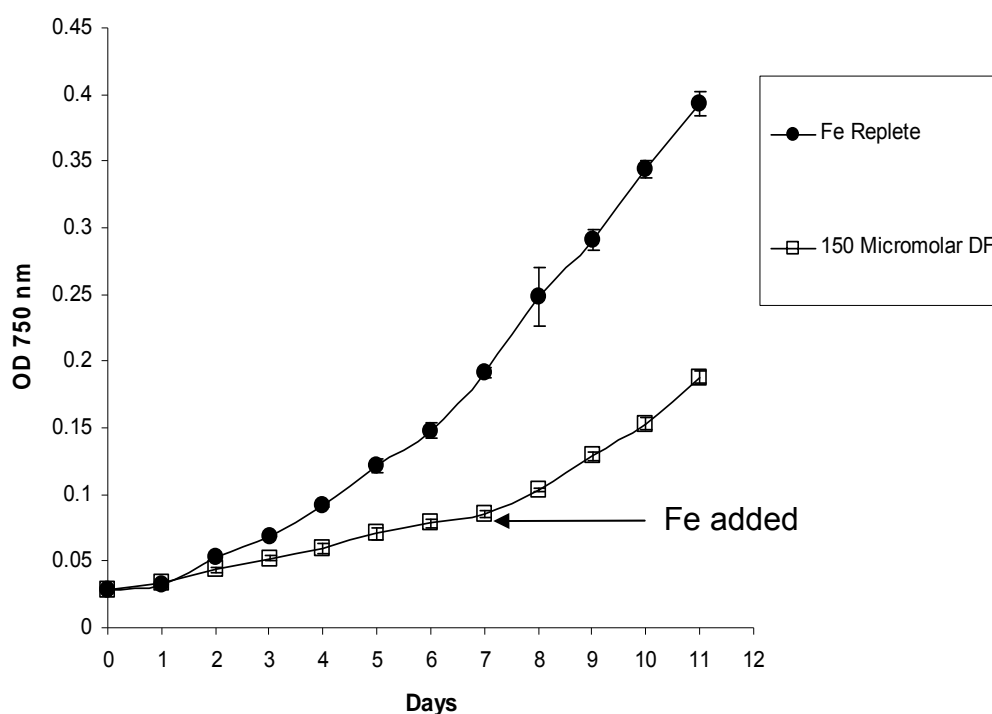


Figure 3.4: Growth curves showing mean \pm SE (n=3) increase in biomass of *Coccolithus pelagicus* cultures grown under iron replete conditions and in the presence of 150 μ M deferoxamine before and after the addition of iron.

The mean \pm SE (n=3) specific growth rates (μ) and generation times (G) of the cultures used in the iron addition experiment were calculated before and after iron addition and are shown in *table 3B*.

<i>Culture</i>	<i>Mean(n=3) Specific Growth Rate (μ) (per day)</i>	<i>Generation Time (G) (Days)</i>	<i>μ expressed as a % of the iron replete μ</i>
Fe Replete cultures	0.202 (SE \pm = 0.00082)	3.43	100%
Fe limited cultures(before iron addition)	0.136 (SE \pm = 0.0024)	5.09	67%
Fe limited cultures (after iron addition)	0.196 (SE \pm = 0.0037)	3.54	97%

Table 3B: Mean SE \pm (n3) specific growth rates, generation times and iron limited growth rates as a percentage of iron replete growth rates of *Coccolithus pelagicus* cultures used in the iron addition experiment.

The specific growth rate of the iron limited cultures increased upon addition of iron.

The specific growth rate increased within one day and reached that of the iron replete cultures. This is apparent in the data presented in *figure 3.4* which shows that the rate of biomass accumulation increased markedly after the addition of iron and in *table 3B* which clearly displays the change in growth rate when iron is made available.

Chlorophyll *a* concentrations were monitored in the iron replete and in the iron limited cultures before and after iron addition. The results of the chlorophyll concentration measurements are shown in *figure 3.5*.

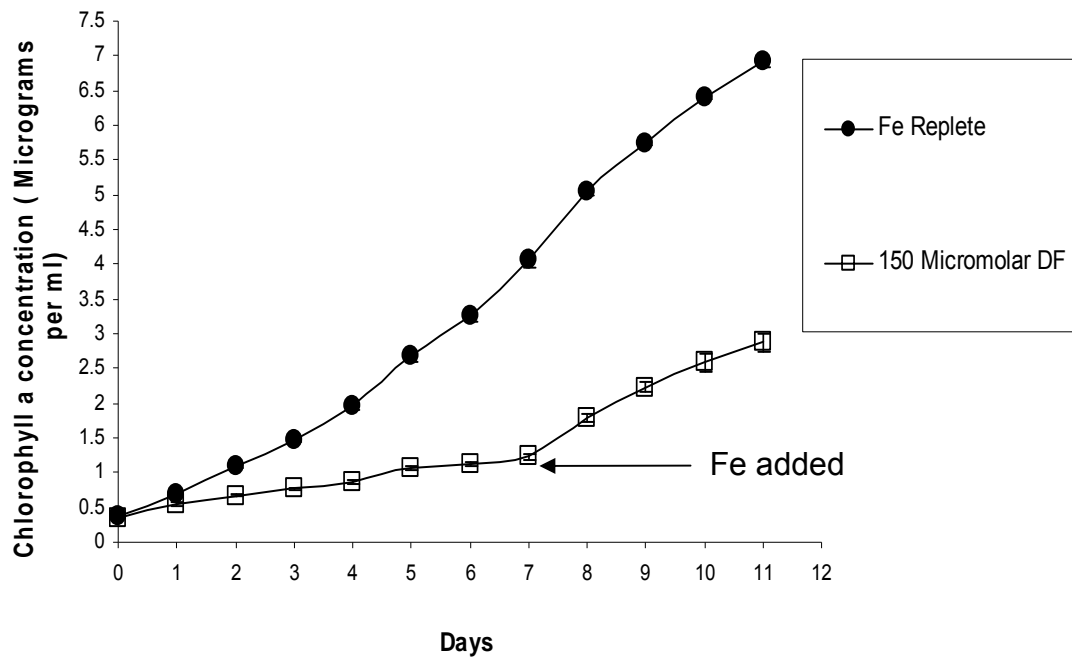


Figure 3.5: Mean \pm SE (n=3) change in chlorophyll concentration over time in cultures of *Coccolithus pelagicus* grown under iron replete conditions and in the presence 150 μ M deferoxamine before and after addition of additional iron.

As was the case with growth rate after iron addition to iron limited cultures (figure 3.4), the rate of increase in chlorophyll *a* concentration also increased upon alleviation of iron limitation (figure 3.5).

In order to determine if the chlorophyll concentrations observed represented a real difference in the amount of chlorophyll *a* per cell, the chlorophyll concentration normalized to biomass over time was calculated and expressed as chlorophyll *a* concentration per 1.0 optical density unit at 750 nm (figure 3.6).

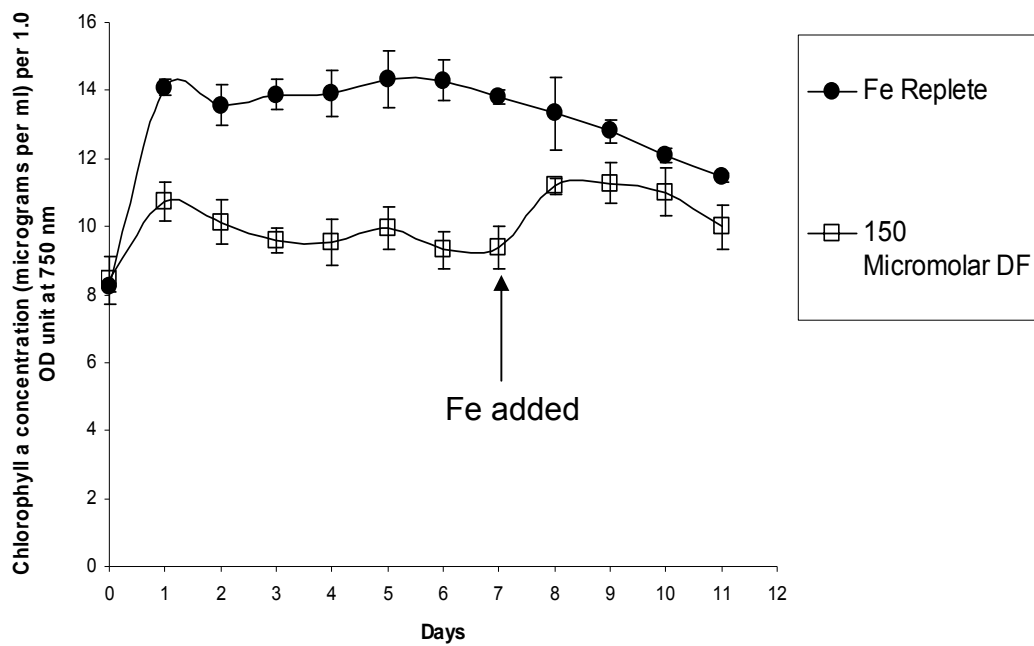


Figure 3.6: Curves showing change in chlorophyll *a* concentration per unit biomass in cultures of *Coccolithus pelagicus* grown under iron replete conditions and in the presence of 150 μM deferoxamine before and after the addition of iron.

The amount of chlorophyll *a* per unit biomass decreased over time in both the iron replete and iron limited cultures, although the decline was much less rapid in the iron replete cultures. The chlorophyll *a* concentration per unit biomass increased markedly upon iron addition to iron limited cultures of *Coccolithus pelagicus* before levelling out and beginning to decrease in line with the iron replete cultures once more. The chlorophyll *a* concentrations per unit biomass in the iron limited cultures did not reach the same levels as the iron replete cultures even after alleviation of iron limitation which was consistent with the increase in specific growth rates of the iron limited cultures which did not quite match that of the iron replete cultures. An initial rapid increase in the concentration of chlorophyll *a* per unit biomass over the first day following inoculation with an iron limited culture was observed in both the iron

limited and iron replete control cultures, with the iron replete cultures reaching the highest concentrations.

3.1.2 – Growth data for cultures used in RNA extractions

Coccolithus pelagicus replicate cultures from which cDNA was prepared for use in RT real time PCR experiments were monitored for increase in biomass over time.

The specific growth rates (μ) and generation times (G) of each replicate were calculated and the data are shown below in *figure 3.7* and *table 3C*.

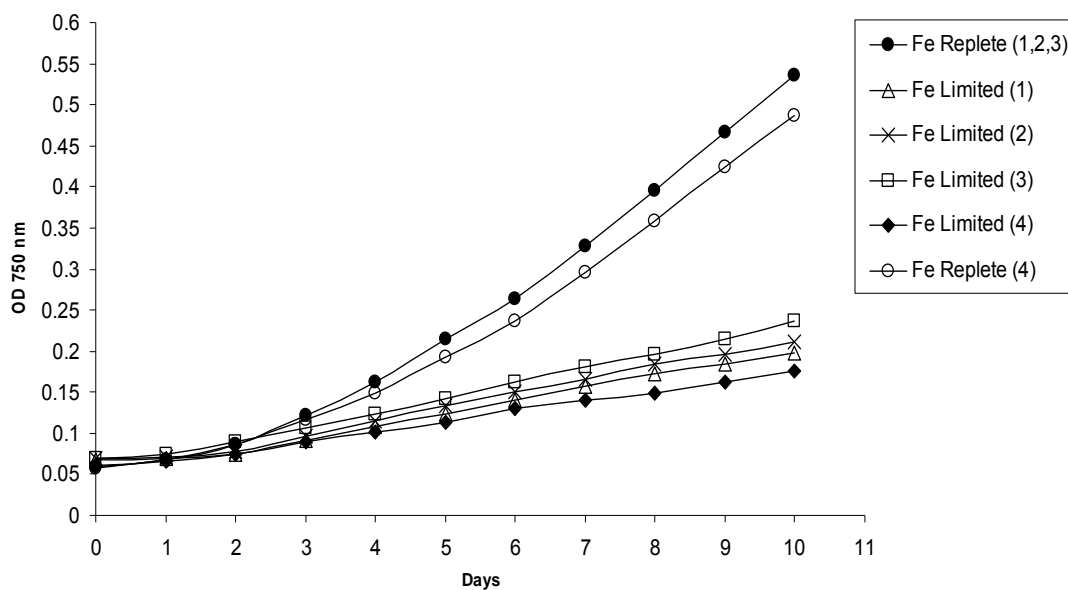


Figure 3.7: Growth curves for *Coccolithus pelagicus* replicate cultures from which RNA was extracted. The growth curves show increase in biomass over time when grown under iron replete conditions and in media containing 150 μ M deferoxamine. The Fe Replete (4) and Fe Limited (4) replicates were inoculated with a different stock from the other replicates shown.

<i>Culture / replicate</i>	<i>Specific growth rate (μ) (per day)</i>	<i>Generation time (G) (Days)</i>	<i>μ expressed as a % of the iron replete μ</i>
Fe Replete (1,2,3)	0.224	3.09	100%
Fe Replete (4)	0.214	3.23	100%
Fe Limited (1)	0.115	6.027	51%
Fe Limited (2)	0.117	5.92	52%
Fe Limited (3)	0.116	5.97	51.8%
Fe Limited (4)	0.097	7.14	45%

Table 3C: Specific growth rates, generation times and iron limited growth rates expressed as a percentage of their respective iron replete control growth rates of replicate cultures of *Coccolithus pelagicus* used to produce cDNA for RT real time PCR experiments.

The growth curves in figure 3.7 show the increase in biomass over time of the *Coccolithus pelagicus* cultures that were used to extract RNA for use in primer optimisation experiments and RT real time PCR. There is some variability between the growth rates of the four iron limited cultures despite each culture being treated with the same concentration of deferoxamine. Such variability was commonly observed throughout the duration of many growth experiments. The cultures appear to suffer a lag phase which lasts one to two days perhaps due to the fact that a 10% of total volume inoculant was used for all of the cultures shown in figure 3.7. The iron limited culture (4) displayed a notably slower growth rate compared to the other three cultures while the growth rate of iron limited culture (2) was the fastest, despite still being considerably slower than the iron replete cultures.

When deferoxamine chelates iron it produces a pale yellow colour at the concentrations of deferoxamine used in these growth experiments which resulted in the culture medium having a slightly pale yellow colour prior to inoculation. To ensure that this would not interfere with the spectrophotometric growth measurements, the absorbance of sterile ASW culture medium containing 200 μ M deferoxamine (the highest concentration used in any of the growth experiments) was measured using ASW medium without deferoxamine as a blank for the spectrophotometer. The ASW containing 200 μ M deferoxamine did not display any absorbance at 750 nm and therefore did not interfere in the determination of biomass.

*3.2 – Microscopic examination of iron replete and iron limited *Coccolithus pelagicus* cultures*

When iron replete and iron limited cells of *Coccolithus pelagicus* were examined under a light microscope at 630 x magnification it was found that there were some notable differences in the appearance of the cells.

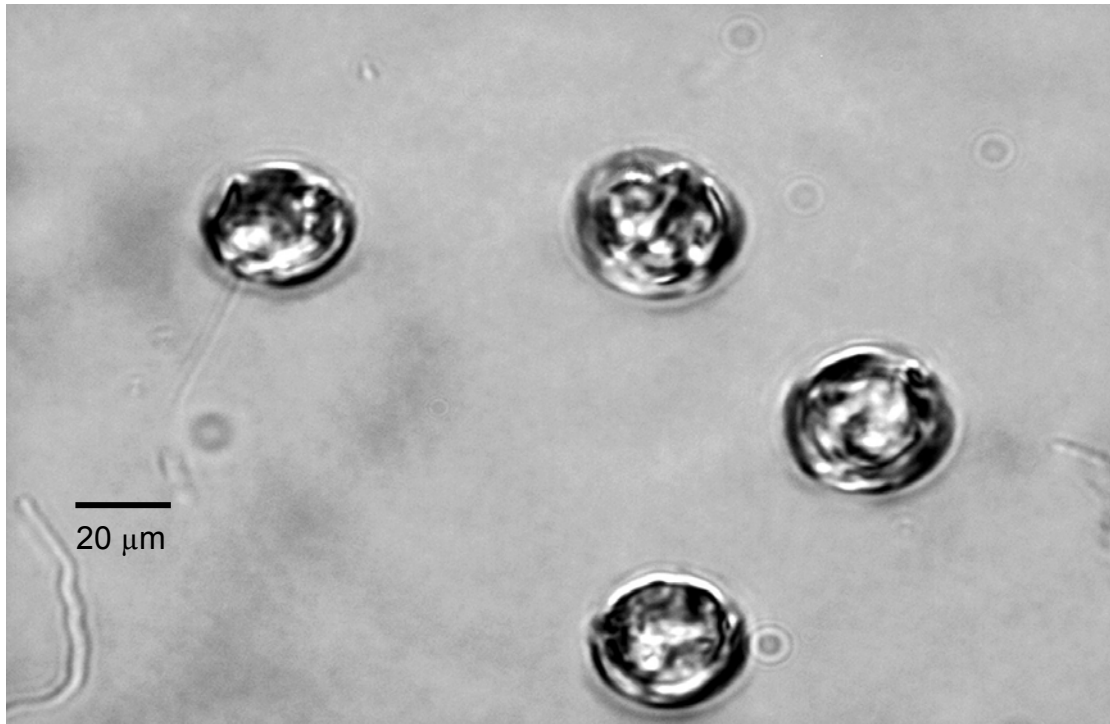


Figure 3.8: Micrograph of iron replete cells of *Coccolithus pelagicus* at 630 x magnification under a light microscope.



Figure 3.9: Micrograph of iron limited cells of *Coccolithus pelagicus* at 630 x magnification under a light microscope.

The iron replete cells shown in *figure 3.8* appeared more refractile than the iron limited cells displayed in *figure 3.9* which suggests that the iron replete cells were more heavily calcified. At least one of the iron replete cells in *figure 3.8* was motile, a flagellum can be seen protruding from the cell and pointing towards the bottom of the image in the cell toward the top left of the micrograph. By contrast, fewer flagellated cells were observed in the Fe limited cultures. The iron-limited cells also appeared to be of a more uneven shape perhaps indicative of incomplete or malformed coccoliths.

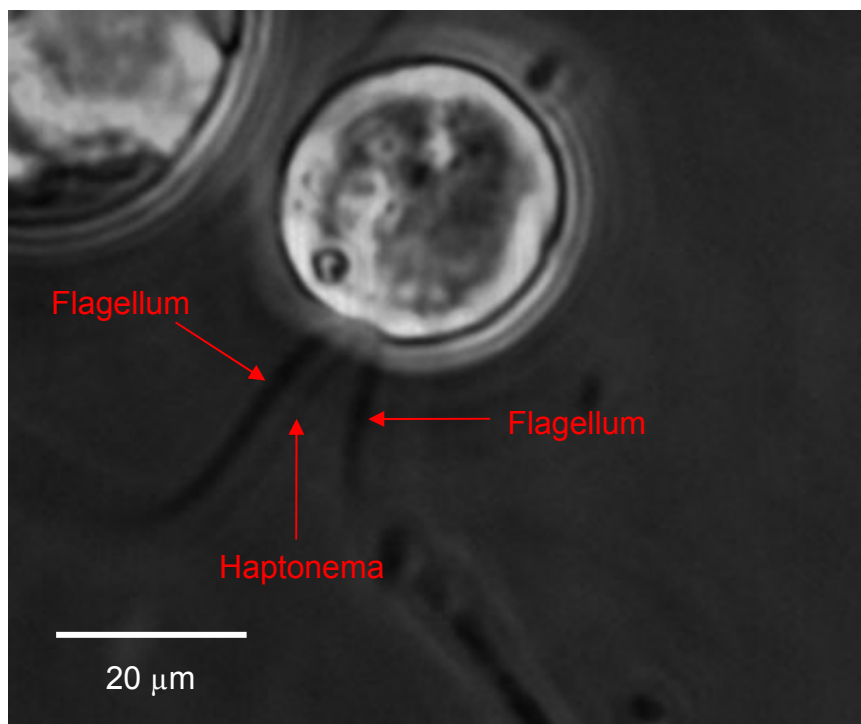


Figure 3.10: Micrograph of an iron replete cell of *Coccolithus pelagicus* at 630 x magnification under a light microscope. The two flagella and the haptonema are highlighted.

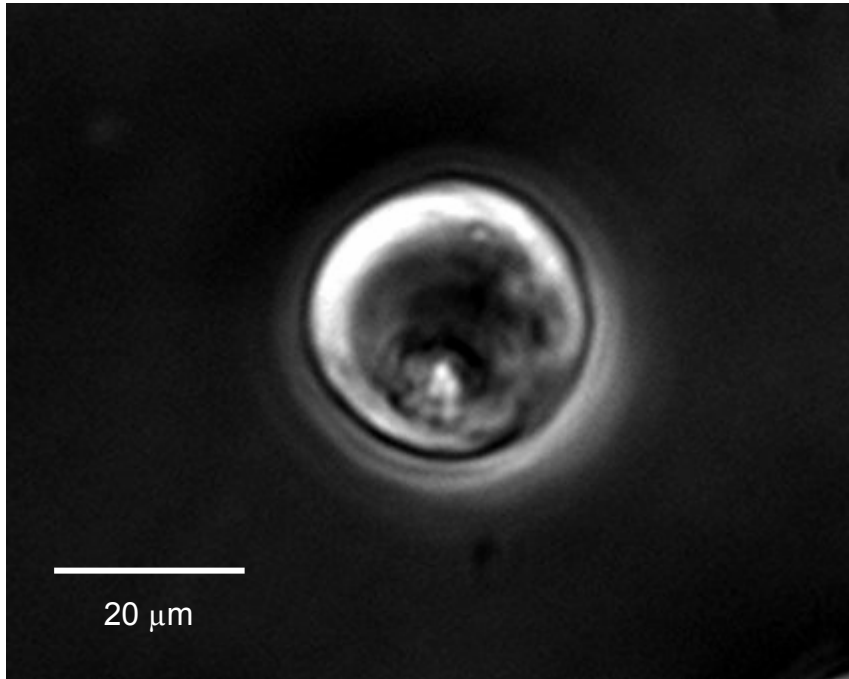


Figure 3.11: Micrograph of an iron limited cell of *Coccolithus pelagicus* at 630 x magnification under a light microscope.

A close up view of iron replete (*figure 3.10*) and iron limited (*figure 3.11*) *Coccolithus pelagicus* cells confirmed the structural differences between cells in each culture when examined under a light microscope. Paired flagella and a haptonema were immediately apparent in iron replete cells while these structures appeared to occur less frequently in cells from the iron limited culture. In the close up view of an iron replete cell shown in *figure 3.10* the paired flagella and central shorter haptonema are clearly visible, as was the case for many of the iron replete cells. In *figure 3.11* showing a close up view of a typical iron limited cell there are no flagella or haptonema present. Counts of flagellated / non-flagellated cells in the iron replete and iron limited cultures showed that cells with actively moving flagella occurred twice as frequently in the iron replete cultures as in the iron limited cultures. 18% of iron replete cells counted had moving flagella while in the iron limited cultures this was the case for only 9% of the cells counted.

3.3 - 1 Dimensional SDS PAGE analysis of *Coccolithus pelagicus* proteins

The change in the proteome between iron replete and iron limited cells of *Coccolithus pelagicus* was examined by means of 1-dimensional SDS-PAGE and 2-dimensional SDS-PAGE. Both 1D SDS PAGE and 2D SDS PAGE revealed that the proteome of iron limited cells had changed in comparison to the proteome of iron replete cells.

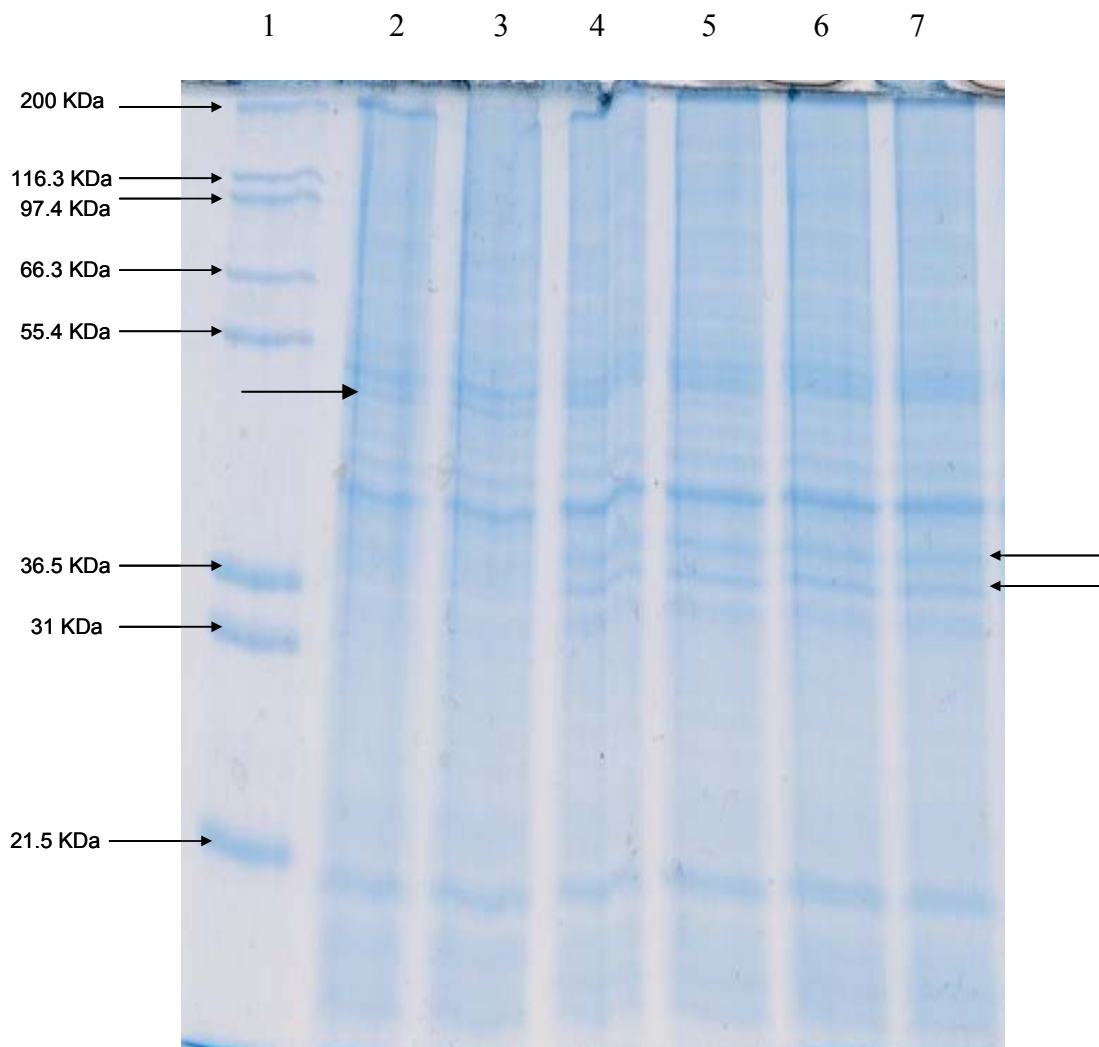


Figure 3.12: Coomassie blue stained 1D SDS-PAGE gel showing two proteins detected only in cells of four iron limited *Coccolithus pelagicus* cultures and one protein detected only in iron replete cultures. Lanes 1-7 contain the following: 1 = Mark 12™ protein standards, 2-3 = Iron replete cultures, 4-7 = Iron limited cultures. Arrows to the right of the image show two protein bands in iron limited samples that were present at lower concentrations or absent in iron replete samples. The single arrow on the left shows a protein band in the iron replete samples that was present in lower concentrations or absent from iron limited samples.

Several strongly stained bands of the same molecular weight were apparent in both iron replete and iron limited samples run on the 1D SDS gel. There were two obvious bands that were present only in samples from one of the culturing conditions. Two stained bands were observed at molecular weights of approximately 36-40 KDa in lanes that contained proteins from iron limited cultures. These bands could not be seen in the two iron replete cultures examined by means of 1D SDS-PAGE.

*3.3.1 - Two-Dimensional SDS PAGE analysis of *Coccolithus pelagicus* proteins*

Differences in the proteins present in iron replete and iron limited *Coccolithus pelagicus* cultures was further examined using 2D – SDS PAGE and 2D gels were analysed using the ImageMaster software. 2D gels showing the differences in the proteins present between the two culture conditions are shown on the proceeding pages:

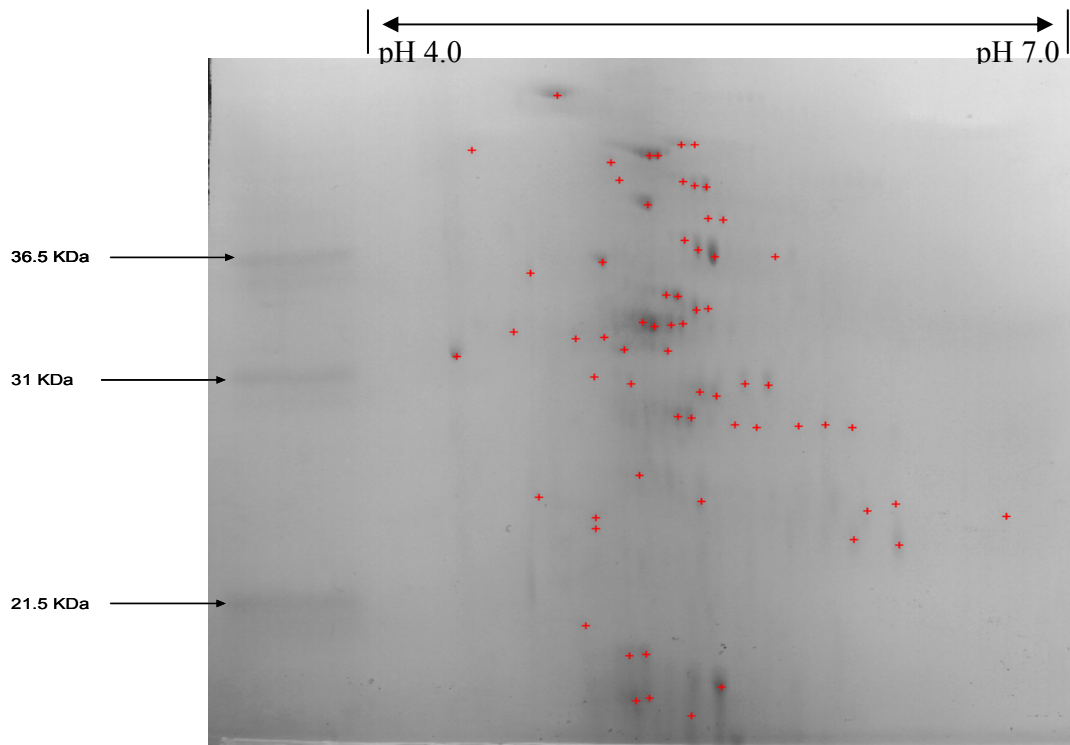


Figure 3.13: 2D-SDS PAGE gel showing proteins in the cells of an iron replete culture of *Coccolithus pelagicus* detected by the ImageMaster software.

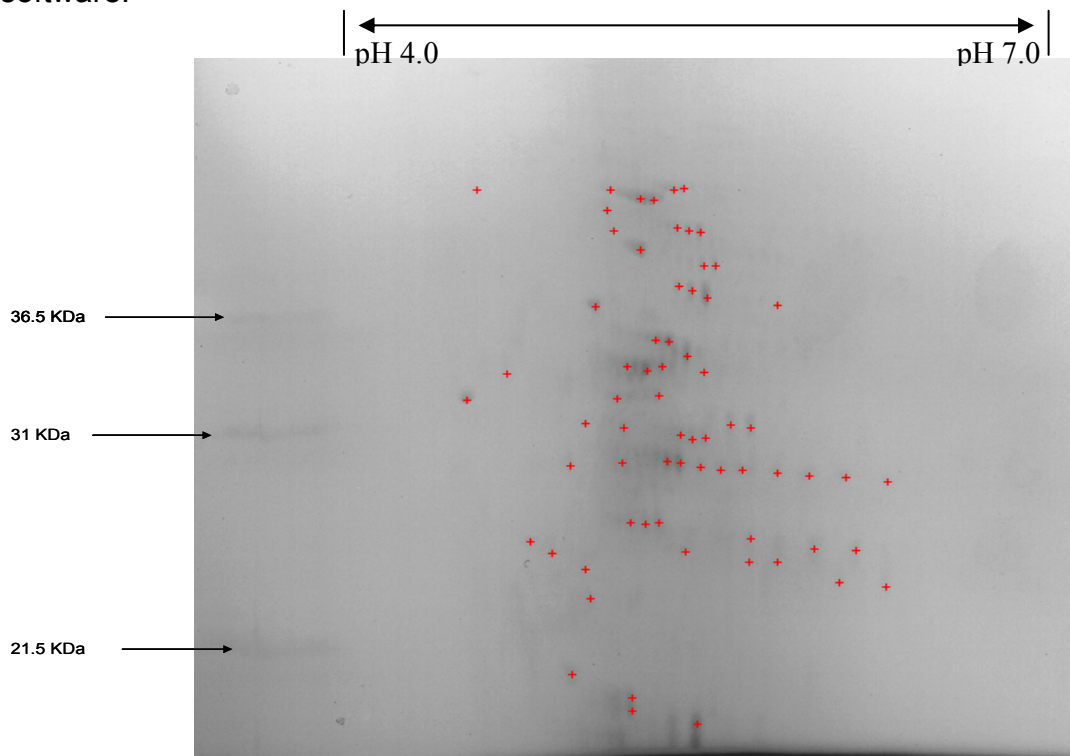


Figure 3.14: 2D-SDS PAGE gel showing proteins in the cells of an iron limited culture of *Coccolithus pelagicus* detected by the ImageMaster software.

The overall pattern of the protein spots detected on both the iron replete 2-D gel and the iron limited 2-D gel was similar, although there were a number of differences between the gels. These differences are highlighted in *figures 3.15* and *3.16*.

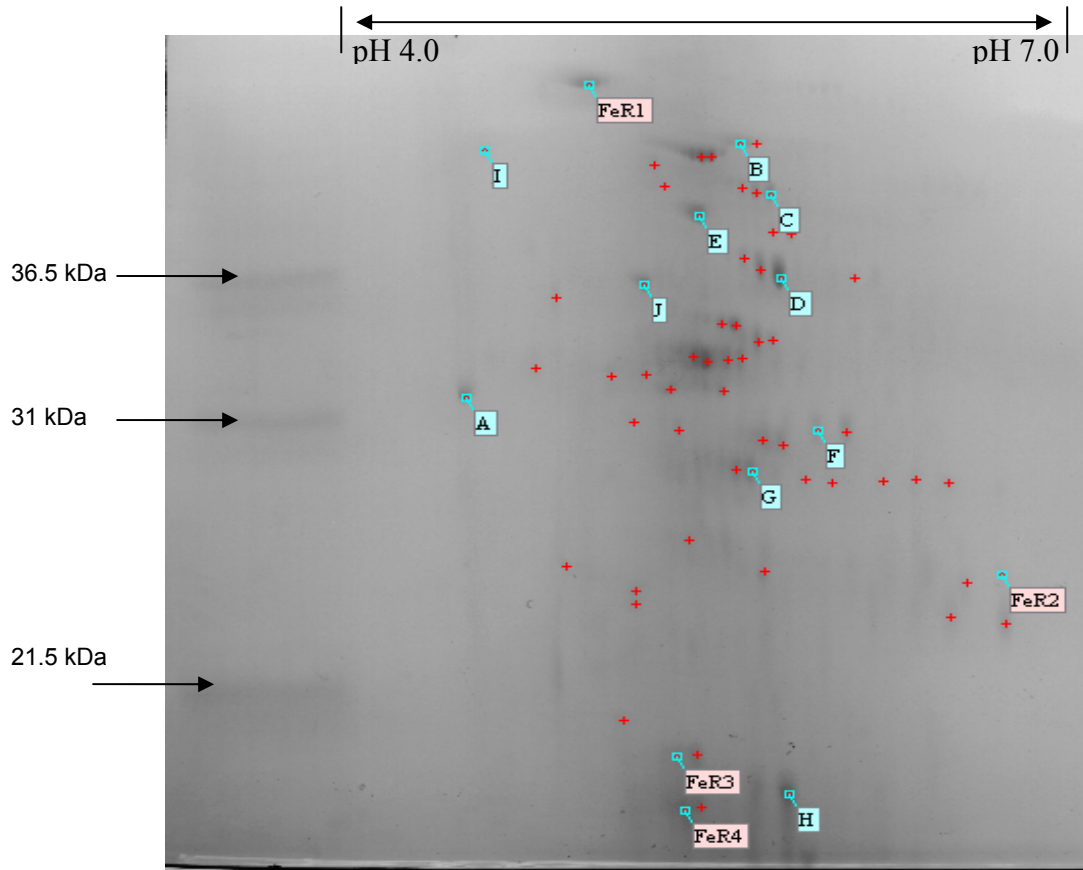
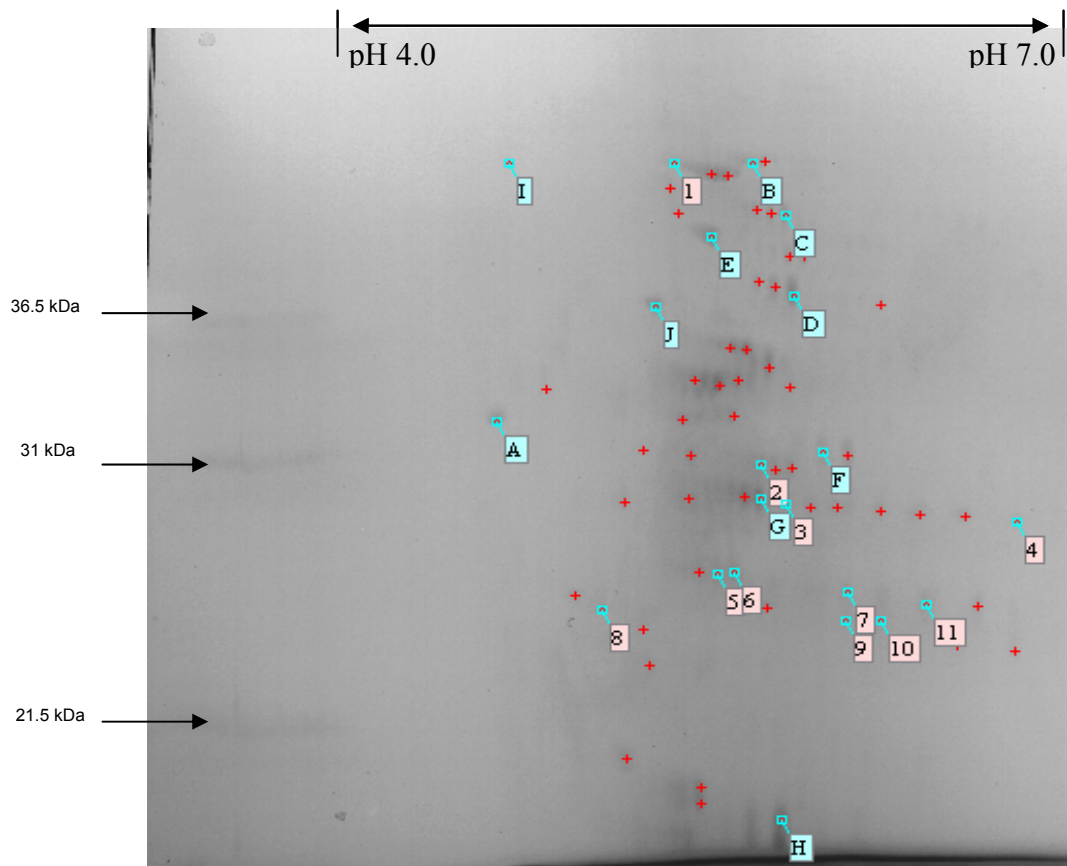


Figure 3.15: 2D-SDS PAGE gel showing proteins present in the cells of an iron replete culture of *Coccolithus pelagicus* with reference proteins annotated (A-J) and differentially expressed proteins annotated (FeR1-FeR4).

The iron replete 2D gel contained four differentially expressed proteins, and in particular the protein spot labelled FeR1 was prominent on the gel and was picked from the gel for sequencing at a later date.



*Figure 3.16: 2D-SDS PAGE gel showing proteins present in the cells of an iron limited culture of *Coccoolithus pelagicus* with reference proteins annotated (A-J) and differentially expressed proteins annotated (1-11).*

In total eleven differentially expressed proteins were detected on the iron limited 2D gel.

Protein spots annotated A-J were detected on 2-D gels showing total protein extracted from iron replete and iron limited *Coccoolithus pelagicus* cultures (*figures 3.15* and *3.16*) and they represent proteins present under both conditions. They were used as reference proteins to guide the ImageMaster software to overlay the gel images and match other protein spot pairs that were present in both gels. The protein spots annotated FeR1 – FeR4 in the iron replete gel (*figure 3.15*) and the protein spots annotated 1 – 11 in the iron limited gel (*figure 3.16*) are differentially expressed proteins detected by the ImageMaster software and confirmed by visual inspection.

The protein spot annotated FeR1 in the iron replete gel (*figure 3.15*) is intensely stained and is clearly not present in the iron limited gel (*figure 3.16*). The protein FeR1 is a clear indication that the proteome of iron replete *Coccolithus pelagicus* cultures differs from that of the iron limited cultures while the presence of the differentially expressed proteins A-J shows clear evidence of changes in the expression in at least 11 distinct proteins in iron-limited cultures.

3.3.2 - Mass spectroscopic analysis of iron replete protein spot FeR1 and western blotting

The most prominent protein (FeR1) present in the 2D-SDS PAGE gels (*figure 3.15*) was extracted from the gel and subjected to mass spectroscopic analysis (1D nLC-MS-MS) in an attempt to identify the differentially expressed iron replete protein. The mass spectroscopy results (data not shown) were ambiguous and several possible identities were obtained for the extracted protein spot. Upon further analysis of the results it was determined that only one of the possible identities; actin, fell within the criteria that could be discerned for the 2D-SDS PAGE analysis. All of the other possible identities suggested by the mass spectroscopic analysis were eliminated on the basis of their molecular weight, isoelectric points or if they were most likely to be a contaminant resulting from the extraction of the gel spot or the subsequent trypsin digest and analysis.

In order to confirm that the extracted protein spot was actin western blots were performed using a commercially available anti-actin antibody (*figure 3.17*). Even under stringent experimental conditions it was not possible to eliminate all background from the western blots. The available antibody bound several protein

bands in both the iron replete and iron limited sample lanes and also bound to some of the standard markers. Increasing the stringency of the experimental conditions resulted in no detectable antibody binding. The poor quality of the available antibody, in particular its lack of specificity, led to ambiguous western blot results and thus it was not possible to confirm the identity of the extracted protein spot as actin. A primary antibody dilution of 1:400 provided the best, yet highly ambiguous and inconclusive results.

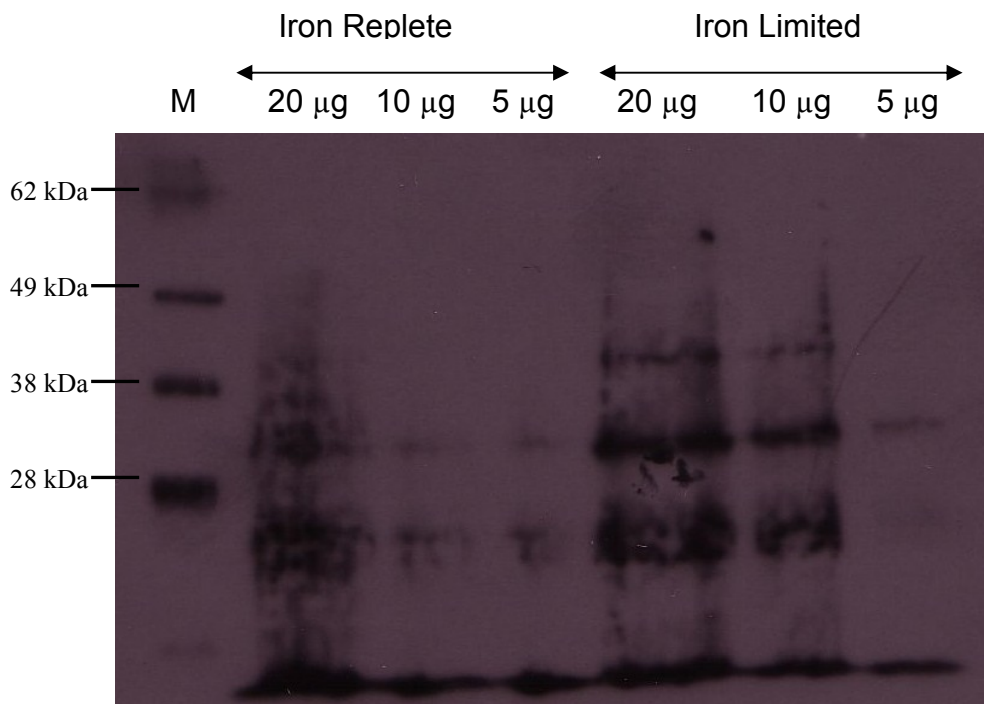


*Figure 3.17: Western blot showing crude cell extracts from iron replete and iron limited *Coccolithus pelagicus* cells probed with rabbit anti-actin antibody (1:400), (secondary antibody – goat anti-rabbit HRP, 1:10,000). 3 lanes were loaded with 20 µg, 10µg and 5 µg of iron replete protein, and another 3 lanes were loaded with 20 µg, 10µg and 5 µg of iron limited protein. M = SeeBlue® pre-stained standard protein markers (Invitrogen™).*

3.4 – Discussion

The results from the growth experiments demonstrate that the use of deferoxamine to chelate iron in growth media is an effective method of producing iron limited cultures of *Coccolithus pelagicus*. Deferoxamine overwhelmingly chelates iron and earlier studies suggest that it has no impact on the uptake of other biologically important metals (Wells, 1999). To date it has not been reported as being detrimental to the growth of phytoplankton in laboratory or field studies, other than growth inhibition resulting from its ability to chelate iron (Hutchins *et al.*, 1999(A) Wells, 1999; Eldridge *et al.*, 2004; Naito *et al.*, 2008). During ship-board laboratory studies in which deferoxamine was added to size fractionated samples of natural phytoplankton communities it was found that while iron uptake rates slowed, short term uptake of carbon was not affected even at the somewhat higher concentrations of deferoxamine used in the study (500 nM). This suggested that the inhibitory effect of deferoxamine on phytoplankton productivity was not due to general toxicity (Wells & Trick, 2004) but was a sole consequence of its effective chelation of iron. The same study found that across all phytoplankton size classes the addition of 3 nM deferoxamine to natural populations reduced iron uptake rates by at least 90% relative to that of controls with no chelator added. Interestingly, the iron uptake rates in the larger size class (>5µm) were more severely reduced by deferoxamine, while the smaller size class (>0.2 – 5µm) appeared to be able to access deferoxamine bound iron to varying extents. This suggests that deferoxamine may be a particularly suitable chelator for studies of iron limitation in the larger eukaryotic phytoplankton as was found to be the case with *Coccolithus pelagicus* in this investigation. Furthermore, it has been reported that addition of deferoxamine to samples of natural iron replete

phytoplankton communities results in changes in biological parameters including biomass and nutrient concentrations which are similar to those observed in iron limited populations in high nutrient low chlorophyll areas (Hutchins *et al.*, 1999(A); Wells, 1999; Eldridge *et al.*, 2004). At least with the larger size classes of phytoplankton, deferoxamine appears to be an effective means of mimicking low iron levels in the marine environment within a laboratory setting.

The considerably reduced specific growth rates observed in *Coccolithus pelagicus* grown in the presence of deferoxamine suggest effective iron limitation was achieved in this study. Deferoxamine-treated cultures also display proportionately lower chlorophyll concentrations per unit biomass than their iron replete counterparts and it was found that lower specific growth rates were overcome upon alleviation of iron-limitation through iron supplementation. The change from reduced to higher specific growth rates and from low to higher chlorophyll concentrations per unit biomass in iron limited cultures after iron addition strongly indicates that it was the relative unavailability of iron in the medium rather than any other factor such as deferoxamine toxicity that produced the differences between the iron limited and iron replete cultures.

The observation that iron replete cells have a different microscopic appearance compared to iron limited cells both in the apparent extent of calcification and in the irregularity of the shape of iron limited cells, further suggests that there are significant differences between the cells under the two conditions. The larger number of iron replete cells possessing moving flagella may be indicative of a larger proportion of cells being in the motile phase of the *Coccolithus pelagicus* life cycle.

The smaller proportion of flagellated cells in the iron limited culture may also reflect a need to conserve energy when a reduced concentration of iron is available. The operation of a flagellum is a metabolic process that demands a great deal of the cell's energy and elimination of this organelle may represent a considerable energy saving to iron limited cells. As iron limited cells are essentially energy limited owing to the critical role of iron in both photosynthesis and respiration, the additional energy demands of maintaining an active flagellum may render it un-sustainable in cells unable to operate at their metabolic optimum.

Coccolithus pelagicus is known to have a non-motile haploid phase in its life cycle which is less calcified than the motile diploid phase (Rayns, 1962). Therefore, one reason for the difference in microscopic appearance observed in deferoxamine-treated cultures is that a higher proportion of the cells are in the non-motile haploid phase in comparison to iron-replete cultures. Maintaining cells in a haploid phase of the life cycle offers a potential means of conserving energy in iron limited cells, owing to the reduced biosynthetic costs associated with maintaining a haploid genome.

The eleven differentially expressed proteins detected in the iron limited 2D gel and the four differentially expressed proteins in the iron replete 2D gel in conjunction with the differences observed on the 1D SDS gel confirm that the proteome of the cells is different between the two growth conditions. This proteomic evidence in conjunction with optical density, chlorophyll *a* concentration measurements, iron addition experiments and microscopic observation confirms that *Coccolithus pelagicus* cultures grown in *f*/2 enriched ASW media in the presence of 150 μ M deferoxamine

results in a level of iron limitation sufficient to cause changes at the molecular level and provides suitably iron limited cells for further study.

Due to its greater specificity deferoxamine was selected as the preferred iron chelator to be used to produce iron limited cells for this study. EDTA was also effective at producing slower specific growth rates and lower chlorophyll concentrations relative to iron replete controls, but it was required at far higher concentrations. This was probably due to the fact that EDTA not only chelates iron but also chelates other divalent cations while deferoxamine has an overwhelming affinity for iron. Some of the additional EDTA will chelate copper, manganese, magnesium and zinc for example, which may account for the far higher concentrations of EDTA needed to produce the same extent of iron limitation that is observed when deferoxamine is used. EDTA is a less suitable chelator for studies of iron limitation in *Coccolithus pelagicus* as the promiscuous nature of this chelator and the millimolar concentrations required in order to cause significant iron limitation mean that changes in gene expression due to chelation of other trace metals cannot be ruled out. Nevertheless, a number of previous studies of iron-limitation with both natural populations and laboratory cultures have used EDTA as a chelator (reviewed by Gerringa *et al.*, 2000) Although using deferoxamine in growth media to chelate iron was consistently effective at producing iron limited cultures of *Coccolithus pelagicus* there was variability between cultures in terms of the severity of iron limitation observed. The severity of iron limitation was judged based on the specific growth rates of cultures, slower specific growth rates indicating more severe iron limitation. Specific growth rates varied over a range of 17% between the iron limited cultures used to produce cDNA for real time PCR experiments and this variation was evident in the gene

expression data obtained using RT real time PCR (see chapter 5). When dealing with low concentrations of trace metals such as iron it is often difficult to maintain equal concentrations in all cultures. When cultures are sampled for growth measurements, for example, dust from the air can contribute additional iron to the media. Despite minimising contamination through the use of aseptic technique and acid washing glassware that was used in the preparation of growth media, it was difficult to completely eradicate all contaminating trace metals from the growth media. When these factors were considered, a variation of 17% in specific growth rate over the range of iron limited cultures used for experimentation was deemed to be acceptable. Even the most rapidly growing of these cultures were still growing far more slowly than the iron replete controls.

Although the 2D gels showed that eleven novel proteins were present in the iron limited cells, none were present at high concentration making them difficult targets as a biomarker. By contrast FeR1 would be a good candidate protein as a marker of iron replete cells although at the time of analysis this was not the main objective of this study. The sensitivity of the Colloidal Coomassie stain is within the range of 38 ng per band or 250 ng per mm². This stain was selected for use as opposed to the more sensitive silver stain, as silver stain makes mass spectral analysis impossible. The sensitivity of the Colloidal Coomassie blue was deemed sufficient to detect proteins which would be present in concentrations high enough to make them suitable potential biomarkers for iron limitation, worthy of further investigation. Any protein present at concentrations below the threshold of Colloidal Coomassie blue sensitivity are unlikely to prove good biomarkers for iron limitation owing to the fact that an

ideal biomarker should show a large difference in abundance between the two iron conditions.

Chlorophyll *a* concentrations per unit biomass did not appear to remain constant throughout the duration of iron limited growth. This may indicate that iron limited cells of *Coccolithus pelagicus* prioritise cell division over chlorophyll *a* biosynthesis under these conditions. If there is a reduction in cell size and an increase in the ratio of accessory pigments : chlorophyll *a* this may allow the cultures to continue growing with reduced chlorophyll *a* concentrations and account for the trend observed. A reduction in chlorophyll / cell of up to 54% has been reported for *Thalassiosira weissflogi* grown in EDTA buffered seawater with iron additions across a range of 10 – 1000 nm (McKay *et al.*, 1997). This is consistent with the findings for *Coccolithus pelagicus* in this study. After an initial increase in chlorophyll per unit biomass upon inoculation into fresh growth media, there was a relatively rapid decline in the cultures grown at low iron concentrations as cells divide but were unable to rapidly synthesise chlorophyll. Reduction in cell size in response to iron limitation has been reported in other species (Stefels & van Leeuwe, 2002, Leynaert *et al.*, 2004). A moderate reduction in the chlorophyll *a* concentration per unit biomass over time was also observed in the iron-replete cultures but this is unlikely to be the result of an inability to produce chlorophyll over the period of growth. It may be the case that shed coccoliths affect the optical density measurements and exaggerate the cell number to an extent sufficient to slightly skew the chlorophyll *a* per unit biomass measurements. It may also be the case that at later stages of growth another nutrient in the iron replete cultures becomes limiting due to rapid growth of the cultures,

resulting in lower chlorophyll biosynthesis but not affecting cell division as appears to be the case for iron limited cells at a much earlier point.

Highly ambiguous western blot results made it impossible to confirm the identity of the iron replete protein spot FeR1 (*figure 3.17*). Actin was pursued as a possible identity for the differentially expressed protein because it most closely fitted the criteria that could be observed from the 2D SDS gel from which it was obtained. Human actin is approximately 43 kDa and isoelectric points of the various isoforms range from 5.4 to 6.0, this is similar in other species ranging from mammals to slime moulds (Zechel & Weber, 1978). Unfortunately the commercially available anti-actin antibody appears to have poor specificity and may be binding to several different actin isoforms in the western blots. The antibody also bound many of the marker proteins in the blots even under stringent conditions which further illustrates its lack of specificity. The amino acid sequence for actin is unusually well conserved throughout different organisms, ranging from humans and other animals to plants and unicellular organisms (reviewed by Sheterline & Sparrow, 1994). It is likely this high degree of sequence conservation that reduces the ability of any anti-actin antibodies to distinguish between different actin isoforms. Until such time as a better quality anti-actin antibody is available it may prove difficult to achieve conclusive western blot results for protein spot FeR1, if it is in fact actin.

Chapter 4 – Analysis of differentially expressed sequences in the iron replete and iron limited subtracted libraries.

4.1 – Chapter introduction

In the proceeding chapter the results obtained from sequencing the iron replete and iron limited subtracted libraries are presented and analysed. Sequences unique to either the iron replete or iron limited subtracted libraries were subjected to BLAST analysis in an attempt to identify or assign a putative identity to each. Only a fraction of the sequences from the iron limited subtracted library could be identified with a degree of confidence and an overview of the iron limited subtracted library is given here. The relative proportion of each identified sequence as a fraction of the entire subtracted library is presented. The subtracted iron limited cDNA sequences are presented alongside their BLAST analysis results and the implications of the assigned identities are discussed. Multiple sequence alignments that were used to design degenerate primers to target the GAPDH and flavodoxin transcripts (Chapter 5) are also shown.

4.1.1 – Composition of the subtracted cDNA library

Nucleotide sequences obtained from the iron replete and iron limited subtracted libraries returned a variety of hits with acceptable e-values from the NCBI database upon being subjected to BLAST analysis. Both the Blastn and BlastX analysis tools were used to identify the sequences. While there were several BLAST hits which provided strong matches to sequences in the NCBI database, most of the sequences in

both the iron replete and iron limited subtracted libraries returned no significant matches, hits on hypothetical proteins or whole genomes from algae and higher plants. In total, 272 clones from the iron limited subtracted library and 48 from the iron replete subtracted library were sequenced successfully. BLAST analysis of the iron limited subtracted library returned results with the following composition:

Significant matches to known proteins or sequences in which conserved domains were detected.	36.4%
Matches to hypothetical proteins, genomes, or sequences which returned no hit.	63.6%

Table 4A: Table showing the overall sequence composition of the iron limited subtracted library.

A significant Blast hit was considered to be a hit on a sequence of known function with an e-value of 0.1 or less or the detection of conserved domains. Hits on hypothetical proteins or genomes with any e-value were not considered any further. The sequences analysed further using RT real time PCR (chapter 5) accounted for 19% of total number of sequences from the iron limited subtracted cDNA library. Several hits appeared frequently within the iron limited subtracted library (Figures 4.1 and 4.2). The following sequences were the most abundant among the sequences which returned significant hits upon Blast analysis, *Table 4B* shows the full name of each sequence alongside the abbreviation used to refer to it:

Gene identified in subtracted cDNA library	Abbreviation used throughout text
20S Proteasome subunit	20S Prot
Chlorophyll light harvesting protein isoform 2	Chl LHP
Protein containing a cytochrome b5 like heme / transition metal binding domain	Cyt b5
Ubiquinol-cytochrome c reductase binding protein	Cyt bc1
DnaJ heat shock response like protein	DnaJ
Chloroplast light harvesting protein isoform 8	CM4E12
Predicted membrane protein	PMP
Chloroplast photosystem I protein E	PsaE
Thioredoxin h	Thio
Ubiquitin-conjugating enzyme E2	UCE
Fucoxanthin chlorophyll <i>a/c</i> binding protein	FucoBP

Table 4B: List of the full names of identified sequences in the iron limited subtracted library and the abbreviated names used to refer to them throughout the text and in figures 4.1 and 4.2.

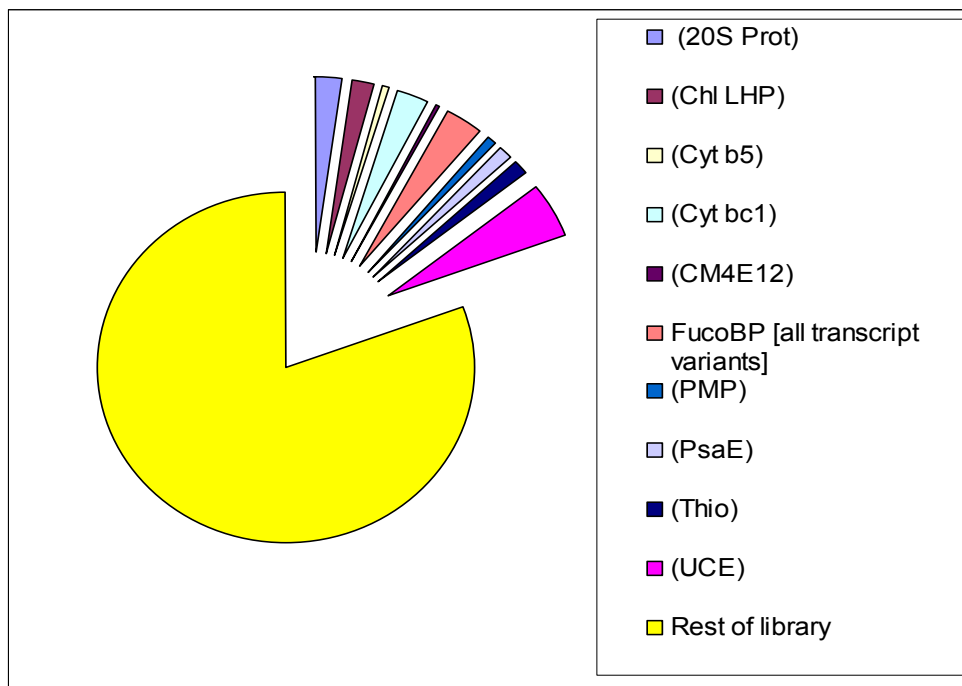


Figure 4.1: Relative proportion of each RT real time PCR analysed iron limited sequence in the iron limited subtracted cDNA library. The abbreviations used to identify each sequence are listed alongside the full sequence name with the nucleotide sequences listed in section 4.1.1.

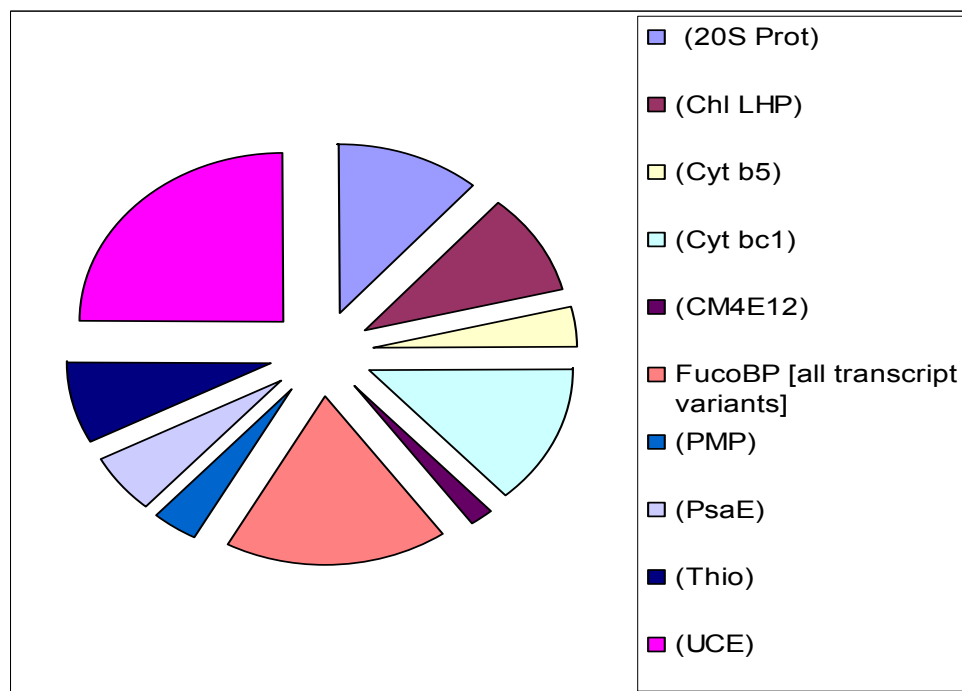


Figure 4.2: Relative proportion of each RT real time PCR analysed iron limited sequence within the 19% of the sequences in the library that were examined. The abbreviations used to identify each sequence are listed alongside the full sequence name with the nucleotide sequences listed in section 4.1.1.

Ferredoxin cDNA was detected once in the iron replete subtracted library but not in the iron-limited library.

4.1.2 – Blast analysis of the subtracted cDNA library

Details of sequences obtained from the iron limited subtracted library and their corresponding Blast analysis results are shown below. The top Blast hit is shown. If this was a hypothetical protein the next Blast hit showing an identified protein and having a significant e-value is also shown with the source organism:

Fucoxanthin-chlorophyll *a/c* binding protein (FucoBP): Blastn

GAATTCGCCCTTAGCGTGGTCNCGNTCCGAGGTACATTATCAACGACCTGCTCGGCG
CCCCTGTGCCATTCAATGTTGGCTTGTAAGCAACCGTTGTCCCTCAGCTTGGGGTC
GGTGGATATCGAAAGCCTTCAGCCTAAAGCTTCTGCTGGCTGACACCAAGCGTTGTG
AGAGTGTCCATGAACTTATTCTATCCATGTTACCTTTTGCACCTTGATTACGCCCTA
AACTGGCATTGCCGTTAAAACGACATGACCTTCCGAAAAAAAAAATAAAAAAAAAA
AAAAAAAAAAAAAAAAAAGCTTGANCTGCCCGGGCGCCGCTCGAAAGGGCGAATT
C

[AB240951.1](#) mRNA for fucoxanthin chlorophyll *a/c* binding protein [Pleurochrysis carterae]

5e-10

20S Proteasome subunit (20S Prot): BlastX

GAATTCGCCCTTAGCGTGGTCCCGNCCGAGGTACATGCGCACGGAGTGCATCAACCA
CAGATATGTCTATGAACAGCCGATGCAAGTTGGCCGCTTGTGACGCAAGTGGCTGA
CAAGTCGCAGCTAGGCACACAGCGTATCGGCAGCCGCCATACGGTGTTCGGTCTGCT
TGTCGCTGGCGTGGATCAAACCGGACCTCATCTGTATGAGACGCAGCCCTCTGGGCA
GTACCTGCCCGGGCGGCCGCTCGAAAGGGCGAATTC

[ref|XP_001770750.1](#) predicted protein [Physcomitrella patens subsp. Patens]

1e-20

[ref|XP_001691250.1](#) 20S proteasome alpha subunit F [Chlamydomonas reinhardtii]

3e-19

Chloroplast light harvesting protein isoform 2 (Chl LHP): BlastX

GAATTCGCCCTTAGCGTGGTCGCGGCCGAGGTACATCCTACCATGAAATTGATGGAG
TGCTATGCTGAAACAGATGAAAATCGACGATGCCATGTTTGTGTTCCGTGAGATTCA
GTGCATGATGCGGGTTGGTGCACCTCGAGGCCAGCTGTCAACCAAGTCGATTAAGACA
ATCGAAGTAGATTTAGAGTAGCTTGCCGCCGGTTCGCGAGCTCCTGCCCAACCATGCC
GGCGATGGCGAACATAGCCAGGCGGCCGTTATTTCAGCTCCTTCGTTGCCAGGTTCTT
GTACCTGCCCGGGCGGCCGCTCGAAAGGGCGAATTC

[gb|ABA55555.1](#) chloroplast light harvesting protein isoform 2 [Karlodinium micrum]

3e-05

Protein containing a cytochrome b5 like heme / steroid / transition metal ion binding
domain (Cyt b5): BlastX

GAATTCGCCCTTTCGAGCGGCCCTTCNGGCAGGTACGTCTCGTGCTTCTGATAAAA
CCCGTGCCACTCAGCGATCCCGCCAAGCTGCTCGTCGGTGAGACCGTCAATCGCATC
AGTAAGGCCCTCTGGTGACGATTCTCCCGTTGAAAAAGCGCGTGTGGCATCACGGCC
AACAAAATGCGCATATGAGCGACCGGCCTTATAAAATTTTGCACCTGTGTTACAGTC
GAAGATGTCTCCGATGATTGCAATGTAAATGGGCTGTCCGTTGAGGCCATTGAACAG
CTTGAGTTCGTCGGTAGTGAAAATGCGAGTTCGTCATGCCTATACGAGCTTTGGG
ACGCATGGCGCGAGCAAGCATCGGAGAAGCAACAAGCACAGCAACGGCAAGAACCAC
TGCTGATGTGGCCGCGACCACGCTAAGGGCGAATTC

[gb|EEC06067.1](#) cytochrome b5 domain-containing protein, putative [Ixodes
scapularis]

3e-17

[ref|NP_567451.1](#) ATMAPR4 (ARABIDOPSIS THALIANA MEMBRANE-
ASSOCIATED PROGESTERONE BINDING PROTEIN 4); heme binding /
transition metal ion binding [Arabidopsis thaliana]

3e-16

Ubiquinol-cytochrome c reductase binding protein (Cyt bc1): BlastX

GAATTCGCCCTTTCGAGCGGCCGCCCGGGCAGGTACTTGCTCATCTCGTGCTGACGT
GAGGAATTTATTCATCTCGTGCTGACGTAAGGGAATATCCGGGCAGCGTCCTTTACT
TGAGGTAGTACTCTTTCTTCTCCTGCTTACCTCGTCCAGGTACGGCGCCAAGTACG
AATCATAGGGATCGTACGCACTCGCGATCTCAAGCGGGAGCTCCTTGTGGGCGGGCGG
AGAGCATCATCGCGCGCTTGAGCCGCTGCTCGCGCGGACGAGGAGCGGCTCGGGCA
GCCGCTTCAGCGCAAGCTTACCTCCTCCGTCTCCACCAAGGAGTCCTCGTACATGA
GGCCGTAGCGGGAGAGTTCCC GGCCGACCTCGGCCGCGACCACGCTAAGGGCGAATT
C

[ref|XP_001505521.1](#) PREDICTED: hypothetical protein [Ornithorhynchus anatinus]

(platypus)

2e-10

[ref|NP_001125376.1](#) ubiquinol-cytochrome c reductase binding protein [Pongo

abelii] (Sumatran orangutan)

4e-10

DnaJ heat shock response like protein (DnaJ): BlastX

GAATTCGCCCTTTCGAGCGGCCNCCCGGGCAGGTACGCGGCCTTGAGGGCAAGGAAA
GCCTCATCCCCCTCGTCTTCTAAACCCGCGGGCGGCGAGCTTATCGGGGTGCACGCGC
AGAGACGCGGTCTTGATGCCCTTCTTGATCTCTTGCAAGGAAGCACTCGGAAGCACA
TCCATCATGTCATAGTAGCTCTGATCCTTGTTTCATCAGCTCCAGCCAATTTTCACT
GATGCAACTATAGCGAGCAGGCCGCCGAAAGAGCCACGGCCTTGCGGCGGTTTCCG
TCCTTACGACACGCGGTGAGGTCATCAAAA ACTCCAAAGGTACCTCGGCCGCGACC
ACGCTAAGGGCGAATTC

[gb|EEC51869.1](#) predicted protein [Phaeodactylum tricornutum CCAP 1055/1]

3e-05

[ref|NP_001020582.1](#) DnaJ (Hsp40) homolog, subfamily A, member 4 [Rattus

norvegicus] (Norway Rat)

1e-04

CM4E12 - Chloroplast light harvesting protein (CM4E12): BlastX

GAATTCGCCCTTAGCGTGGTCGCGGCCGAGGTACCAGCTGCCTGGCACCGTTCTCGG
CCAGCTGATGTTTTCCATTGCCGTCGCTGAGGGCATCCGCGGCAGCATTATTTACAA
GAAGGACTCCGTCCCAGGCGAGCACGGCTTTGACCTGCCGGCTTCATCCCCAAGTT
CTGCAACACACCTGAGAAGATGGCCGAGATGAAGCTCAAGGAGCTCAAGCACTGCCG
CATTGCCATGATTGCTATCACTGGCTTCTTCTTCCAGGAGACCATCACCGGCCATGT
TGTGCCGTTCTTTAAACTATTGAAGCTGCTAATTTCCACTAATTTCCGTATTAGGG
TTTGAGCCCAGACGTGGAAGTCCAGCGGTTCCCCTTGAATGCTGTGACTGGCTCT
TCAAGTCTCTCCAGAGCCGGCGGCAGACCGGCATGGAAAGTCTCGACCTGTGATTTT
TGTACCTGCCCGGGCGGCCGCTCGAAAGGGCGAATTC

[gb|ABA55524.1](#) chloroplast light harvesting protein isoform 8 [*Isochrysis galbana*]

e = 0.037

Predicted membrane protein (PMP): BlastX

AGCGTGGTCGCGGCCGAGGTGCGACAGCNTNNCGGACTCGACGCCACAAGCGGAGTA
GCGGCAGCAGCGGCTGTAGCATTGGAAGGGACTGCTCCTGCACACGCTGGGATGGGC
ATTCATCAGATGTCGACCGGCTCAGGCTCCTCATTCTGCCCTGTGCGCTGGCACTG
CAAGCTGCGCATCTACCAGCTACACACCTCATGCACGCGCAAGGCATGGGTGTGCCA
AAGTTGGCCACTGCCCCGACGCTTTCGTCTGTGAGCCTTCGAGTCAAATCAGATTCT
GAAAAGGTCACCAAAGATCCCAGCGGAGGTCCTGAGAAGTTCGGGCTGGAGGCAGGC
TTGTTTTCTGCTGCAAAGGGCAAGGACATGTCAAAGCGGGTGATCTGCTCAAGCAG
TATGGCGGGGCATATCTCCTGACCTCCATTTCTCTCGCGCTCATCTCTTTTTCTCTG
TGCTACTTCGCGATTGATCGAGGTGTCGATGTGGCTGCGTTGCTGCAGCGAGTCGGA
ATCGAGGTCAGTACCACCTCAGAGACCGTGGGGACCGTGGGCATCGCGTATGCTATC
CACAAGGCTGCGTCGCCGATCAGGTTCCCAGCAACCGTCCGCGCTCACTCCCATCGTA
NCCCGTAAATTTTTTGGCCAGAAGGATGCTGACAAAAGTATTAGGAGAGCCGGTCT
CAATGAAACTCAAGTTGGACGGCTTTGTGACGGCTGCAAGCGGCTTCGTGTCTCTTT
GCCAAGTCGACTGCATGCTTTTGTGAGTGAAATGTTTTGGCTTGTCTTCGTTGAATN
ANACTGNCGTACTTGAACCCGCCTAAAATAAAATCTGGGGTTGGAAAATAGGGGTCT
ATTGTTTCTGTAAACGGGAAATTGNAGCGAANTCGAANTTTCCGAAAAAAAAAAAAA
AAAAAAAAAAAAAANTTNTACCTGCCCGGNGGNCGNCA

[emb|CAO48682.1](#) unnamed protein product [*Vitis vinifera*]

1e-25

[emb|CAL57011.1](#) Predicted membrane protein (ISS) [*Ostreococcus tauri*]

6e-20

PsaE (PsaE): BlastX

GAATTCGCCCTTTCGAGCGGCCGCCCGGGCAGGTTCGCAGACGCAGCCAGCACCGCCG
CAGCCATGCTTCGCTCCATGATCATTGCCGCGCTCTGCGCCGTCTGCGCTGCCTTCA
CGCCCAACTCGGCCATGCACGCGACACGCAGCACTGTCTCTGCGCAGTCTATCCAGA
TGGTCTCGCGTGGCTCCGTGGTGCCTGTGATGCGGCCGGAGTCGTAAGTGGTTCCAGG
AGACCGCACTGTTGCGACGATTGCCAAGGGTGGCGACAGGTACCCTGTTGTGGTTC
GCTTTGACAAGGTGAACTACGCTGGCGTTCGCGACGAACAACCTTCGCTGTTGATGAGC
TGGTGGAGGTGTCTGCGCCGGCTCCGAAGCCAGCTGCCAAGTCTGAGTAAATATGTG
ACCTGCAAAATATTCAGGCTCCATGGAATTGCGTTGACTATATTACATTCTTCACTT
GAA
AAAAAAAAAAAAAAAAAAAAAAAAAAAAAAAAANGNTTGTACCTCGGCCNANCANNTAAGGGN
NAATTN

[gb|AAW79344.1](#) chloroplast photosystem I protein E [Isochrysis galbana]

3e-22

Thioredoxin (Thio): BlastX

GAATTCGCCCTTAGCGTGGTCGCGGCCGAGGTACATACTCGTGCTGTCCAGGTGCCA
TCAGTAGTGTAAGTCTGATCCGCAAGCGACCATTCCGAGCAAGGCACCCTGGTATGC
CCGCTAGTTGTTGCGCAGACATCAAGCTAAATCAGCCACAGCAGACCCGGAGCTTTGC
CTCGTCAGCACCTTTTACGACGTTTACGATCTCTCCGTTTCGCCAAAATTGAAATGT
TGGCATCGAGCTCACACCGAGGTCGGCAGCCAGTTCGCCAGCTCATCCACGTCGAT
CTTGACGAAGACTACGTCTGGGTACCTGCCCCGGGCGGCCGCTCGAAAGGGCGAATTC

[gb|EEC48068.1](#) Thioredoxin h [Phaeodactylum tricornutum CCAP 1055/1]

6e-10

Ubiquitin conjugating enzyme (UCE): BlastX

```
GAATTCGCCCTTAGCGTGGTCNCGGCCGAGGTACAATCGCATGCGCGGAGGGACGCT
CTGCTCTGCTGTGCGCAAGCTTTGAGCACTTGCCATGGCGACTTTGTCCCATTCGCA
AGATGCTCTTGCGTGTGCGAAAGTCGGCGACGGGCGGCCTCGGGGTTTGCAGGGCTG
GCGCAGTTGGGGTCTGTCTCAGAAGCGAGCGAATAGCGATCAGGATTGAACACACCGAA
TAGATAGGCGACCAGTTGTCTCTGGATCAAGTCCATGCAAAGAGTGCCGTCTGGGTAG
ATGTTTCGGATGGAACATTTTCGGAAGTGAATCGCACGCGCGGAGGCTTGTCTAGGGTAT
TGATCAGTAAATGTCAGCCGCATGGAAAAGACGCCTCCCTCCCAGGCTGTGTCTGTC
GGGCCGAAGATGGTGCCGCCCCATACAAAAATGTTTTTCATCGGCAAGGGGACTGGCG
CTGACACCCTCGGGTGGTTCTGCTTCATTGTTTTTTAGGTCACTCATAAGGCGAAGC
GTAGACGGCTTTATCGACGACATCACACCCTGCTGCAAGGGGGCTTGCTCTTCTCCT
GAACCCGCGGGACCTGCCCGGGCGGCCGCTCGAAAGGGCGAATTC
```

[ref|XP_001703225.1](#) hypothetical protein CHLREDRAFT_133208 [Chlamydomonas reinhardtii] 8e-49

[ref|XP_001739461.1](#) ubiquitin-conjugating enzyme E2-17 kDa [Entamoeba dispar SAW760]

3e-41

Figure 4.3: Results from BlastX analysis performed on unique sequences found in the iron limited subtracted library. Each sequence from the library is shown and the EcoR1 restriction sites from the cloning vector and adaptors from the subtraction cloning are highlighted in yellow. The presence of different adaptors on each end of the nucleotide sequence confirms that they are differentially expressed or highly up-regulated sequences.

4.2 – Multiple sequence alignments of fucoxanthin binding protein (FucoBP)

sequences detected in the subtracted library

Multiple sequence alignments of the sequences presented in *figure 4.4* from the iron limited subtracted library indicated that 7 different fucoxanthin binding protein (FucoBP) sequences were detected. The fucoxanthin binding protein (FucoBP) sequences contain stop codons in identical positions but the specific stop codon used

In addition to cDNAs encoding proteins involved in light-harvesting (fucoxanthin binding proteins and chloroplast light-harvesting protein) one further differentially expressed photosynthesis-related cDNA was recovered several times from iron-limited cultures. This cDNA showed strong homology to the *psaE* gene, the product of which is involved in stabilising the docking of ferredoxin (and flavodoxin) to photosystem I. A number of cDNAs related to sequences encoding proteins known to be up-regulated in response to stress (including oxidative stress) were also recovered. These included DnaJ, thioredoxin, and a number of proteins involved in protein turnover such as a ubiquitin-conjugating enzyme and 20S proteasome subunit. None of these cDNAs were recovered in the limited number of cDNAs analysed from iron-replete cells.

Despite reports of substantial up-regulation of flavodoxin by iron limitation in other phytoplankton, no cDNAs were recovered that were related to this protein from either iron-replete or limited cells. To assess whether *C. pelagicus* contains a flavodoxin gene, degenerate primers were designed based on multiple sequence comparisons of the protein from other chromophyte algae.

4.2.1 - Multiple sequence alignments for Flavodoxin and GAPDH

In order to design primers for detection of flavodoxin and GAPDH transcripts multiple sequence alignments were performed and used to identify conserved regions suitable for primer binding.

*** Indicates a position where the peptide is identical in all sequences.**

: Indicates highly conservative substitutions at that position.

. Indicates conservative substitutions at that position.

Karenia	MRAIVISLTCLACGGYGRRVHPQRDSLEK GASRLEAFVMDGSKLAQKGMQERLERQAANG
Phaeodac	MNTQFVSALLLAS-----AAITNG-----
Ehux	-----
osteo	-----
Thallassio	-----
Karenia	KEAKLCQVLAATNPAAAFQAAGTGISTPLRARRVGMSPGMSVGLYYSTSTGNTETVAEYI
Phaeodac	-----FAFVN-THRYTAS-----TTALEAG-----VKIYYSSSTGNTETQVAEYI
Ehux	-----MGVGLLYSTTTGNTETVAGYL
osteo	-----
Thallassio	-----QVGVFFGTSTGSTEEAAELI
Karenia	AGAA-----GIEDWKDIGDADDAEITGHDAIIVGAPTWHTGADSERSGTSWDEWLYNTLP
Phaeodac	SKAG-----GDLPMDDIGDATNEEVEGLDCLIVGAPTWHTGADEQRSGETSWDDWLYTTLP
Ehux	S-----AEIGVDAVDIADAEDLASFDGLIIGAPTWHTGADSERSGTAWDYLYGDLT
osteo	-----MDIADVA-VSDLSSYDSLIVGAPTWHTGADEGRSGTAWDE-AYGDIR
Thallassio	VSEFGDVAAGPIDIDGVAGSVAKEFAKYDALVVGTPTWNTGADTERSGETGWDEIYYSEMQ
	. : : . * : : : * : * : * : * : * : * : * : * : * : * : *
Karenia	NLDFS GKKVAIFG VGDSS-----SYSDNYCDAAGELYDL
Phaeodac	NLKVE GKKVAVFG VGDQQ-----SYGDNFCDAAGELYDL
Ehux	SADLK GKKVAIFGLGDQARPTPLAHASTHAQPPHSRRRPPPVQAGYGDNFCDADELKSC
osteo	SLDLS GKKVAVFG VGDSS-----AYGEYFCDAIEELHSA
Thallassio	DLDIAGKKVAVFG LGDSV-----SYCENYADATGELHDV
	. . . * : : : * : * : * : * : * : * : * : * : * : * : *
Karenia	FTGKGAKVFGMTPSDEGYDYTESKSVVDDK FVGRMFDEDSYSDESEERAKSWVEQLKSEG
Phaeodac	FSAKGCKVFGMT-STEGYDHTESKAEVDGK FVGLMFDEDNQYELSEERAKAWIGQLKSEG
Ehux	FEKQGAEVIG-AWSADGYDHTESKSEAGGTFVGLACEDNQPDQSEERVKAWVAQLKSEG
osteo	FRDTGAEMCGGNVSKDDYDFADSKALVDGV FVIGLPLDEDNESHKSEERAKNWCKQLSNAG
Thallassio	FEALGCKMMGYT-SVDGYLHEESKAQRGEKFCGLPLDAVNQEELTEERVQKVAALIAE-
	* * : : * * : : * : : * : * * * : : * : * : * : * : *
Karenia	FM-
Phaeodac	FF-
Ehux	MPL
osteo	F--
Thallassio	---

Figure 4.5: Multiple peptide sequence alignment for flavodoxin. The binding sites for two alternative degenerate forward primers are highlighted in green and yellow while the binding site for the reverse primer is highlighted in blue. The sequences used in the alignment are from *Emiliania huxleyi*, *Karenia brevis*, *Phaeodactylum tricornutum*, *Ostreococcus tauri* and *Thalassiosira pseudonana*.


```

Phaeodactylum      ASCTTNGLAPMVKAIHDEFVIEEALMTTVHAMTATQAVVDSSSR-KDWRGGRAASGNIIP
Thalassiosira        ASCTTNGLAPMVKAIHDEFDIQEALMTTVHAMTATQAVVDSSSR-KDWRGGRAASGNIIP
Ascophylum          ASCTTNGLAPTVKVINDFVIKDALMTTVHAMTATQMVVDGTSK-KDWRGGRCASSNIIP
Gonyaulux             ASCTTNGLAPAVKAVNDAFQIKRGLMTTIHAMTASQPTVDSASK-KDWRGGRAASGNIIP
Ehux                  -----IRDKR-----ATASQLTVDGSMKGADWRAGRAASANIIP
Isochrysis            ASCTTNGLAPLVKTIINDKFGIKQGLMTTVHAATASQVVVDSSSMKGADWRAGRAASANIIP
pavlova               ASCTTNGLAPLVKHIDQTYGIAEGLMTTVHATTASQLTVDGSMKGSWDWRAGRAASANIIP
                      : :                               **:*.**.: :  **.*.**:***

Phaeodactylum      SSTGAAKAVTKVIPSLVGKITGMAFRVPTIDVSVVDLTAKLEKSTTYEEICAVIKAKSE-
Thalassiosira        SSTGAAKAVTKVIPSLQGKLTGMAFRVPTIDVSVVDLTCKLGKATTYEEICAVIKAKSE-
Ascophylum          SSTGAAKAVTKVIPQLKGKLTGMAFRVPTPNVSVVDLTCTLEKSTSYEEICAAVKSASES
Gonyaulux             SSTGAAKAVAKVVPVVKGLTGMFRVPTIDVSVVDLTCELEKATTYEEICAEIKRRSE-
Ehux                  SSTGAAKAVAKAYPVMKGLTGMFRVPTVDVSVVDLTCELETPPTYDEIKAEVKLASE-
Isochrysis            SSTGAAKAVAKCYPVMKGLTGMFRVPTVDVSVVDLTCELETPCTYDEIKAEVKLASE-
pavlova               SSTGAAKAVAKCYPASKGLTGMFRVPTIDVSVVDLTCRLVKSTTYDELKASVKAASE-
                      *****:* *  **:* ***** :*****. * .. :*: * :* **

Phaeodactylum      GEMKGFGLGYDEPLVSTDFEGDLRSSIFDADAGIMLNPNFVKLIAWYDNEYGYSGRVVDL
Thalassiosira        GEMKILGYCDEPLVSTDFESDRSSIFDAGAGIMLNPTFVKLVAWYDNEWGYSGRVVDL
Ascophylum          GPMAGIIGYTEEPLVSTDFISDSRSSIFDAGAGIMLNPNFVKVVAWYDNEWGYSQRVMDL
Gonyaulux             GDMKGFGLGYTDEPLVSTDFETNTISCTFDKAGIMLDPTFVKLVWYDNEWGYSCRVVRP
Ehux                  TYAKGIVGYTEDQVVSDFVGETCSTVFDAGAGIMLTPTFVKLVSWYDNEWGYSTRLVLDL
Isochrysis            TYAKGIVGYTEDQVVSDFVGETCSTVFDAGAGIQLTPTFVKLVSWYDNEWGYS-----
pavlova               GSMKGFGLGYTEDQVVSQDFVSEMSTTFDAGAGIMLNPNFVKLISWYDNEWGYS-----
                      *:*** : : ** * . * ** * * * * .***: *******

```

Figure 4.6: Multiple peptide sequence alignment for GAPDH. The forward and reverse primer binding sites are highlighted in yellow. The organisms from which the sequences were derived are *Phaeodactylum tricornutum*, *Thalassiosira pseudonanna*, *Ascophylum nodosum*, *Gonyaulux poledra*, *Emiliania huxleyi*, *Isochrysis galbana* and *Pavlova lutheri*.

To ensure that the cDNAs recovered from the subtracted library were differentially expressed under iron limitation degenerate primers were designed for conserved regions within the house-keeping gene encoding GAPDH. Multiple sequence comparison of the GAPDH peptide sequences from related chromophytes including the haptophytes, *I. galbana*, *E. huxleyi*, and *P. lutheri* showed a number of regions of overall homology including those selected for primer development (Figure 4.6).

4.3 – Discussion

A small proportion of the iron limited subtracted library was selected for further study. Although a larger number of sequences were present in the library, the few that were selected for further study were selected under the following criteria: each returned a low e-value, appeared more than once in the subtracted library and the

putative identities of the proteins were reasonable within the context of iron limitation.

Multiple fucoxanthin / chlorophyll binding proteins were detected in the iron limited subtracted library. Five different fucoxanthin binding protein sequences were detected which shared a certain degree of homology in the coding region but differed dramatically in their 3' untranslated regions and in their stop codons. These differences suggest the differential expression of individual members of a multigene family in response to iron limitation.

Up-regulation / differential expression of accessory pigments may result in a higher ratio of accessory pigments : chlorophyll *a* than would be observed under iron replete conditions. This has been reported in iron limited cultures of the diatom *Phaeodactylum tricornerutum* (Greene *et al.*, 1991, 1992) and the haptophyte *Phaeocystis* (van Leeuwe & Stefels, 1998). In the case of *Phaeocystis*, synthesis of 19'-butanoyloxyfucoxanthin and 19'-hexanoyloxyfucoxanthin was increased at the expense of fucoxanthin which is the main carotenoid under iron replete conditions. This response may help to dissipate excess energy absorbed by the cells by reducing the efficiency of energy transfer to the photosystems when low iron availability has impaired the effectiveness of the electron transport chains. This would help to maintain the redox balance of the photosynthetic electron transport chain and reduce the likelihood of formation of reactive oxygen species (van Leeuwe & Stefels, 1998). As the *Coccolithus pelagicus* cultures in this investigation are highly unlikely to have suffered any light limitation, requiring additional pigments to gather light under the growth conditions in the incubator, it is conceivable that up-regulation / differential

expression of fucoxanthin binding protein transcripts in iron limited cells could be a photo-protective response.

Unfortunately the fucoxanthin binding protein sequences obtained in the subtracted cDNA library were only a small segment of the 3' end of the transcript with only 51 nucleotides of the coding region present. Based on a multiple sequence alignment it was found that there were 5 different fucoxanthin binding protein transcripts that were exclusive to the iron limited subtracted cDNA library. Most of the variance in the sequences was in the 3' untranslated regions. Sequence homology in the coding region but not in the 3' untranslated region may indicate that the 5 fucoxanthin binding protein sequences are the result of differential expression of a multigene family in response to iron limitation.

psaE detected in the iron limited subtracted library is a photosystem I protein which facilitates the docking of soluble electron acceptors (particularly ferredoxin/flavodoxin) to the photosystem in order to allow efficient electron transfer (Rousseau *et al.*, 1993). It has also been reported to be involved in protecting the cell from photo-oxidative damage by preventing the formation of reduced oxygen species in the cyanobacterium *Synechocystis* sp. PCC 6803 (Jeanjean *et al.*, 2008). This study found that in *PsaE*-null mutants of *Synechocystis* sp. PCC 6803 expression of genes encoding iron superoxide dismutase (*sodB*) and catalase (*katG*) were up-regulated relative to the wild type. The resultant increased activity of these enzymes which are involved in combating reactive oxygen species was thought to be a compensatory response to the increased generation of reactive oxygen species in the *psaE*-null mutant. The study concluded that the presence of the PsaE protein at the reducing

side of photosystem I serves to prevent the formation of toxic oxygen species resulting from electron leakage to oxygen in the light. Since iron limited phytoplankton cells essentially suffer from an excess of absorbed light energy due to the reduced efficiency of the photosynthetic electron transport chains it is likely that in *Coccolithus pelagicus* up-regulation of the *psaE* transcript is a photo-protective response. Increased amounts of the PsaE protein may increase the efficiency of electron transfer to soluble electron acceptors docked with photosystem I and reduce the risk of electrons being leaked from the system and reacting with oxygen species at this point in the electron transport chain.

The predicted membrane protein transcript (PMP) was selected for further study due to the fact that it returned a very low *e* value although the exact function of this protein has not been determined. One possibility is that it may represent an enzyme in the cell membrane involved in iron acquisition. However, this is based only on the fact that it appeared in the iron limited subtracted library presented in this investigation and is predicted to be associated with a membrane. The function of the predicted membrane protein was not investigated further and within the scope of this investigation its up-regulation under iron limited conditions was the extent to which it was examined.

Thioredoxin is a ubiquitous redox signalling enzyme involved in a multitude of signalling activities throughout the cell. It is known that thioredoxins play a major role in responses to oxidative stress either through redox signalling or more directly by acting as electron donors to the members of the peroxiredoxins (Dietz, 2003). The role of thioredoxins in regulating cellular activities is so varied that it is unlikely to make a good biomarker for iron limitation due to the fact that iron limitation /

oxidative stress is unlikely to be the only conditions under which up-regulation of thioredoxins will occur. Interestingly thioredoxin has been shown to be involved in catalase regulation in *Chlamydomonas reinhardtii*, a situation which has not been reported for higher plants on which most studies of thioredoxins have been focussed (Lemaire *et al.*, 2004). As catalase is an enzyme involved in combating oxidative stress – a problem which iron limited phytoplankton cells inevitably must deal with, it is conceivable that the detection of thioredoxin in the iron limited subtracted library may indicate that it is involved in the regulation of the response of *Coccolithus pelagicus* cells to iron limitation induced oxidative stress. Interestingly the thioredoxin detected in the iron limited subtracted library is thioredoxin h which is a cytosolic isoform whose reduction proceeds via an NADPH-dependent thioredoxin reductase enzyme, as opposed to a ferredoxin-dependent thioredoxin reductase (Besse *et al.*, 1996; Cho *et al.*, 1999). This may indicate a preference for thioredoxins that do not demand a share of the cell's reduced ferredoxin supply under iron limited conditions.

Ubiquitin conjugating enzyme (UCE) was the most abundant of the sequences detected in the iron limited subtracted library representing 4.78% of the total clones sequenced. The 20s proteasome subunit accounted for 2.2% of the clones sequenced and was the third most abundant identifiable transcript in the library. Such a large proportion of the iron limited subtracted library being represented by enzymes involved in protein degradation may be an indication of the use of the protein degradation machinery to continuously recycle proteins in the cell. This may be in order to recycle iron containing proteins and keep the cellular iron pool in a flexible state or it may also be a more general response resulting from the need to recycle

amino acids due to a lack of iron cofactor for enzymes involved in amino acid biosynthesis. A need to recycle the cellular pool of amino acids may also be related to a reduced supply of ammonium for incorporation into amino acids. The impairment of nitrogen assimilation in phytoplankton cells imposed by iron limitation has been reported in several species (Raven *et al.*, 1992; Maldonado & Price, 1996; Milligan & Harrison, 2000). If the ability of the cell to supply reduced forms of nitrogen is impaired then this is likely to result in less ammonium being available to the cell for incorporation into amino acids. It may also be the case that there is a need to rapidly break down and reassemble the photosynthetic and respiratory electron transport chains during periods of light and dark in order to maintain a flexible iron pool in the cell.

Chapter 5 – RNA extractions, DNase digests, primer optimisation and real time PCR results

5.1 – Chapter introduction

Agarose gels from RNA extraction and primer optimisation experiments are presented to demonstrate the quality of experimental and sample preparation for reverse transcription real time PCR (RT Q-PCR) experiments. High quality RNA extraction, thorough DNase treatment and primer optimisation are essential for accurate RT Q-PCR experiments and the data shown in this chapter demonstrates that such criteria was met. The data showing the optimum annealing temperatures for each set of primers used in RT Q-PCR are shown and the evidence that each primer set amplifies only a single product from a mixed cDNA template is also shown. RT Q-PCR gene expression data is presented as a series of histograms which detail the extent to which transcripts were up or down regulated in iron limited *Coccolithus pelagicus* cells. Where there was any ambiguity in the RT Q-PCR fluorescence profiles, suggesting the possibility of multiple products resulting from DNA contamination, the reactions were run out on agarose gels to demonstrate the presence of a single product only. That data is presented here.

5.1.1 – Examination of extracted DNase treated RNA on agarose gels

All RNA extracted for use in subtraction cloning and reverse transcription PCR to generate template for real time PCR was run on 1.5% agarose gels to assess the integrity of the ribosomal RNA bands and the level of DNA contamination. In total 4 RNA extractions were conducted on separate iron replete and iron limited cultures of *Coccolithus pelagicus*:

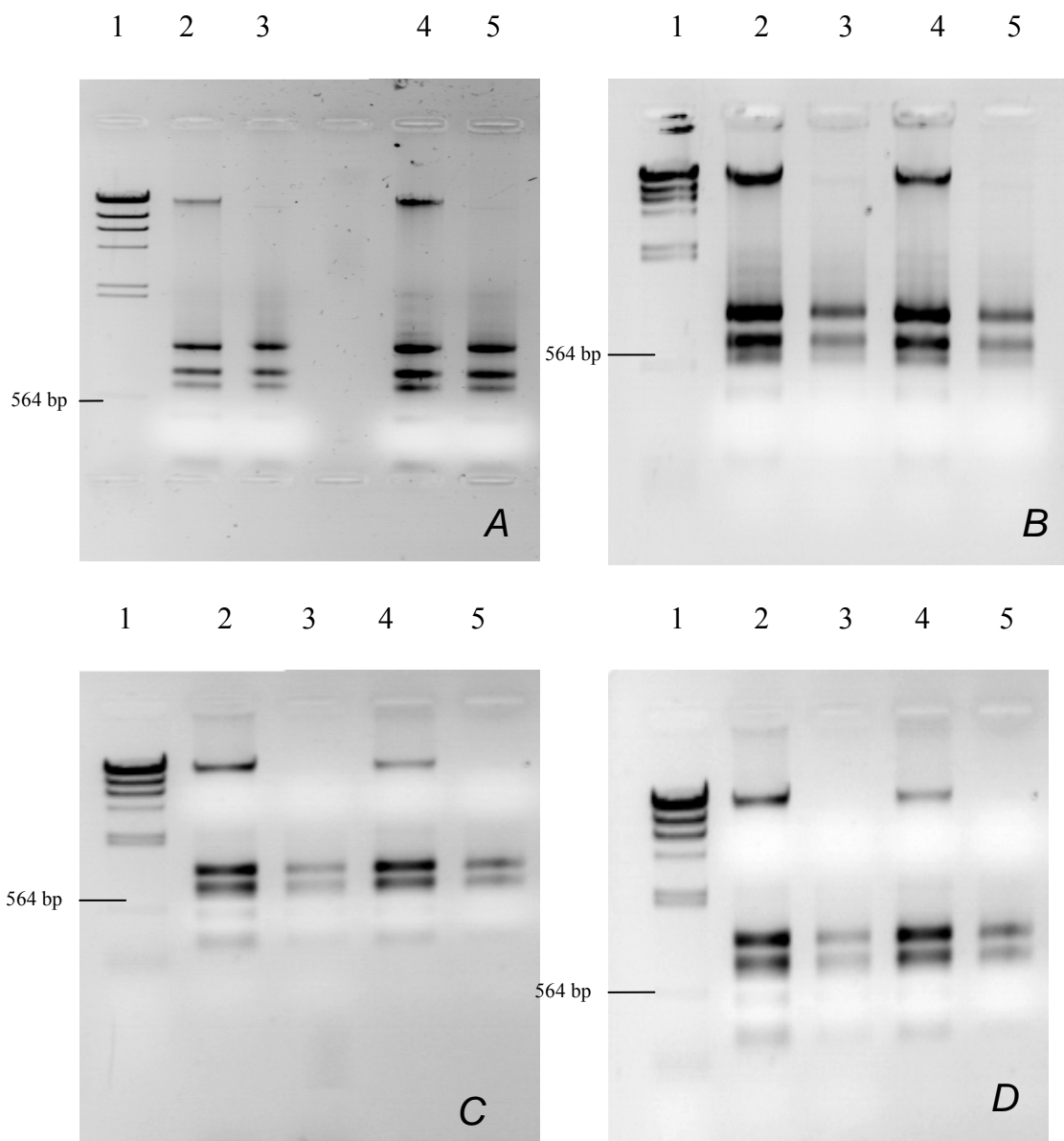


Figure 5.1: 1.5% agarose gels showing RNA extractions before and after treatment with the Turbo DNA-free kit. In all four gels the lanes were loaded as follows: 1 – *Hind* III λ phage markers, 2 – iron replete RNA before DNase treatment, 3 – iron replete RNA after DNase treatment, 4 – iron limited RNA before DNase treatment, 5 – iron limited RNA after DNase treatment. In each gel showing Fe replete and Fe limited RNA samples prior to and after DNase treatment (A,B,C and D) the contaminating DNA (highest molecular weight band) is greatly reduced or absent in the samples after DNase treatment compared to those samples without DNase treatment.

Figure 5.1 shows that the DNase treatment performed on each of the RNA extractions was effective at greatly reducing the amount of contaminating DNA in the original

RNA sample. The integrity of the RNA was observed to be maintained throughout the DNase treatment as indicated by the sharpness of the 28S and 18S rRNA bands on the gels.

The concentrations of RNA in all four RNA preparations were determined spectrophotometrically. The absorbances, dilution factors and calculated concentrations are detailed in Table 5A:

RNA SAMPLE	DILUTION FACTOR	ABSORBANCE AT 260 nm	Concentration ($\mu\text{g ml}^{-1}$)
1 – Replete	1:250	0.056	560
1 – Fe limited	1:250	0.022	220
2 – Replete	1:250	0.025	250
2 – Fe limited	1:250	0.014	140
3 – Replete	1:250	0.012	120
3 – Fe limited	1:250	0.024	240
4 – Replete	1:250	0.02	200
4 – Fe limited	1:250	0.016	160

Table 5A: Table showing the dilution factor, absorbance at 260 nm and calculated concentrations ($\mu\text{g ml}^{-1}$) of RNA after treatment with the Turbo DNA-free kit.

5.2 – Thermal gradient PCR primer optimisation.

The optimum annealing temperatures for each set of primers designed to target sequences detected in the iron limited subtracted cDNA library were determined using thermal gradient PCR. Cloned plasmids containing the sequence of interest were used as template in the reactions and the products were analysed by running them out on agarose gels. The annealing temperature determined to be the optimum was the temperature step just before any reduction in product yield was observed at a higher annealing temperature. The results of the thermal gradient PCR reactions are shown below:

57°C – 67°C thermal gradient - Predicted membrane protein (PMP) and Fucoxanthin binding protein (3) (FucoBP (3)) :

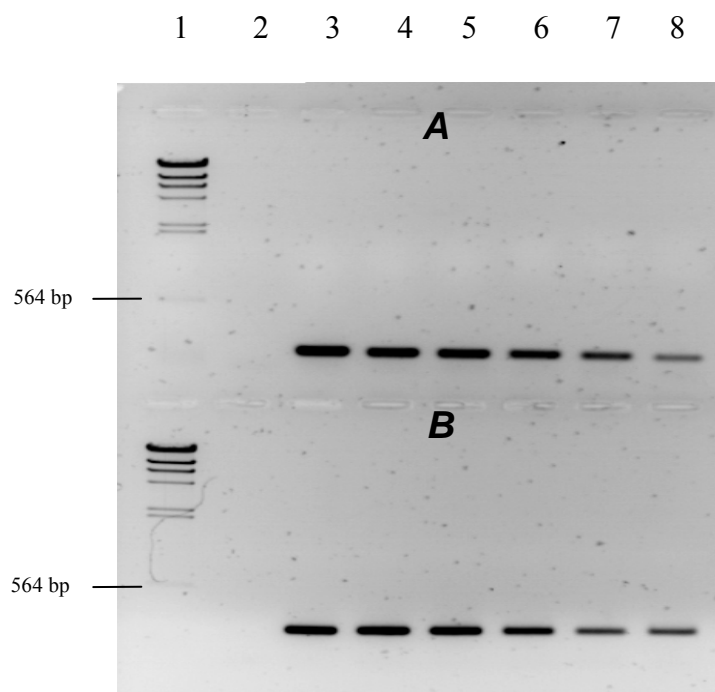


Figure 5.2: 1% agarose gels showing products from 57°C – 67°C thermal gradient PCR. Gel A = PMP, Gel B = FucoBP (3). On both gels: 1 = *Hind* III λ phage markers, 2 = negative controls. The temperature gradient was: 3 = 57°C, 4 = 59°C, 5 = 62.6°C, 6 = 64.9°C, 7 = 66°C, 8 = 67°C.

60°C – 70°C thermal gradient - Fucoxanthin binding protein (7) (FucoBP (7)),

Thioredoxin (Thio), Fucoxanthin binding protein (6) (FucoBP (6)) :

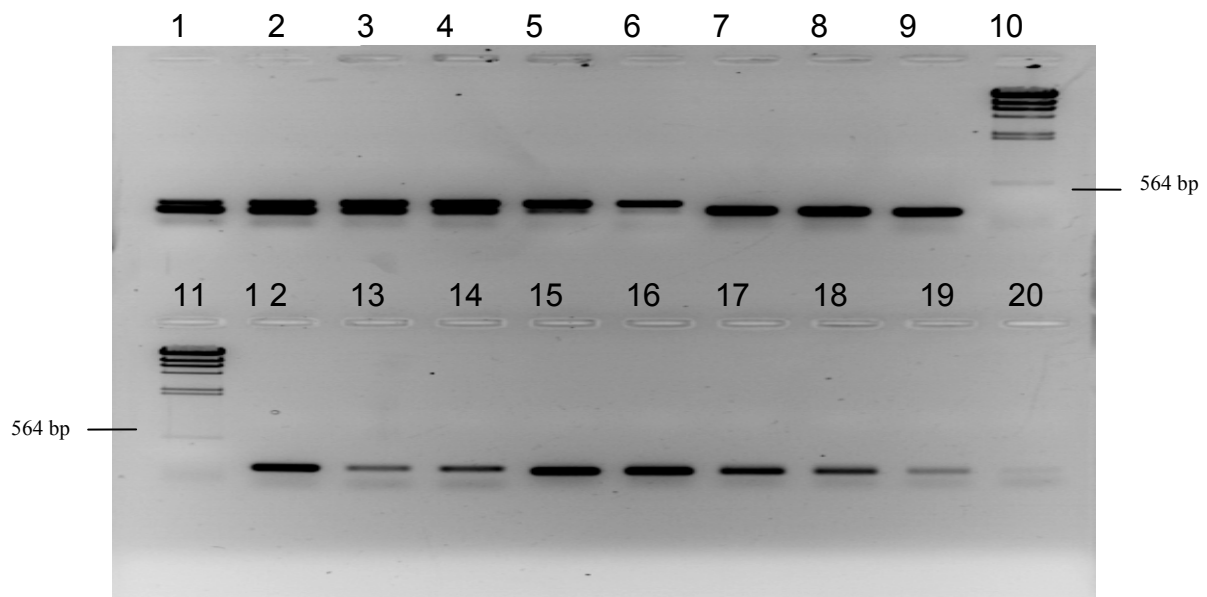


Figure 5.3: 1% agarose gels showing products from 60°C – 70°C thermal gradient PCR. Lanes 1 – 6 = FucoBP (7), Lanes 7 – 9 and 12 – 14 = Thio, Lanes 15 – 20 = FucoBP (6). Lanes 10 and 11 = *Hind* III λ phage markers. All 3 reactions were run on gradients with the following increments: 60 °C, 62 °C, 64.4 °C, 65.6 °C, 68 °C, 70 °C.

60 °C - 70 °C thermal gradient – Ubiquinol-cytochrome c reductase binding protein

(Cyt bc1), Fucoxanthin binding protein (2) (FucoBP (2)), Fuco (4), Ubiquitin-

conjugating enzyme E2 (UCE), Fucoxanthin binding protein (1) (FucoBP (1)),

Fucoxanthin binding protein (5) (FucoBP (5)):

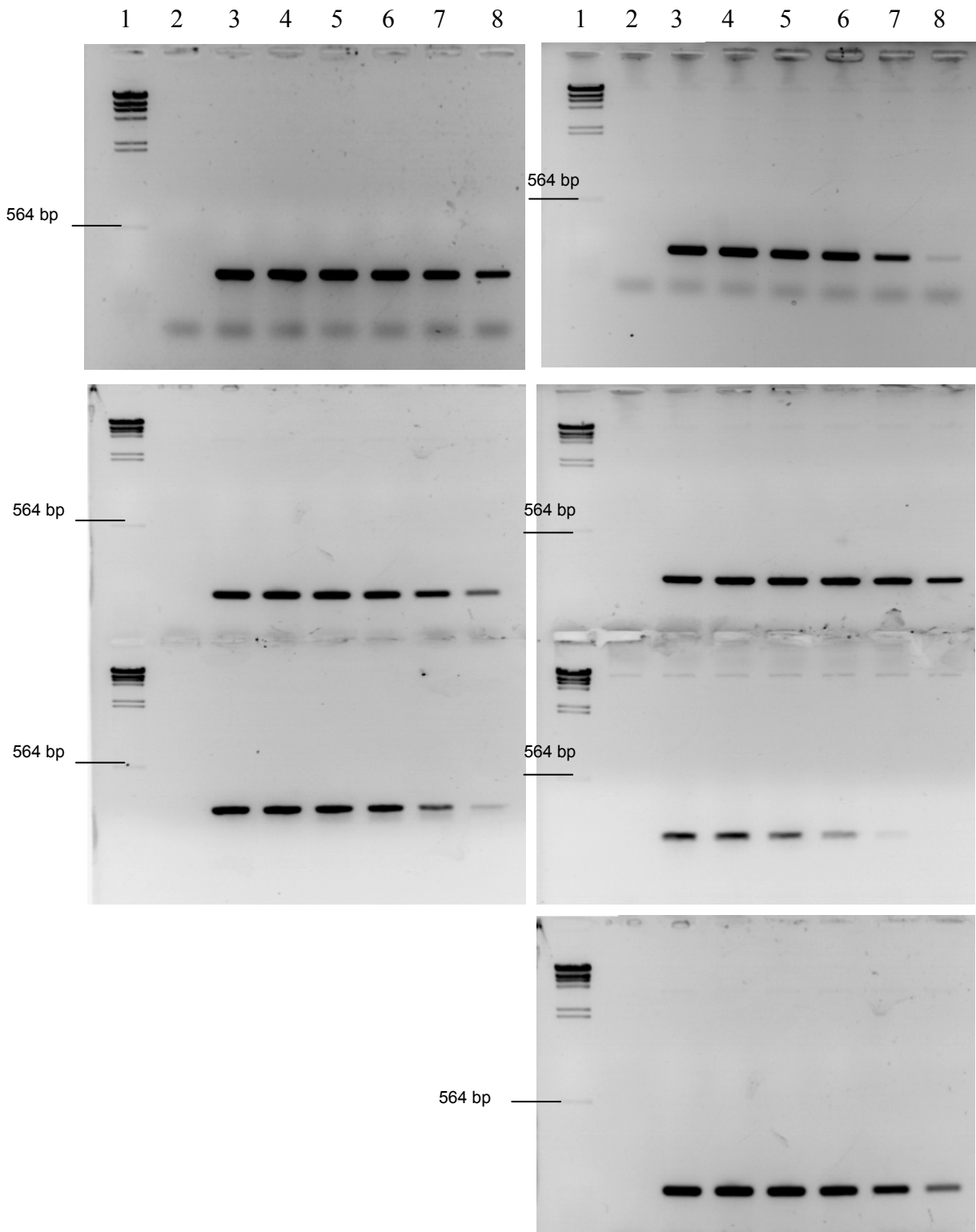


Figure 5.4: 1% agarose gels showing products from 60°C – 70°C thermal gradient PCR. A = Cyt bc1, B = FucoBP (2), C = FucoBP (4), D = UCE, E = FucoBP (1), F = FucoBP (3) G = FucoBP (5). On both gels: 1 = *Hind* III λ phage markers, 2 = negative controls. The temperature gradient was: 3 = 60°C, 4 = 62°C, 5 = 64.4°C, 6 = 65.6°C, 7 = 68°C, 8 = 70°C.

62°C – 72°C thermal gradient – Photosystem I protein E (psaE), 20S Proteasome subunit (20S Prot), Chloroplast light harvesting protein isoforms 8 (CM4E12), Cytochrome b5 domain-containing protein (Cyt b5), Chloroplast light harvesting protein isoform 2 (Chl LHP):

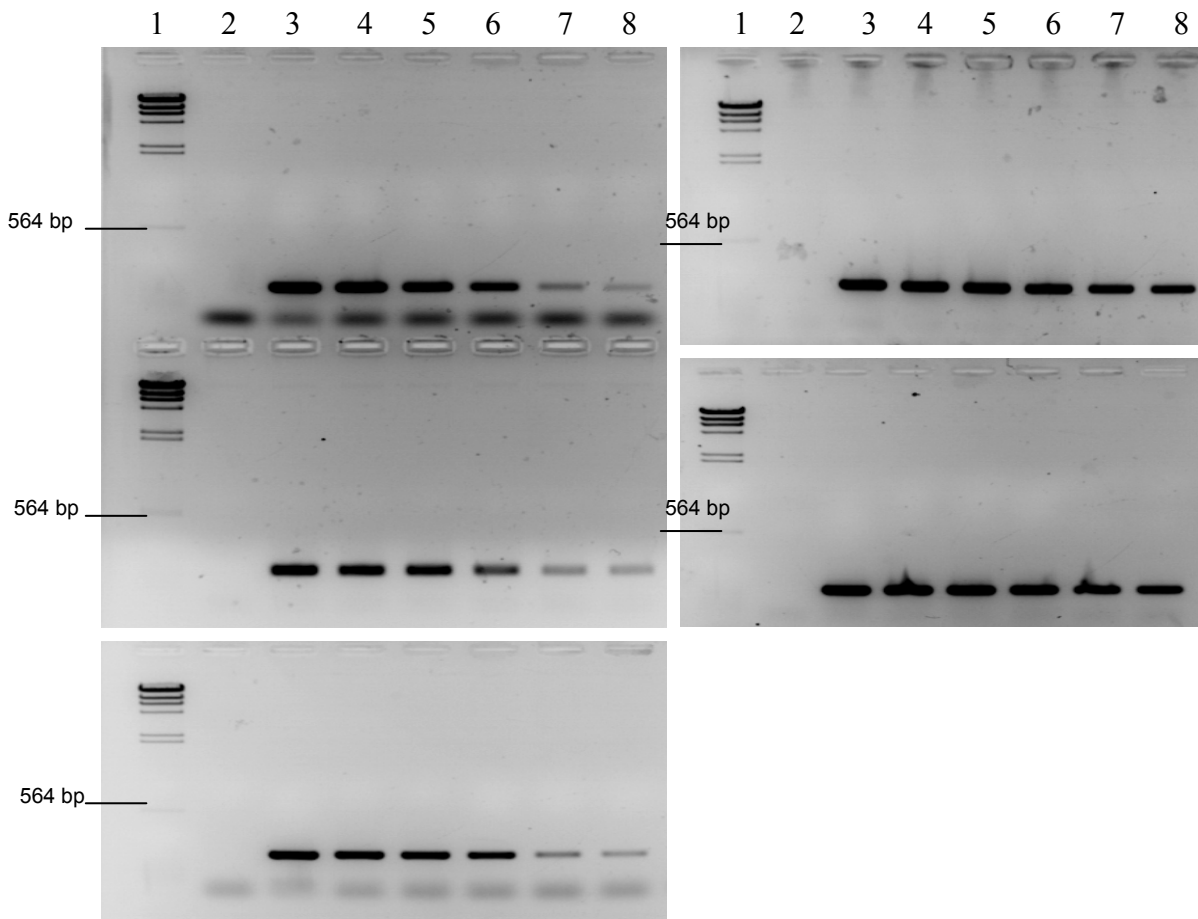


Figure 5.5: 1% agarose gels showing products from 62°C – 72°C thermal gradient PCR. A = PsaE, B = 20s Prot, C = CM4E12, D = Cyt b5, E = Chl LHP. On all of the gels: 1 = *Hind* III λ phage markers, 2 = negative controls. The temperature gradient was: 3 = 62.9°C, 4 = 65.2°C, 5 = 66.4°C, 6 = 67.6°C, 7 = 69.9°C, 8 = 72°C

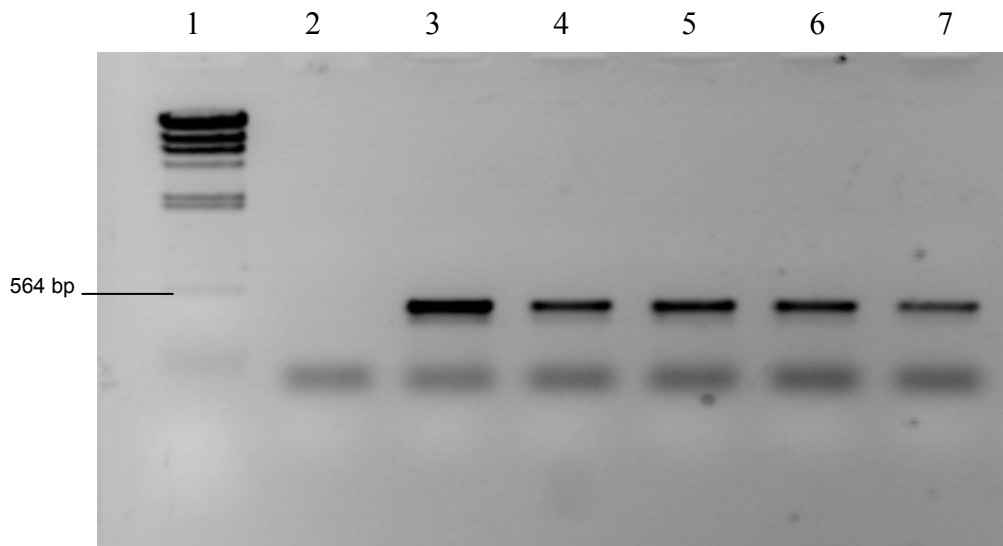


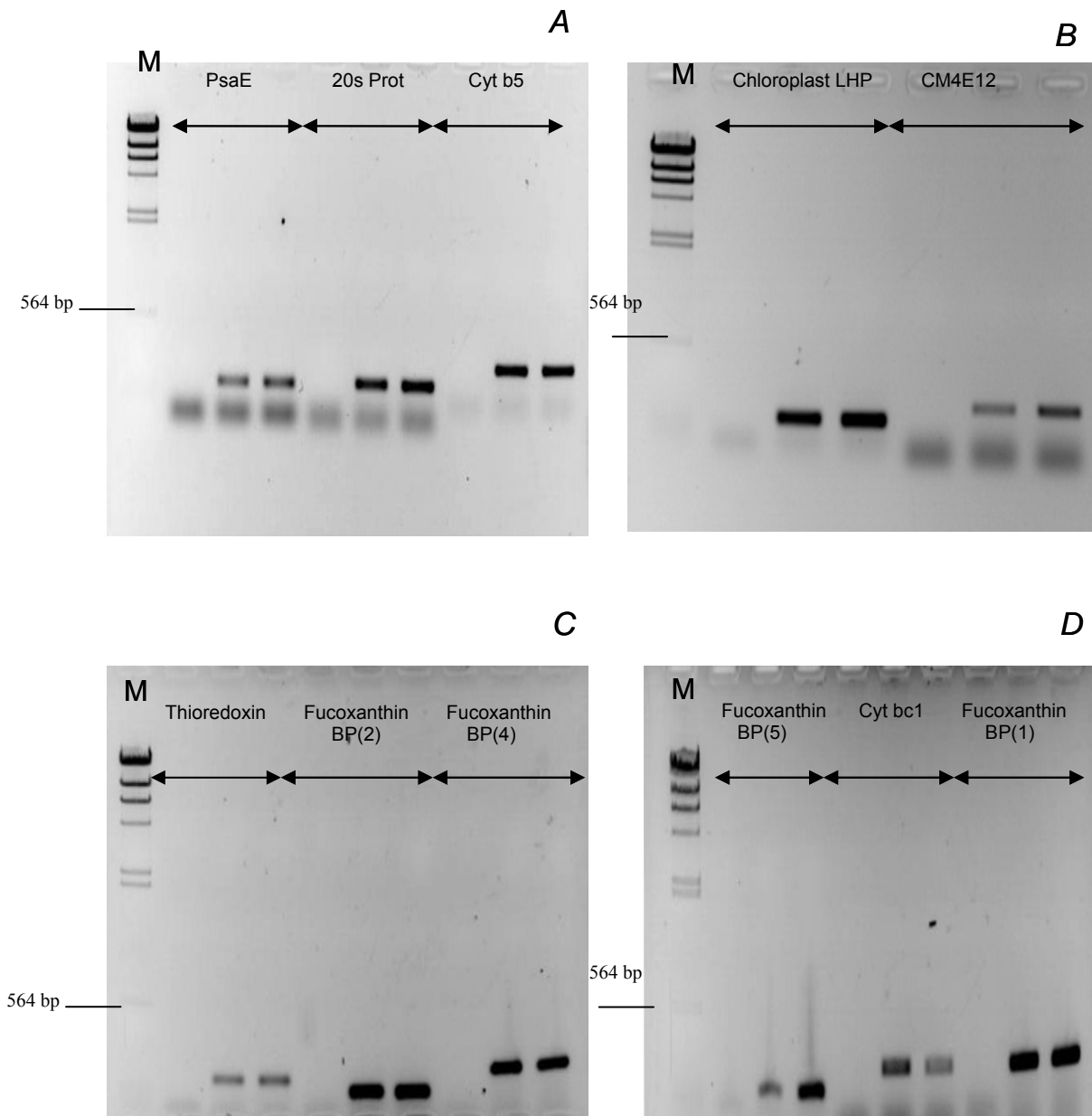
Figure 5.6: 1% agarose gels showing products from 38°C – 48°C thermal gradient PCR with GAPDH primers. 1 = *Hind* III λ phage markers, 2 = negative control, 3 = 38C, 4 = 40 °C, 5 = 42.4 °C, 6 = 44.8 °C, 7 = 48 °C.

It was determined that several different annealing temperatures ranging from 38 °C to 68 °C were required for optimal PCR results with the primers and so RT real time PCR experiments had to be carried out on several different runs of the real time thermal cycler in order to examine all of the sequences selected for further study.

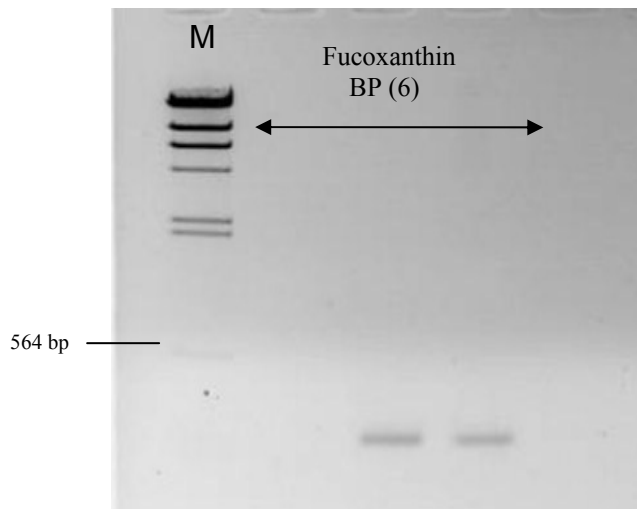
5.2.1 – Testing primers for use in RT real time PCR with cDNA templates.

When the primers designed to amplify sequences detected in the iron limited subtracted library were tested in PCRs using cDNA templates from iron replete and iron limited cells single products of the appropriate size were detected on agarose gels. One single exception was the iron replete cDNA in the PCR containing the ubiquitin conjugating enzyme (UCE) primers (see *Figure 5.7*). In this reaction there was a very faint second product visible on the gel which was not detected in RT real time PCR reactions or RT minus controls using subsequent cDNA preparations.

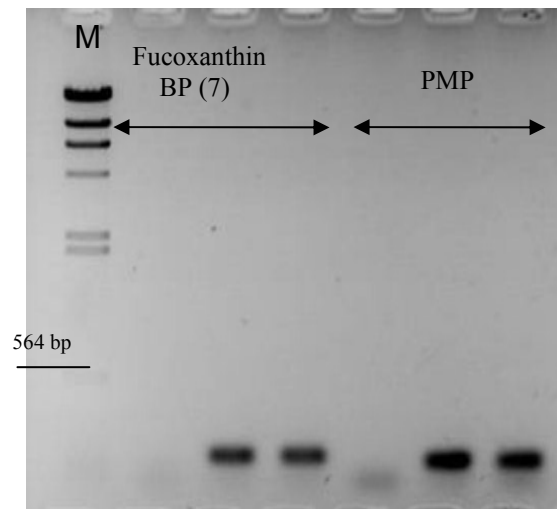
Figure 5.7: 1% agarose gels showing products from PCR reactions with cDNA templates used to optimise primers for real time PCR. The gels were loaded as follows: In all gels M = Hind III λ phage markers. For each target transcript 3 PCRs were run. These 3 reactions were a negative control, the PCR product from iron replete cDNA and the PCR product from iron limited cDNA. In all of the gels every set of 3 lanes were loaded in that sequence from left to right. The gels show the PCR products from the following reactions: A = PsaE, 20s Prot, Cyt b5. B = Chloroplast LHP, CM4E12. C = Thioredoxin, Fucoxanthin BP (2), Fucoxanthin BP (4). D = Fucoxanthin BP (5), Cyt bc1, Fucoxanthin BP (1). E = Fucoxanthin BP (6). F = Fucoxanthin BP (7), PMP. G = DnaJ, UCE. H = Fucoxanthin BP (3). I = Ferredoxin. J = GAPDH.



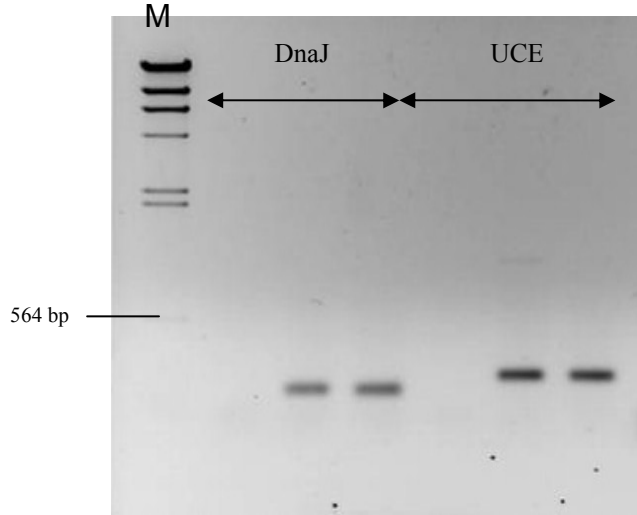
E



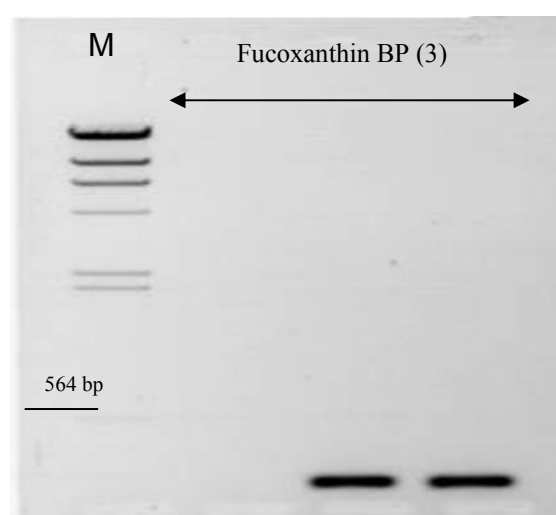
F



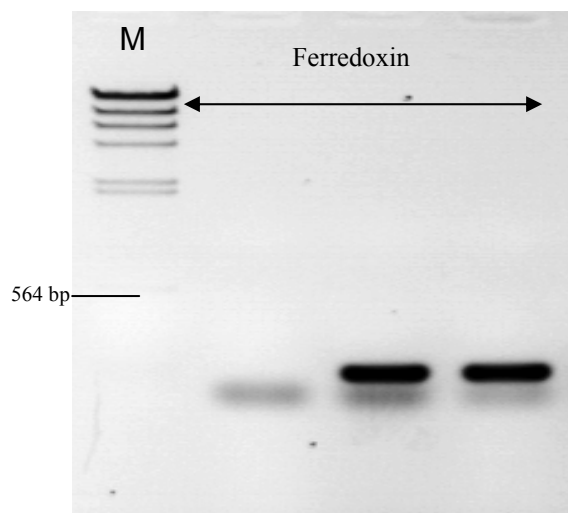
G



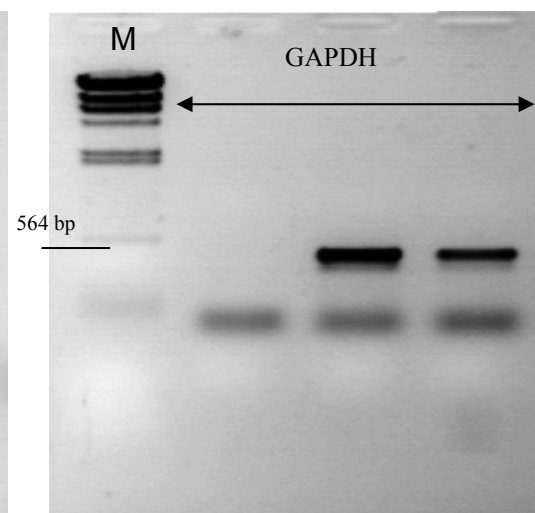
H



I



J



Primer dimers were not eliminated from four of the seventeen PCR reactions conducted to test primers. This potential problem was addressed in real time PCR by using a negative control containing no template to observe the extent to which any primer dimers affect background fluorescence. Given that the real time PCR signal was recorded post-extension rather than following primer annealing it was anticipated that little or no interference would be observed.

5.3 – RT Real time PCR results

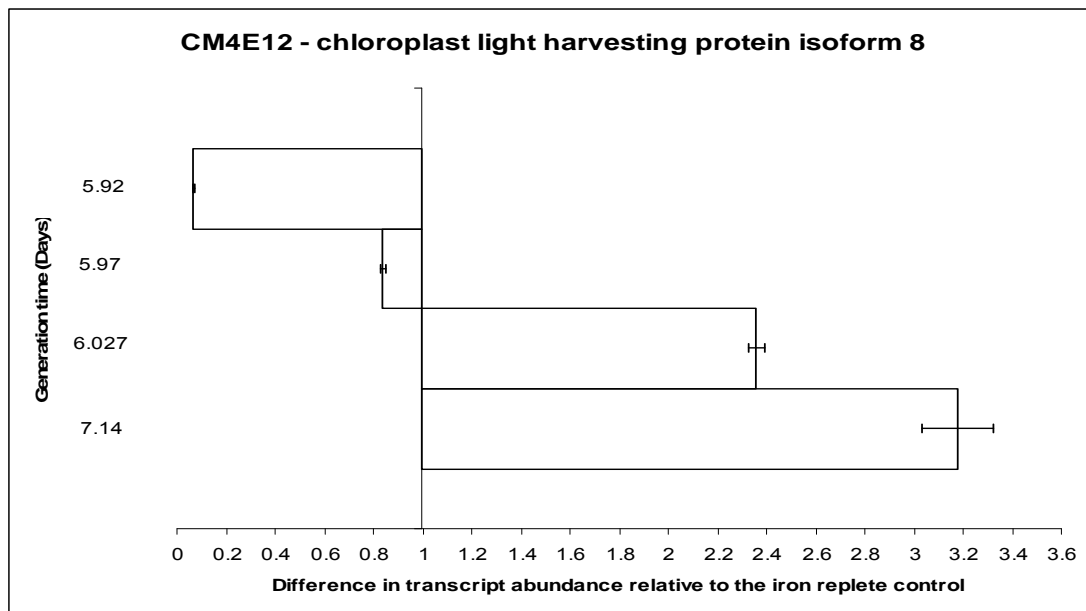
After primer optimisation real time PCR experiments were carried out in order to determine the extent to which transcripts detected in the iron limited subtracted library were up-regulated in iron limited cells of *Coccolithus pelagicus*. An initial round of real time PCR experiments without replication, were conducted using cDNA from four iron replete and four iron limited cultures. The data obtained from the reactions was normalised to the transcript abundance of the housekeeping gene GAPDH and used to select sequences to run in triplicate during subsequent real time PCR experiments.

Based on preliminary results from an initial round of real time PCR experiments it was decided to conduct further experiments with replication on six of the transcripts detected in the iron limited subtracted cDNA library. These reactions were carried out in triplicate, the threshold cycle (Ct) values obtained were averaged and normalised to the mean (n=3) abundance of transcript detected for the housekeeping gene GAPDH. Specific growth rates were calculated for each culture from which cDNA was produced for use in real time PCR. It was found that the specific growth

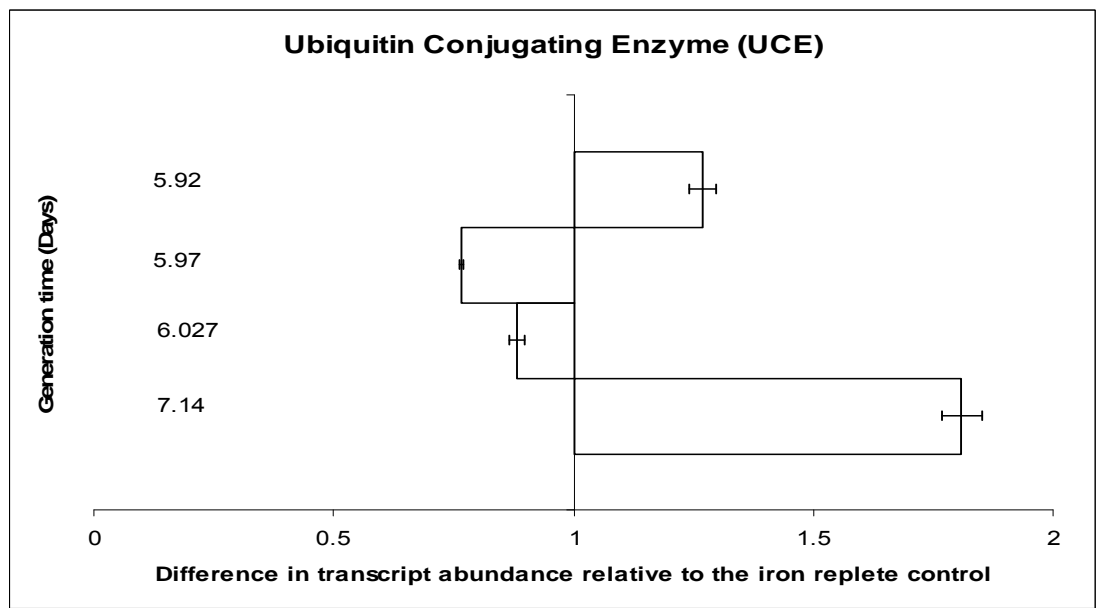
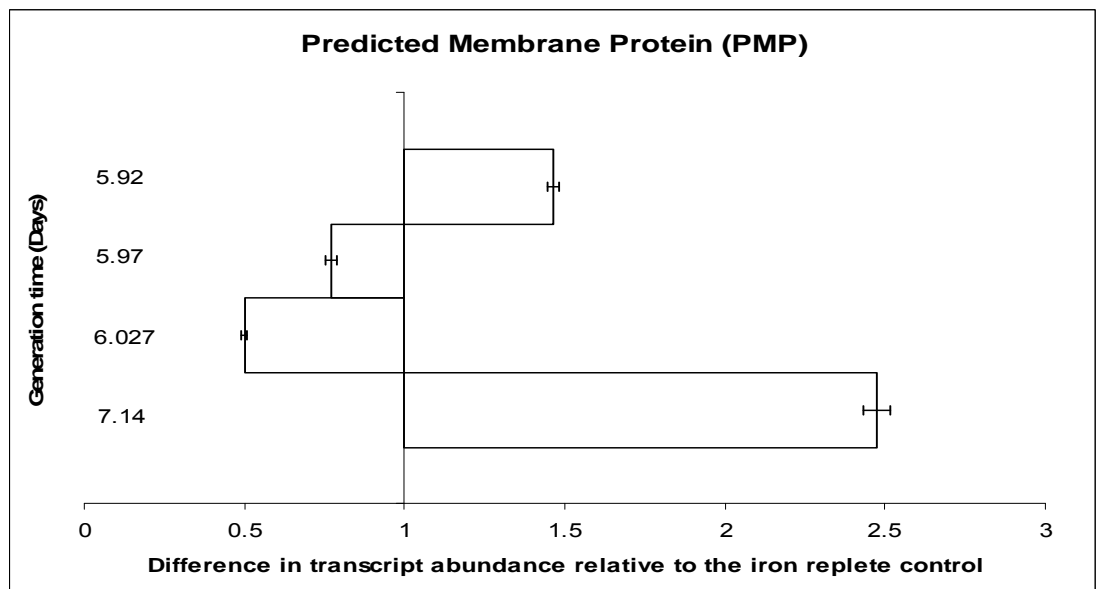
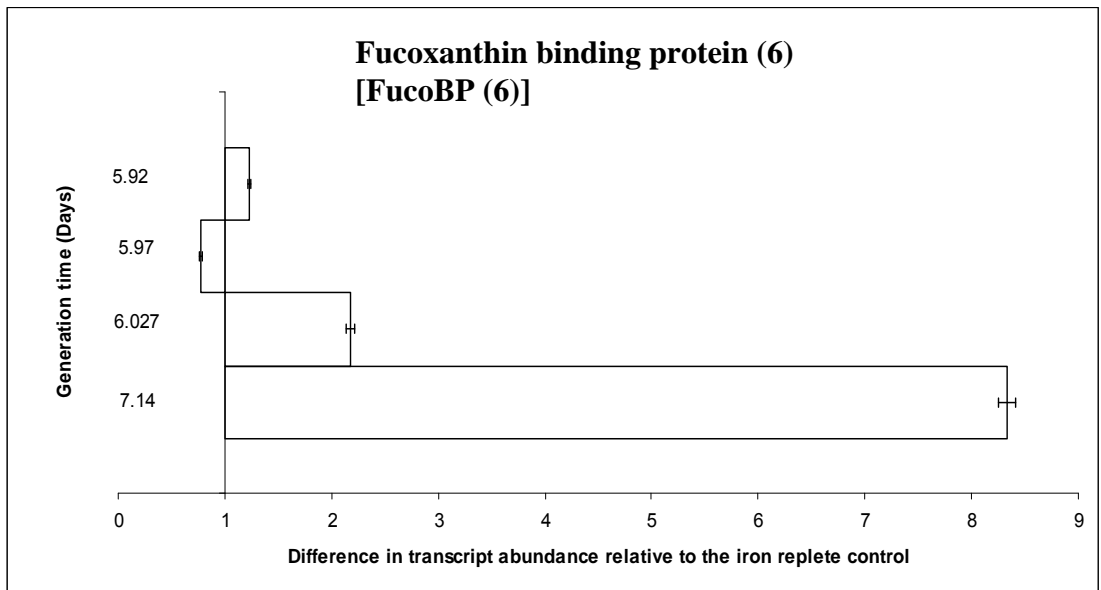
rates of the four iron limited cultures used to produce cDNA varied by 17%. These results are presented in Table 3C in Chapter 3.

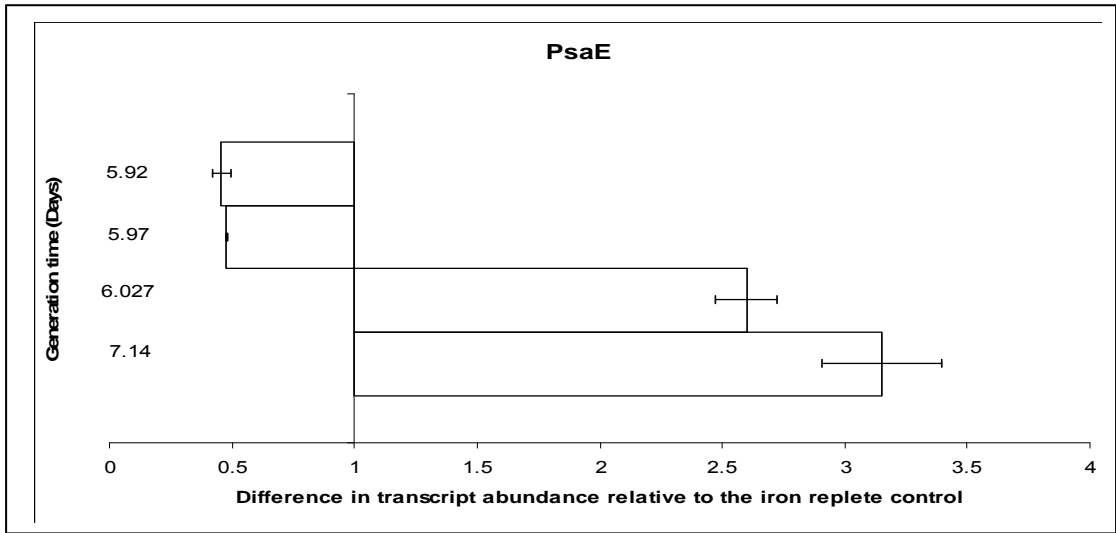
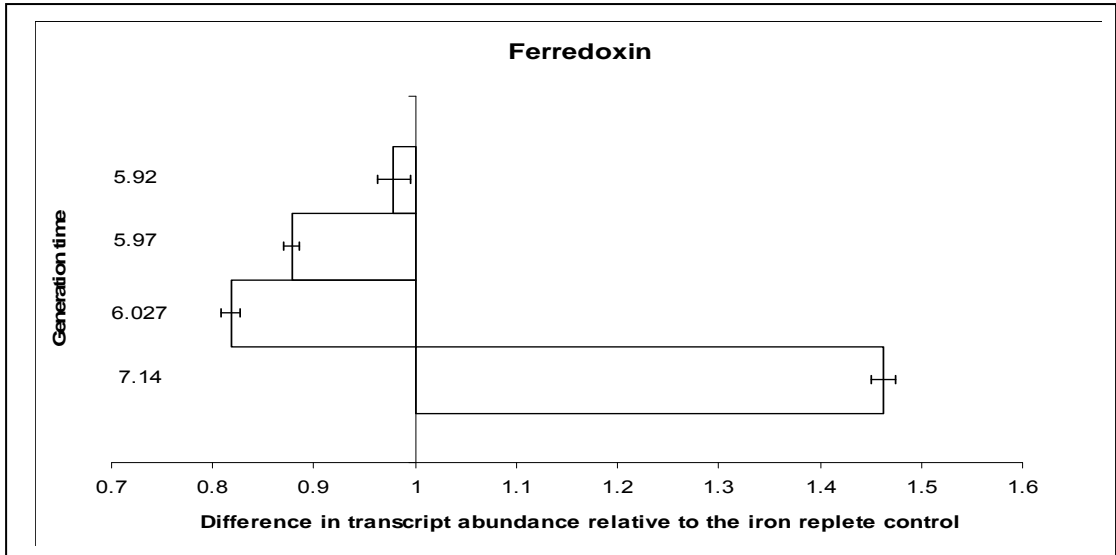
RT real time PCR experiments were conducted using cDNA derived from four iron replete and four iron limited cultures. The iron limited culture most representative of the original iron limited culture that was used to produce the subtracted library is iron limited replicate (4). The iron limited culture used to produce the subtracted cDNA library had a specific growth rate of 0.101 and the specific growth rate of iron limited replicate (4) ($\mu = 0.097$) was closer than any of the other iron limited replicates used in RT real time PCR studies.

Figure 5.8: Histograms showing mean $SE \pm$ (n=3) abundance of transcripts in iron limited *Coccolithus pelagicus* cultures relative to iron replete controls. A value of 1.0 indicates that a transcript is neither up nor down-regulated. A value greater than 1.0 indicates that a transcript is up-regulated in the iron limited cultures.

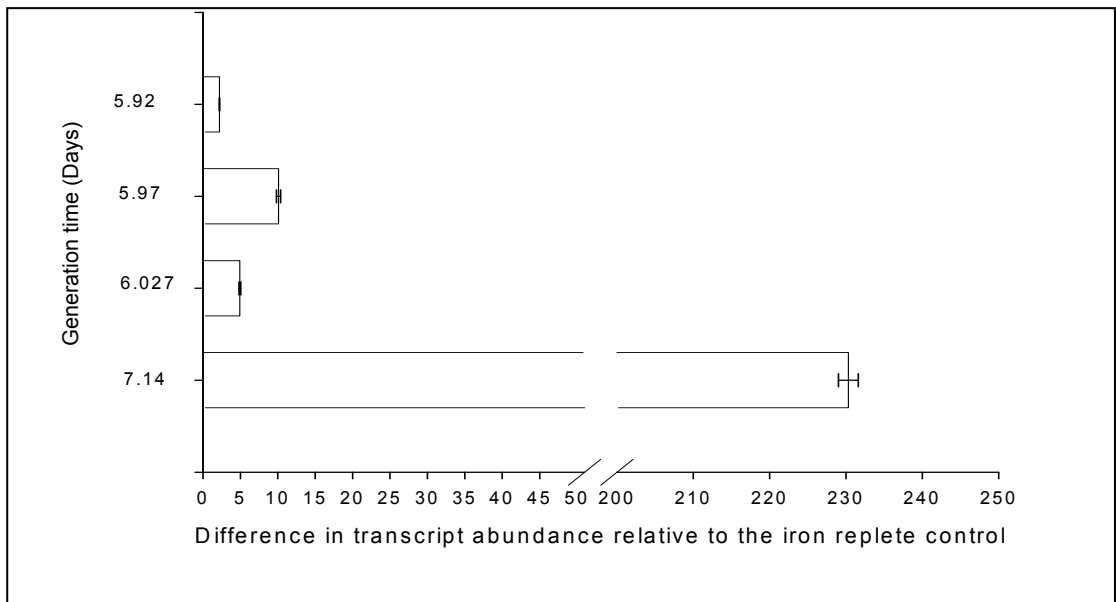


Only one single threshold cycle (Ct) value was detected among all of the iron replete reactions with the CM4E12 primers and so the maximum PCR cycle number (40) has been used as the Ct value where none was detected. The results for CM4E12 represent the minimum difference between the iron replete and iron limited samples as the real Ct value for the iron replete reactions could be much greater than the assigned value of 40.





Chloroplast Light Harvesting Protein (Chl LHP)



The chloroplast LHP transcript was the only cDNA that was up-regulated in all four of the iron limited cultures. It also showed the greatest levels of up regulation out of all of the transcripts examined. In particular the chloroplast LHP transcript was found to be one of the most up-regulated transcripts in terms of overall transcript abundance. In cDNA sample 4 the transcript was shown to be 230 times more abundant relative to the iron replete control.

Across all four cDNA samples every transcript was up-regulated the most in cDNA sample (4) which was produced from the culture (culture 4) that was found to have the slowest specific growth rate. cDNA sample 3 consistently showed no significant up-regulation of any of the examined transcripts with the exception of the chl *a* binding protein transcript which was found to be 2.2 times more abundant in the iron limited culture than in the iron replete culture.

The ferredoxin transcript was not significantly up-regulated or down-regulated in any of the iron limited cDNA samples. The real time PCR data suggests that ferredoxin transcript levels do not differ significantly between iron limited and iron replete cultures of *Coccolithus pelagicus*.

5.3.1 – Analysis of RT real time PCR products on agarose gels

The real time PCR dissociation curves for the –RT controls of the predicted membrane protein (PMP) and ferredoxin reactions showed small peaks in some of the reactions which were at a different melting temperature than those of the main

product (see the dissociation curves in the appendix). Those reactions which showed these unexpected peaks in the dissociation curves were run out on 1% agarose gels to confirm that only one product was present and that it was of the expected size. This was the case in all of the aforementioned reactions as can be seen from *figures 5.9 – 5.12* below.

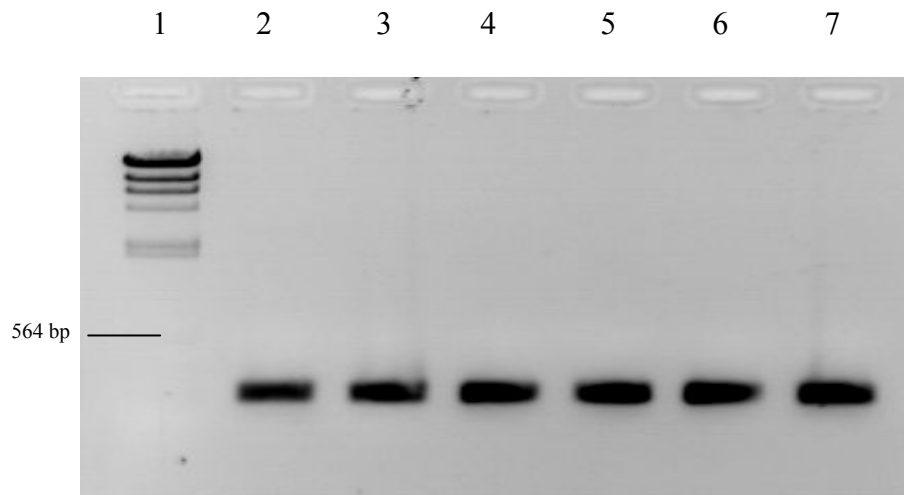


Figure 5.9: 1% agarose gel showing PCR product from RT real time PCR experiment using predicted membrane protein (PMP) primers. 1 - *Hind* III λ phage markers, 2-7 – Single PCR products of expected size (152 bp).

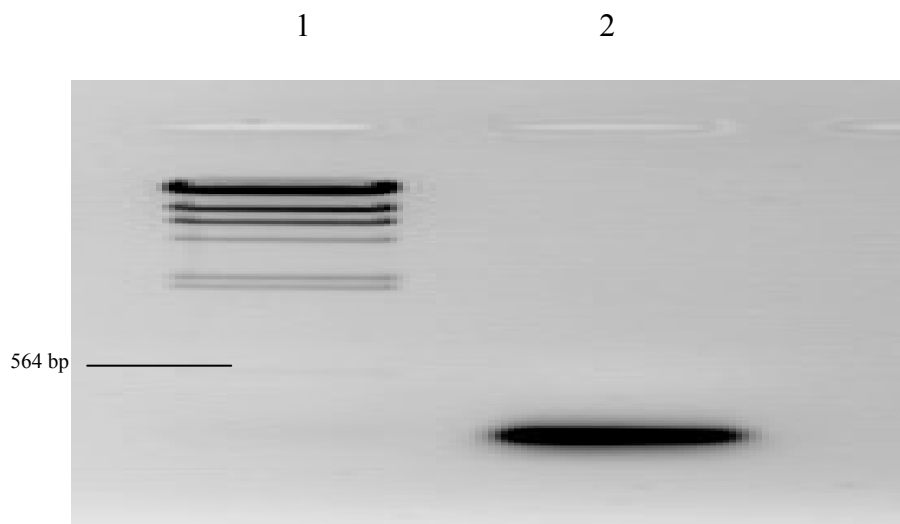


Figure 5.10: 1% agarose gel showing PCR product from RT real time PCR experiment using Ferredoxin primers. 1 - *Hind* III λ phage markers, 2 – Single PCR product of expected size (103 bp).

The RT real time PCR dissociation curves (see appendix) of the GAPDH and Chlorophyll *a* binding protein products displayed more than one peak for the main reactions. In the case of the GAPDH products the peaks were within 2°C of one another. In order to confirm that only a single PCR product of expected size existed in the reactions, one of the iron replete cDNA products and one of the iron limited cDNA products were run out on 1% agarose gels. It was found that all of the aforementioned reactions contained single products of expected size.

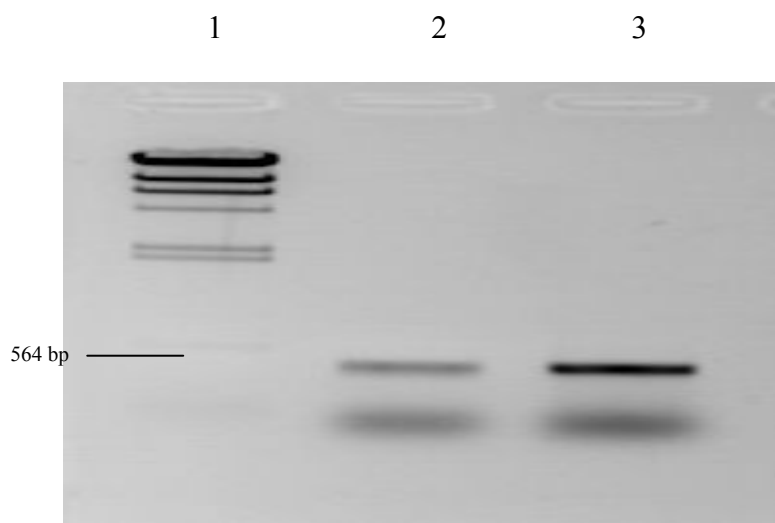


Figure 5.11: 1% agarose gel showing primer dimers and PCR product from RT real time PCR experiment using GAPDH degenerate primers. 1 - *Hind* III λ phage markers, 2 + 3 – Single PCR products of expected size.

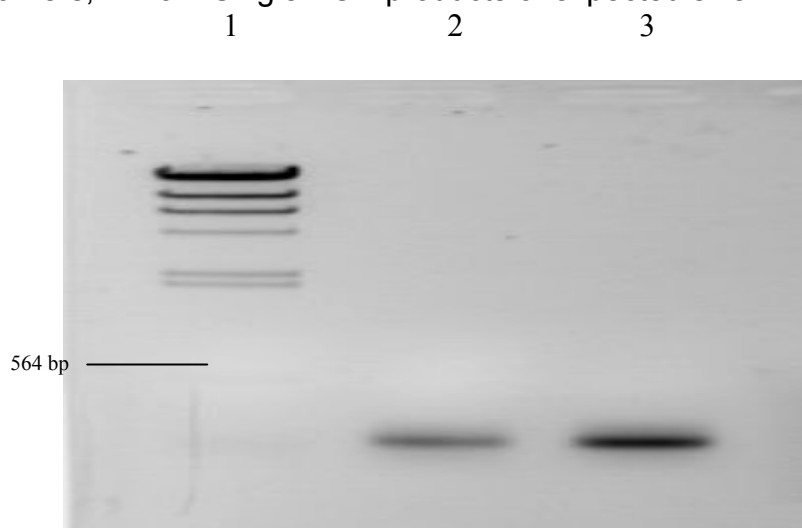


Figure 5.12: 1% agarose gel showing PCR product from RT real time PCR experiment using Chl LHP primers. 1 - *Hind* III λ phage markers, 2 + 3 – Single PCR products of expected size (198 bp).

5.4 – Discussion

Variability in specific growth rates and therefore severity of iron limitation was apparent in the gene expression data obtained from RT real time PCR experiments (figure 5.8). Iron limited cultures 2 and 3 which had the fastest specific growth rates of the iron limited cultures consistently showed the least up-regulation of transcripts detected in the subtracted library. In contrast the iron limited culture with the slowest specific growth rate displayed the highest levels of up-regulation across all of the transcripts examined reflecting its more severe state of iron limitation. Culture 3 showed no significant up-regulation in many of the transcripts examined. The transcript which was up-regulated most in the slowest growing cultures was the chloroplast light harvesting protein, a result consistent with the other cultures. The data suggests that the level of up-regulation of the transcripts detected in the iron limited subtracted library was tightly correlated to the severity of iron limitation over what is likely to be a narrow range of iron concentrations. It appears that very small amounts of iron contamination in laboratory glassware or from the air can greatly affect gene regulation in *Coccolithus pelagicus*.

Although using deferoxamine in growth media to chelate iron was consistently effective at producing iron limited cultures of *Coccolithus pelagicus* there was variability between cultures in terms of the severity of iron limitation observed. The severity of iron limitation was judged based on the specific growth rates of cultures, slower specific growth rates indicating more severe iron limitation. Between the iron limited cultures used to produce cDNA for real time PCR experiments the specific growth rates varied over a range of 17% and this variation was evident in the gene

expression data obtained. When dealing with nanomolar concentrations of trace metals such as iron it is often difficult to maintain equal concentrations in all cultures. When cultures are sampled for growth measurements dust from the air can contribute iron to the media. Despite minimising contamination through the use of sterile technique and acid washing glassware that is used in the preparation of growth media, it is difficult to completely eradicate all contaminating trace metals from the growth media. When these factors were considered, a variation of 17% in specific growth rate over the range of iron limited cultures was deemed to be acceptable. These cultures were still growing far slower than the iron replete controls.

It was found that the abundance of the ferredoxin transcript did not vary significantly between the iron replete and iron limited cultures. Furthermore no flavodoxin transcript was detected in the iron limited subtracted library and the flavodoxin gene could not be detected in iron limited cDNA with degenerate primers. This observation is suggestive of several possibilities. It may be the case that *Coccolithus pelagicus* does not possess the flavodoxin gene and therefore has no alternative but to continue expressing ferredoxin even when iron limited. If flavodoxin was being expressed in the iron limited cultures it would be highly unlikely that it would not appear in the iron limited subtracted library. Many species of eukaryotic phytoplankton do not produce flavodoxin when suffering iron limitation (Erdner *et al.*, 1999). While not conclusive, the results of this investigation suggest that *Coccolithus pelagicus* may not have the capacity to produce flavodoxin under conditions of moderate iron limitation.

Another possibility is that the *Coccolithus pelagicus* cultures in this study were not iron limited enough to induce expression of flavodoxin, being only iron limited as opposed to iron starved. However, a laboratory study in which two diatoms were examined found that induction of flavodoxin expression is a response to declining iron concentrations in the environment and was detected before any apparent physiological impairment or growth rate inhibition had occurred (McKay *et al.*, 1997). As the iron limited *Coccolithus pelagicus* cultures in this study were suffering from chlorosis and impaired growth rates it would be expected, based on the observations from other studies, that these conditions would be sufficient to induce expression of the flavodoxin gene if it were present.

Iron limitation in *Coccolithus pelagicus* does not appear to have a repressive effect on the transcription of the ferredoxin gene. Ferredoxin protein levels may not be the same between iron limited and iron replete cells, however. Iron availability may regulate the translation of the ferredoxin mRNA resulting in levels of ferredoxin under the two conditions that would not be in equal proportions, as the transcript levels would seem to imply. A laboratory study (Laudenbach *et al.*, 1988) found that in the cyanobacterium *Anacystis nidulans* R2 the ferredoxin transcript was detected in cells grown in iron concentrations which also induced flavodoxin expression.

Although the ferredoxin transcript was present regardless of the iron concentration of the growth medium, it was only translated under conditions that were not iron limiting. Under iron limitation the flavodoxin transcript was transcribed and translated. Addition of iron to the *A. nidulans* cultures resulted in the degradation of flavodoxin transcripts within one hour and the reappearance of ferredoxin protein in the cells. This implies that iron has a repressing effect on flavodoxin transcription

and that it may also regulate the translation of the continually present ferredoxin transcript.

There is a contradiction between the proportions of the sequences in the subtracted library possessing both Clontech adaptors and their up-regulation as determined by RT real time PCR. In particular the UCE was not found to be up-regulated to any great extent despite being the most abundant identifiable transcript in the subtracted library. As the RNA used to create the subtracted library was not the same RNA used in the RT real time PCR experiments – owing to the problem of obtaining sufficient quantities from biomass that does not take excessive time periods to produce in cultures. While the specific growth rates of the cultures used in RT real time PCR studies did not differ dramatically from the one used in the production of the subtracted cDNA library, it would be advisable in any future experiments to conduct real time PCR experiments on the same RNA sample from which a subtracted library was created. This likely explains the differences observed between implied abundance and differential expression of transcripts in the subtracted library and the RT real time PCR results.

Some of the RT real time PCR reaction products which yielded dissociation curves which were not as ideal as the other reactions were run on agarose gels to confirm that only one single product was present. Some small peaks may be present in –RT controls due to minute levels of DNA contamination. However, it is extremely unlikely that this contamination exists in the reactions being measured as the samples in these reactions had undergone an additional DNase digest as part of the reverse transcription protocol (gDNA wipeout). The Chl LHP dissociation curves appeared to

show two peaks with close melting temperatures. This would normally indicate two different products. However, when observed on an agarose gel there was clearly only a single product. Such an observation may be indicative of multiple copies of this gene with slightly differing sequences being represented in the cDNA template, perhaps as a result of alternative splicing.

CHAPTER 6 – CONCLUSIONS AND FUTURE WORK

The aim of this study was to investigate the acclimation of *Coccolithus pelagicus* to iron limitation from a molecular viewpoint. It has been demonstrated that the fungal siderophore deferoxamine is a suitable ferric iron chelator for use in studies of iron limitation (Chapter 3). Growth of *Coccolithus pelagicus* in the presence of deferoxamine results in changes in gene expression (*figure 5.8*) and in the proteome of the cells (*figures 3.12, 3.15, 3.16*). It induces classic signs of iron limitation – slower growth rates (*figure 3.1 & table 3A*) and reduced chlorophyll *a* concentrations per unit biomass (*figure 3.3*). A secondary aim of this investigation was to identify potential biomarkers of iron limitation in *Coccolithus pelagicus*. Several up-regulated transcripts (fucoxanthin binding protein (6), PMP, CM4E12, *psaE*) and one highly up-regulated transcript (Chl LHP) were identified (*figure 5.8*) and these may prove worthy of further examination for their potential as biomarkers to complement the already existing approaches used to confirm iron limitation in the field (LaRoche *et al.*, 1995; van Leeuwe & Stefels, 1998; Erdner *et al.*, 1999; McKay *et al.*, 1999; Inda & Peleato, 2003; DiTullio *et al.*, 2007; Hernandez *et al.*, 2008).

In order to prove suitable as biomarkers these transcripts should be significantly up-regulated under conditions of iron limitation in a multitude of phytoplankton species and should display an up-regulated response specific to iron limitation as opposed to being up-regulated as a general stress response.

PsaE is a potentially useful target for use as a biomarker of iron limitation. It is present in the photosystem I complexes of phytoplankton (Rhiel & Bryant, 1993; Yu

et al., 1993; Zhao *et al.*, 1993; Fromme *et al.*, 2003), and it is highly conserved (Golbeck & Bryant, 1991), indicating that it serves an important role. Its highly conserved sequence and presence throughout a range of phytoplankton taxa may make it useful for confirming iron limitation in mixed phytoplankton communities, if it can be established that up-regulation in response to iron limitation is common among phytoplankton. Its high degree of sequence conservation may also potentially make it easier to develop PCR or immunological based methods for detecting it in the majority of species of a mixed community were it to be used as a biomarker.

The high level of up-regulation detected for the chlorophyll binding protein (Chl LHP) in this study indicates that it may hold potential as a biomarker. If the up-regulation of Chl LHP shows the same magnitude in response to iron limitation in other phytoplankton then the clear contrast in expression levels between iron limited and iron replete conditions makes it an attractive candidate as a biomarker.

Chlorophyll binding protein expression is not unique to iron limitation however, they are up-regulated in other circumstances such as light limitation and it would have to be confirmed that Chl LHP up-regulation was a response exclusive to iron limitation before it could be employed as an indicator of iron limitation.

The data presented in this study suggest that iron limitation results in up-regulated expression of mRNAs which encode proteins involved in photosynthesis and protein degradation (*figures 4.3 & 5.8*). The reduced chlorophyll *a* concentrations per unit biomass (*figure 3.3*) and the significant up-regulation of transcripts encoding proteins of the photosynthetic apparatus indicate that photosynthesis is the primary target of iron limitation in *Coccolithus pelagicus*. This is consistent with other studies of iron

limited phytoplankton species which reported photosynthesis as the main target of iron limitation (Milligan & Harrison, 2000; Davey & Geider, 2001).

The significant up-regulation of one of several alternative fucoxanthin binding protein transcripts in response to iron limitation, reported in this investigation, compliments the findings that elevated levels of alternative types of fucoxanthin such as 19'-hexanoyloxyfucoxanthin are present in iron limited cells of *Phaeocystis antarctica* (van Leeuwe & Stefels, 1998; DiTullio *et al.*, 2007). It was reported that high ratios of 19'-hexanoyloxyfucoxanthin to other pigments such as chlorophyll *c*, chlorophyll *a* and fucoxanthin were observed in iron limited *Phaeocystis antarctica*. The ratios of these pigments may be potential indicators of iron limitation. Considering chlorophyll *a* per unit biomass is reduced relative to iron replete levels in iron limited *Coccolithus pelagicus*, the up-regulated iron limited fucoxanthin : chlorophyll *a* ratio may be higher than the iron replete control and this may be consistent with the findings in *Phaeocystis antarctica*. If production of alternative types of the main fucoxanthin carotenoid and its corresponding binding proteins is a response to iron limitation among phytoplankton as evidence from this investigation and other studies suggests (van Leeuwe & Stefels, 1998; DiTullio *et al.*, 2007), then this may prove to be a worthwhile candidate as a biomarker of iron limitation.

Expression of chlorophyll binding proteins in response to iron limitation has been reported in other studies. In *Dunaliella salina* iron limitation results in enlarged photosystem I complexes and the expression of a chlorophyll binding protein homolog (Varsano *et al.*, 2006). The chlorophyll binding protein IsiA is expressed in cyanobacteria in response to iron limitation (Geiß *et al.*, 2001; Sarcina & Mullineaux,

2004; Yeremenko *et al.*, 2004; Liu *et al.*, 2006; Singh & Sherman, 2007). The protein has been shown to form aggregates associated with photosystem I which aid in the dissipation of excess light energy (Boekema *et al.*, 2001; Yeremenko *et al.*, 2004; Ihalainen *et al.*, 2005). Evidence from the subtracted library produced in this study (*figure 4.3*), and aforementioned studies of iron limitation in other phytoplankton species suggest that induction of chlorophyll binding proteins may be a common response to iron limitation. The findings of this investigation are in agreement with the wider literature that significant changes are made to photosystem I in response to iron limitation.

Iron limited *Coccolithus pelagicus* cells maybe attempting to enhance protein turnover rates as evidenced by the detection of ubiquitin-conjugating enzyme E2 (UCE) and the 20S proteasome subunit (20S Prot) in the iron limited subtracted library (*figure 4.3*). While to date the up-regulation in response to iron limitation of either of these transcripts has not been reported in the literature, other studies have provided evidence that protein degradation is enhanced in iron limited cells in order to recycle cellular materials as rates of photosynthesis, nitrogen assimilation and mitochondrial electron transport are impaired (Allen *et al.*, 2008). Lower protein contents in iron limited cells of the diatom *Cyclotella meneghiniana* relative to iron replete cells were also reported (Lewandowska & Kosakowska, 2004), this may imply an elevated rate of protein degradation which would be consistent with the function of some of the transcripts detected in the *C. pelagicus* subtracted library, namely the ubiquitin conjugating enzyme and the 20S proteasome subunit which both serve functions in protein degradation.

Curiously, no identifiable transcription factors or transcripts relating to calcification, iron acquisition or nitrogen assimilation were detected in the subtracted library. It is unlikely that *Coccolithus pelagicus* does not express any genes involved in enhanced iron uptake under conditions of iron limitation, it is more likely that these genes are present in the bulk of the subtracted library that could not be identified due to the limited nature of the data available not just for *Coccolithus pelagicus* but for iron limited phytoplankton in general. Further examination of the iron replete subtracted library may identify transcripts encoding proteins involved in calcification which are down regulated or absent in iron limited cells; this would concur with the observation that iron limited cells appear to be less extensively calcified (*figure 3.9*) and may be worth investigating in future. However, examination of genes differentially expressed under iron replete conditions was not the aim of this investigation.

Based on the sequence data and other observations from this investigation, some conclusions can be drawn regarding some of the ways in which *Coccolithus pelagicus* becomes acclimated to iron limitation. There is a reduction in the concentration of chlorophyll *a* per cell (*figure 3.3*) which is a general response among phytoplankton not only to iron limitation but to limitation by other nutrients also (Graziano *et al.*, 1996) and in the case of *C. pelagicus* iron limitation appears to result in malformed coccoliths or a lesser degree of calcification. This may be due to impairment of chlorophyll biosynthesis or it may be a coordinated cellular response to reduce the level of chlorophyll when the photosynthetic electron transport chain cannot process the light energy that is already entering the system. This would be consistent with the up-regulation of proteins which may serve in a photoprotective capacity such as fucoxanthin binding proteins (FucoBP), Chloroplast light harvesting protein isoform 2

(Chl LHP), Chloroplast light harvesting protein isoform 8 (CM4E12), Photosystem I protein E (PsaE). In addition to this it appears that there may be an attempt by the cells to recycle iron cofactor and amino acids through the enhancement of the protein degradation machinery as indicated by the detection of ubiquitin conjugating enzyme E2 (UCE) and 20S proteasome subunit (20S Prot) in the subtracted library.

Unfortunately, due to the limited number of sequences that could be identified a more detailed and conclusive description of *Coccolithus pelagicus* acclimation to iron limitation is difficult to provide.

Differences in specific growth rate (and hence the degree of iron limitation) can alter gene expression patterns dramatically under iron limited conditions. Although there was negligible difference in growth rate between cultures 1, 2 and 3 – culture 1 showed considerably greater up-regulation of transcripts detected in the subtracted library (*table 3C* and *figures 3.7 & 5.8*). This may be due to iron contamination sufficient to alter gene expression but not to significantly alter growth or chlorophyll *a* concentrations in cultures 2 and 3. This implies that only small differences in iron concentration are required to affect gene expression and may indicate a staggered response in gene expression alteration from low level iron deficiency to out-right iron limitation over a narrow iron concentration range. This is opposed to an all out response in which a multitude of genes are up-regulated upon iron availability dropping below a certain point.

Further study is required to examine the relationship between gene expression and specific growth rates in iron limited *Coccolithus pelagicus* cultures. The use of iron limited chemostats to provide a constant supply of culture maintained in a state of iron

limitation would be a suitable approach to examine this further. Examining the differences in gene expression and differences in the proteome of iron limited and out-right iron starved cells may also help to further elucidate the extent of the molecular changes that occur when cells are deprived of iron.

Almost two thirds of the iron limited subtracted library could not be identified by Blast analysis (*table 4A & figure 4.1*). Among this part of the library there may be sequences worthy of further investigation to assess their potential as biomarkers of iron limitation. Use of RT real time PCR and northern blots to establish the extent to which the unidentified sequences in the library are up-regulated are required, followed by studies to determine the function of these unknown proteins.

While identifying potential iron replete biomarkers was not within the scope of this investigation, the FeR1 protein (*figure 3.15*) excised from an iron replete 2D gel is absent from the iron limited 2D gel and present at quite high abundance in the iron replete gel. Despite the fact the western blotting approach described in this thesis was unsuccessful; it would be worthwhile pursuing further efforts to identify this protein in the hope of examining its expression and furthering the current understanding of the molecular changes that occur in *Coccolithus pelagicus* between states of iron sufficiency and iron limitation. In addition to this, it may be useful to produce 2D SDS gels with purified iron limited and iron replete chloroplast proteins, as some of the most up-regulated transcripts presented in this study encode proteins involved in photosynthesis. Proteomic analysis of chloroplast proteins may reveal molecular changes in response to iron limitation controlled at the translational level which could be largely un-altered at the transcriptional level. Since there is the potential for

differentially expressed chloroplast proteins regulated at the translational level to be masked by other non-chloroplast proteins in 2D SDS gels which attempt to examine the entire cell proteome, procedures to isolate intact chloroplasts from *C. pelagicus* should be optimized.

REFERENCES:

Allen, A. E., LaRoche, J., Maheswari, U., Lommer, M., Schauer, N., Lopez, P. J., Finazzi, G., Fernie, A. R. & Bowler, C. 2008. Whole-cell response of the pinnate diatom *Phaeodactylum tricornutum* to iron starvation. *PNAS*. 105 (30), 10438 – 10443.

Anderson, M. A. & Morel, F. M. M. 1980. Uptake of Fe(II) by a diatom in oxic culture medium. *Marine Biology Letters*. 1, 263-268.

Anderson, M. A. & Morel, F. M. M. 1982. The influence of aqueous iron chemistry on the uptake of iron by the coastal diatom *Thalassiosira weissflogii*. *Limnology & Oceanography*. 27, 789-813.

Balch, W.M., Holligan, P.M., Ackleson, S.G & Voss, K.J. 1991. Biological and optical properties of mesoscale coccolithophore blooms in the Gulf of Maine. *Limnology & Oceanography*. 36, 692-643.

Barber, R. T., 1992. Introduction to the WEC88 cruise: an investigation into why the equator is not greener. *Journal of Geophysical Research*. 97 (C1), 09-610.

Behrenfield, M. J. & Kolber, Z. S., 1999. Widespread iron limitation of phytoplankton in the South Pacific ocean. *Science*. 283, 840-843.

- Besse, I., Wong, J. H., Kobrehel, K. & Buchanan, B. B. 1996. Thiocalcin: A thioredoxin-linked, substrate-specific protease dependent on calcium. *PNAS*. 93, 3169-3175.
- Boekema, E. J., Hifney, A., Yakushevskaya, A. E., Piotrowski, M., Keegstra, W., Berry, S., Michel, K. P., Pistorius, E. K. & Kruijff, J. 2001. A giant chlorophyll-protein complex induced by iron deficiency in cyanobacteria. *Nature*. 412, 745 – 748.
- Boyd, P. W., A. J. Watson, C. S. Law, E. R. Abraham, T. Trull, R. Murdoch, D. C. E. Bakker, A. R. Bowie, K. O. Buesseler, H. Chang, M. Charette, P. Croot, K. Downing, R. Frew, M. Gall, M. Hadfield, J. Hall, M. Harvey, G. Jameson, J. LaRoche, M. Liddicoat, R. Ling, M. T. Maldonado, R. M. McKay, S. Nodder, S. Pickmere, R. Pridmore, S. Rintoul, K. Safi, P. Sutton, R. Strzepek, K., Tanneberger, S. Turner, A. Waite, and J. Zeldis. 2000. A Mesoscale Phytoplankton Bloom in the Polar Southern Ocean Stimulated by Iron fertilization. *Nature*, 407, 695-702.
- Boyd, P. W. & Law, C. S. 2001. The Southern Ocean Iron RElease Experiment (SOIREE) – introduction and summary. *Deep Sea Research II*. 48, 2425 – 2438.
- Boye, M., van den Berg, C.M.G. 2000. Iron availability and the release of iron-complexing ligands by *Emiliania huxleyi*. *Marine Chemistry*. 70, 277-287.
- Bratbak, G., Wilson, W. & Heldal, M. 1996. Viral control of *Emiliania huxleyi* blooms? *Journal of Marine Systems*. 9, 78-81.

- Brown, P.R., Burnett, J.A. & Gallagher, L.T. 1992. Calcareous nannoplankton evolution. *Memorie di Scienze Geologiche*. 43, 1-17.
- Campbell, W. H., 1999. Nitrate reductase structure, function and regulation: bridging the gap between biochemistry and physiology. *Annual Review of Plant Physiology. Plant Molecular Biology*. 50, 277-303.
- Cho, M., Wong, J. H., Marx, C., Jiang, W., Lemaux, P. G. & Buchanan, B. B. 1999. Overexpression of thioredoxin h leads to enhanced activity of starch debranching enzyme (pullulanase) in barely grain. *PNAS*. 96, No. 25, 14641-14646.
- Coale, K. H., Johnson, K. S., Fitzwater, S. E., Gordon, R. M., Tanner, S., Chavez, F. P., Ferioli, L., Sakamoto, C., Rogers, P., Millero, F., Steinberg, P., Nightingale, P., Cooper, D., Cochlan, W. P., Landry, M. R., Constantinou, J., Rollwagen, G., Trasvina, A. & Kudela, R. 1996. A massive phytoplankton bloom induced by an ecosystem scale iron fertilisation experiment in the equatorial Pacific Ocean. *Nature*. 383, 495-501.
- Course, P.A., Tarran, G.A. & Green, J.C. 1994. The life history of *Emiliana huxleyi*: evidence for haploid and diploid states using flow cytometry. *Phycologist*. 37, 25.
- Davey, M., Geider, R. J. 2001. Impact of iron limitation on the photosynthetic apparatus of the diatom *Chaetoceros muelleri* (Bacillariophyceae). *Journal of Phycology*. 37, 987-1000.

Delille, B. 2005. Response of primary production and calcification to changes of pCO₂ during experimental blooms of the coccolithophorid *Emiliana huxleyi*. *Global Biogeochemical Cycles*. 19, GB2023, doi: 10.1029/2004GB002318.

Dietz, K. 2003. Plant peroxiredoxins. *Annual Review of Plant Biology*. 54, 93-107.

DiTullio, G., Garcia, N., Riseman, S. & Sedwick, P. 2007. Effects of iron concentration on pigment composition in *Phaeocystis antarctica* grown at low irradiance. *Biogeochemistry*. 83, No. 1-3, 71-81(11).

Doucette, G.J, Erdner, D.L., Peleato, M.L., Hartman, J.J., Anderson, D.M. 1996. Quantitative analysis of iron stress related proteins in *Thalassiosira weissflogii*: measurement of flavodoxin and ferredoxin using HPLC. *Marine Ecology Progress Series*. 130, 269-276.

Duce, R.A., & Tindale, N.W., 1991. Atmospheric transport of iron and its deposition in the ocean. *Limnology and Oceanography*. 36, 1715-1726.

Eldridge, M.L., Trick, C.G., Alm, M.B., DiTullio, G.R., Rue, E.L., Bruland, K.W., Hutchins, D.A., & Wilhelm, S.W. 2004. Phytoplankton community response to a manipulation of bioavailable iron in HNLC waters of the subtropical Pacific Ocean. *Aquatic Microbial Ecology*. 35 (1), 79-91.

- Erdner, D.L., Price, N.M., Doucette, G.J., Peleato & Anderson, D.M. 1999. Characterization of ferredoxin and flavodoxin as markers of iron limitation in marine phytoplankton. *Marine Ecology Progress Series*. 184, 43-53.
- Falkowski, P.G. and Raven J.A. 1997. Aquatic Photosynthesis. Blackwell. pp.375
- Falkowski, P.G., Katz, M.E., Knoll, A.H., Quigg, A., Raven, J.A., Schofield, O., & Taylor F.J.R. 2004. The evolution of modern eukaryotic phytoplankton. *Science*. 305, 354-360.
- Fischer, N., Hippler, M., Setif, P. Jacquot, J. P. & Rochaix, J. D. 1998. The PsaC subunit of photosystem I provides an essential lysine residue for fast electron transfer to ferredoxin. *The EMBO Journal*. 17 (4), 849-858.
- Fromme, P., Melkozernov, A., Jordan, P. & Krauss, N. 2003. Structure and function of photosystem I: interaction with its soluble electron carriers and external antenna systems. *FEBS Letters*. 555, 40-44.
- Geider, R.J. & La Roche, J. 1994. The role of iron in phytoplankton photosynthesis, and the potential for iron-limitation of primary productivity in the sea. *Photosynthesis Research*. 39: 275-301.
- Geiß, U., Vinnemeier, J., Kunert, A., Lindner, I., Gemmer, B., Lorenz, M., Hagemann, M., Schoor, A. 2001. Detection of the *isiA* gene across cyanobacterial strains. *Applied and Environmental Microbiology*. 67 (11), 5247-5253.

Gerringa, L. J. A., de Baar, H. J. W., & Timmermans, K. R. 2000. A comparison of iron limitation of phytoplankton in natural oceanic waters and laboratory media conditioned with EDTA. *Marine Chemistry*. 68, 335-346.

Gobler, C. J. *et al.* 1997. Elemental release and bioavailability following viral lysis of a marine chrysophyte. *Limnology & Oceanography*. 42, 1492-1504 .

Golbeck, J.H., & Bryant, D.A. 1991. Photosystem I. *Current Topics in Bioenergetics*. 16, 83-177.

Graziano, L.M., La Roche, J., Geider, R.J. 1996. Physiological responses to phosphorus limitation in batch and steady state cultures of *Dunaliella tertiolecta* (chlorophyta): a unique stress protein as an indicator of phosphate deficiency. *Journal of Phycology*. 32 (5), 825-838.

Greene, R. M., Geider, R. J. & Falkowski, P. G. 1991. Effect of iron limitation on photosynthesis in a marine diatom. *Limnology & Oceanography*. 36:1772–82.

Greene, R. M., Geider, R. J., Kolber, Z. & Falkowski, P. G. 1992. Iron-induced changes in light harvesting and photochemical energy conversion processes in eukaryotic marine algae. *Plant Physiology*. 100:565–75.

Green, J.C., Course, P.A. & Tarran, G.A. 1996. The life cycle of *Emiliania huxleyi*: a brief review and a study of relative ploidy levels analysed by flow cytometry. *Journal of Marine Systems*. 9: 33-44.

Gregson, A.J., Green, J.C., Leadbeater, B.S.C. 1993. Structure and physiology of the haptonema in *Chrysochromulina* (Prymnesiophyceae). I. Fine structure of the flagella/haptonemal root system in *C. acantha* and *C. simplex*. *Journal of Phycology*. 29 (5), 674-686.

Guikema, J. A. 1987. Differential effects of iron and chlorophyll in the control of membrane synthesis in *Anacystis nidulans*. In. Diggins, J. [Ed.] *Progress in Photosynthesis Research*, Vol. 4. Martinus Nijhoff Publishers, Dordrecht, The Netherlands, pp.785-788.

Harris, R. 1994. Zooplankton grazing on the coccolithophore *Emiliana huxleyi* and its role in inorganic carbon flux. *Marine Biology*. 119, 431-439.

Head, E. J. H. & Harris, L. R. 1994. Feeding selectivity by copepods grazing on natural mixtures of phytoplankton determined by HPLC analysis of pigments. *Marine Ecology Progress Series*. 110, 75-83.

Hernandez, M.T., Mills, R.A., & Pancost, R.D. 2008. Algal biomarkers in surface waters around the Crozet plateau. *Organic Geochemistry*. 39 (8), 1051-1057.

Hoge, F., Swift, R., Yungel, J., Turner, S., Nightingale, P., Hatton, A., Liss, P. & Tindale, N. W. 1994. Testing the iron hypothesis in ecosystems of the equatorial Pacific Ocean. *Nature*. 371, 123–129.

Holligan, P.M., Viollier, M., M., Harbour, D.S., Camus, P. & Champagne-Phillipe, M. 1983. Satellite and ship studies of coccolithophore production along a continental shelf edge. *Nature* 304, 339-342.

Hudson, R. J. M. & Morel, F. M. M. 1990. Iron transport in marine phytoplankton: kinetics of cellular and medium coordination reactions. *Limnology & Oceanography*. 35, 1002-1020.

Hudson, R. J. M. & Morel, F. M. M. 1993. Trace metal transport by marine microorganisms: implications of metal coordination kinetics. *Deep Sea Research I*. 40, 129-150.

Hutchins, D. A. & Bruland, K. W. 1994. Grazer-mediated regeneration and assimilation of Fe, Zn and Mn from planktonic prey. *Marine Ecology Progress Series*. 110, 259-269.

Hutchins, D. A., Witter, A. E., Butler, A. & Luther III, G. W. 1999. Competition among marine phytoplankton for different chelated iron species. *Nature*. 400, 858-861.

Hutchins, D. A., Franck, V. M., Brzezinski, M. A. & Bruland, K. W. 1999(A). Inducing phytoplankton iron limitation in iron-replete coastal waters with a strong chelating ligand. *Limnology and Oceanography*. 44(4), 1009-1018.

Ihalainen, J. A., D'Haene, S., Yeremenko, N., van Roon, H., Arteni, A. A., Boekema, E. J., van Grondelle, R., Matthijs, H. C. P. & Dekker, J. P. 2005. Aggregates of the chlorophyll binding protein IsiA (CP43') dissipate energy in cyanobacteria.

Biochemistry. 44, 10846 – 10853.

Inda, L.A., & Peleato, M.L. 2003. Development of an ELISA approach for the determination of flavodoxin and ferredoxin as markers of iron deficiency in phytoplankton. *Phytochemistry*. 63 (3), 303-308.

Inouye, I., & Kawachi, M. 1994. The haptonema. In: Green J.C., Leadbeater, B.S.C. (eds) The haptophyte algae. The Systematics Association Special Volume No 51, Clarendon Press, Oxford, 73-89.

Jeanjean, R., Latifi, A., Matthijs, H.C.P. & Havaux, M. 2008. The PsaE subunit of photosystem I prevents light-induced formation of reduced oxygen species in the cyanobacterium *Synechocystis* sp. PCC 6803. *Biochimica et Biophysica Acta*. 1777, 308 - 316

Jones, G.J., Palenik B.P. & Morel F.M.M. 1987. Trace metal reduction by phytoplankton: The role of plasmalemma redox enzymes. *Journal of Phycology*. 23, 237-244.

Kim, S.A., & Guerinot, M.L. 2007. Mining iron: Iron uptake and transport in plants. *FEBS Letters*. 581, 2273-2280.

- Kutzki, C. Masepohl, B. & Bohme, H. 1998. The isiB gene encoding flavodoxin is not essential for photoautotrophic iron limited growth of the cyanobacterium *Synechocystis* sp. strain PCC 6803. *FEMS microbiology letters*. 160, 231-235.
- LaRoche, J., Murray, H., Orellana, M., Newton, J. 1995. Flavodoxin expression as an indicator of iron limitation in marine diatoms. *Journal of Phycology*. 31, 520-530.
- Laudenbach, D.E., Reith, M.E & Straus, N.A. 1988. Isolation, sequence analysis, and transcriptional studies of the flavodoxin gene from *Anacystis nidulans* R2. *Journal of Bacteriology*. Vol 170, No.1: 258-265.
- Leadbeater, B.S.C., & Manton, I. 1969. *Chrysochromulina camella* sp. nov. and *C. cymbium* sp. nov., two new relatives of *C. strobilus* Parke and Manton. *Archives of Microbiology*. 68 (2), 116-132.
- Lemaire, S. D., Guillon, B., Le Marechal, P., Keryer, E., Miginiac-Maslow, M. & Decottignies, P. 2004. New thioredoxin targets in the unicellular photosynthetic eukaryote *Chlamydomonas reinhardtii*. *PNAS*. 101, 19, 7475-7480.
- Leynaert, A., Bucciarelli, E., Claquin, P., Dugdale, R. C., Martin-Jezequel, V., Podaven, P. & Ragueneau, O. 2004. Effect of iron deficiency on diatom cell size and silicic acid uptake kinetics. *Limnology and Oceanography*. 49(4), 1134-1143.
- Liu, X., Zhao, J., Wu, Q. 2006. Biogenesis of chlorophyll binding proteins under iron stress in *Synechocystis* sp. PCC 6803. *Biochemistry (Moscow)*. 71 (1), 101-104.

- Lynnes, J. A., Derzaph, T. L. M. & Weger, H. G. 1998. Iron limitation results in induction of ferricyanide reductase and ferric chelate reductase activities in *Chlamydomonas reinhardtii*. *Planta*. 204, 360-365.
- Mahowald, N., Kohfeld, M., Hansson, Y., Balkanski, Y., Harrison, S., Prentice, C., Schulz, M. & Rodhe, H. 1999. Dust sources and deposition during the last glacial maximum and current climate: A comparison of model results with paleodata from ice cores and marine sediments. *Journal of Geophysical Research*. 104, 15895 – 15916.
- Maldonado, M. T. & Price, N. M., 1996. Influence of N substrate on Fe requirements of marine centric diatoms. *Marine Ecology Progress Series*. 141, 161-72.
- Maldonado, M. T. & Price, N. M. 2001. Reduction and transport of organically bound iron by *Thalassiosira oceanica* (bacillariophyceae). *Journal of Phycology*. 37, 298-309.
- Malin, G., Turner, S.M. & Liss, P.S. 1992. Sulfur: the plankton/climate connection. *Journal of Phycology*. 28, 590-597.
- Marius, N., Muller, Avan, N., Anita, & LaRoche, J. 2008. Influence of cell cycle phase on calcification in the coccolithophore *Emiliana huxleyi*. *Limnology and Oceanography*. 53 (2), 506-512.
- Manton, I. 1964. Further observations on the fine structure of the haptonema in *Prymnesium parvum*. *Archives of Microbiology*. 49 (4), 315-330.

Marchetti, A., Parker, M. S., Moccia, L. P., Lin, E. O., Arrieta, A. L., Ribalet, F., Murphy, M. E. P., Maldonado, M. T & Armbrust, V. E. 2009. Ferritin is used for iron storage in bloom-forming marine pennate diatoms. *Nature*. 457, 467-470.

Marschner, H., & Romheld, V. 1994. Strategies of plants for acquisition of iron. *Plant and Soil*. 165 (2), 261-274.

Martin, J. H., 1990. Glacial-interglacial CO₂ change: the iron hypothesis. *Paleoceanography*. 5, 1-13.

Martin, J. H., Coale, K. H., Johnson, K. S., Fitzwater, S. E., Gordon, R. M., Tanner, S. J., Hunter, C. N., Elrod, V. A., Nowicki, J. L., Coley, T. L., Barber, R. T., Lindley, S., Watson, A. J., Van Scoy, K., Law, C. S., Liddicoat, M. I., Ling, R., Stanton, T., Stockel, J., Collins, C., Anderson, A., Bidigare, R., Ondrusek, M., Latasa, M., Millero, F. J., Lee, K., Yao, W., Zhang, J. Z., Friederich, G., Sakamoto, C., Chavez, F., Buck, K., Kolber, Z., Greene, R., Falkowski, P., Chisholm, S. W., Hoge, F., Swift, R., Yungel, J., Turner, S., Nightingale, P., Hatton, A., Liss, P. & Tindale, N. W. 1994. Testing the iron hypothesis in ecosystems of the equatorial Pacific Ocean. *Nature*. 371, 123–129.

McIntyre, A., Ruddiman, W.F., Jantzen, R. 1972. Southward penetration of the North Atlantic Polar Front: faunal and floral evidence of large-scale surface water mass movements over the last 225,000 years. *Deep Sea Research*. 19, 61-77.

McKay, R. M. L., Geider, R. J. & La Roche, J. 1997. Physiological and biochemical response of the photosynthetic apparatus of two marine diatoms to Fe stress. *Plant Physiology*. 114, 615-622.

McKay, R. M. L., Geider, R. J. & La Roche, J. 1997. Physiological and biochemical response of the photosynthetic apparatus of two marine diatoms to Fe stress. *Plant Physiology*. 114, 615-622.

McKay, R.L., La Roche, J., Yakunin, A.F., Durnford, D.G. & Geider, R.J. 1999. Accumulation of ferredoxin and flavodoxin in a marine diatom in response to Fe. *Journal of Phycology*, 35, 510-519.

Moore, K.J., Doney, S.C., Glover, D.M., Fung, I.Y., 2002. Iron cycling and nutrient patterns in surface waters of the World Ocean. *Deep – Sea Research II*. 49, 463-507.

Naito, K., Imai, I & Nakahara, H. 2008. Complexation of iron by microbial siderophores and effects of iron chelates on the growth of marine microalgae causing red tides. *Phycological Research*. 56 (1), 58-67.

Mori, S. 1999. Iron acquisition by plants. *Current Opinion in Plant Biology*. 2, 250-253.

Neilands, J. B. 1984. Methodology of siderophores. *Structure. Bonding*. 58, 1-24.

- Paasche, E. & Brubak, S. 1994. Enhanced calcification in the coccolithophorid *Emiliana huxleyi* (Haptophyceae) under phosphorus limitation. *Phycologia*. 33, 324-330.
- Paasche, E. 2002. A review of the coccolithophorid *Emiliana huxleyi* (Prymnesiophyceae), with particular reference to growth, coccoliths formation, and calcification-photosynthesis interactions. *Phycologia*. 40 (6), 503-529.
- Ratledge, C., P. V. Patel & J. Mundy. 1982. Iron transport in *Mycobacterium smegmatis*: The location of mycobactin by electron microscopy. *Journal of General Microbiology*. 128, 1559-1565.
- Raven, J. A., Wollenwever, B. & Handley, L. L., 1992. A comparison of ammonium and nitrate as nitrogen sources for photolithotrophs. *New Phytol.* 121, 19-32.
- Rayns, D.G. 1962. Alternation of generations in a coccolithophorid, *Cricoshaera carterae* (Braarud and Fagerl.) Braarud. *Journal of the Marine Biological Association*. 42: 481-484.
- Rea, D.K. 1994. The paleoclimatic record provided by eolian deposition in the deep sea: the geologic history of wind. *Reviews of Geophysics*. 32, 159-195.
- Rhiel, E., & Bryant, D.A. 1993. Nucleotide sequence of the *psaE* gene of cyanobacterium *Synechococcus* sp. PCC 6301. *Plant Physiology*. 101, 701-702.

- Riebesell, U. 2004. Effects of CO₂ enrichment on marine phytoplankton. *Journal of Oceanography*. 60, 719-729.
- Riegmann, R., Stolte, W., Noordeloos, A., & Slezak, D. 2000. Nutrient uptake and alkaline phosphatase (EC 3:1:3:1) activity of *Emiliana huxleyi* (Prymnesiophyceae). *Journal of Phycology*. 36, 87-96.
- Robertson, J.E., Robinson, C., Turner, D.R., Holligan, P., Watson, A.J., Boyd, P., Fernandez, E., & Finch, M. 1994. The impact of a coccolithophore bloom on oceanic carbon uptake in the northeast Atlantic during summer 1991. *Deep Sea Research*. 41 (2), 297-314.
- Rousseau, F., Setif, P. & Lagoutte, B. 1993. Evidence for the involvement of PSI-E subunit in the reduction of ferredoxin by photosystem I. *The EMBO Journal*. 12 (5), 1755 – 1765.
- Rue, E. L. & Bruland, K. W. 1995. Complexation of iron(III) by natural organic ligands in the Central North Pacific as determined by a new competitive ligand equilibration / adsorptive cathodic stripping voltametric method. *Marine chemistry*. 50, 117-138.
- Rueter, J. G. & Ades, D. R. 1987. The role of iron nutrition in photosynthesis and nitrogen assimilation in *Scenedesmus quadricauda* (Chlorophyceae). *Journal of Phycology*, 23, 452-457.

- Sarcina, M., & Mullineaux, C.W. 2004. Mobility of the IsiA chlorophyll-binding protein in cyanobacterial thylakoid membranes. *Journal of Biological Chemistry*. 279 (35), 36514-36518.
- Schmidt, W. 2003. Iron solutions: acquisition strategies and signalling pathways in plants. *Trends in Plant Science*. 8 (4), 188-193.
- Seuront, L., Lacheze, C., Doubell, M.J., Seymour, J.R., Van Dongen-Vogels, V., Newton, K., Alderkamp, A.C., & Mitchell, J.G. 2007. The influence of *Phaeocystis galbosa* on microscale spatial patterns of chlorophyll *a* and bulk-phase seawater viscosity. *Biogeochemistry*. 83, 173-188.
- Setif, P., Fischer, N., Lagoutte, B., Bottin, H. & Rochaix, J. D. 2002. The ferredoxin docking site of photosystem I. *Biochimica et Biophysica Acta*. 1555, 204-209.
- Sheterline, P., & Sparrow, J.C. 1994. Actin. *Protein profile*. 1, 1-121.
- Simon, N., Cras, A., Fouldon, E., & Lemee, R. 2009. Diversity and evolution of marine phytoplankton. *Comptes Rendus Biologies*. 332 (2-3), 159-170.
- Singh, A.K., & Sherman, L.A. 2007. Reflections on the function of IsiA, a cyanobacterial stress-inducible, chl-binding protein. *Photosynthesis Research*. 93, 17-25.

Soria-Dengg S, Horstmann U. 1995. Ferrioxamines B and E as iron sources for the marine diatom *Phaeodactylum tricornutum*. *Marine Ecology Progress Series*. 127, 269-277.

Spilmont, N., Denis, L., Artigas, L.F., Caloin, F., Courcot, L., Creach, A., Desroy, N., Gevaert, F., Hacquebart, P., Hubas, C., Janquin, M., Lemoine, Y., Luczak, C., Migne, A., Rauch, M., & Davoult, D. 2009. Impact of the *Phaeocystis galbosa* spring bloom on the intertidal benthic compartment in the eastern English Channel: A synthesis. *Marine Pollution Bulletin*. 58 (1), 55-63.

Stefels, J. & van Leeuwe, M., A. 2002. Effects of iron and light stress on the biochemical composition of antarctic *Phaeocystis* sp. (prymnesiophyceae. I. Intracellular DMSP concentrations. *Journal of Phycology*. 34(3), 486-495.

Strom, S. L. 1993. Production of phaeopigments by marine protozoa: results of laboratory experiments analyzed by HPLC. *Deep Sea Research I*. 40, 57-80.

Tegen, I., Fung, I.y., 1994. Modelling of mineral dust in the atmosphere: sources, transport and optical thickness. *Journal of Geophysical Research*. 99, 22897-22914.

Tegen, I., Fung, I.Y., 1995. Contribution to the atmospheric mineral aerosol load from land surface modifications. *Journal of Geophysical Research*. 100, 18707-18726.

Tomitani, A. 2006. Origin and early evolution of chloroplasts. *Paleontological Research*. 10 (4), 283-297.

van Leeuwe, M. A. & Stefels, J. 1998. Effects of iron and light stress on the biochemical composition of Antarctic *Phaeocystis* sp. (Prymnesiophyceae). II. pigment composition. *Journal of Phycology*. 34, 496 – 503.

Varsano, T., Wolf, S. G., & Pick, U. 2006. A chlorophyll a/b-binding protein homolog that is induced by iron deficiency is associated with enlarged photosystem I units in the eucaryotic alga *Dunaliella salina*. *The Journal of Biological Chemistry*. 281 (15), 10305 – 10315.

Vaulot, D., Birrien, J.L., Marie, D., Cassotti, R., Veldhuis, M.J.W., Kraay, G.W. & Chretiennot-Dinet, M.J. 1994. Morphology, ploidy, pigment composition, and genome size of cultured strains of *Phaeocystis* (Prymnesiophyceae). *Journal of Phycology*. 30, 1022-1035.

Weger, H. G., 1999. Ferric and cupric reductase activities in the green alga *Chlamydomonas reinhardtii*: experiments using iron limited chemostats. *Planta*. 207, 377-384.

Wells, M.L., 1999. Manipulating iron availability in nearshore waters. *Limnology and Oceanography*. 44, 1002– 1008.

Wells, M. L. & Trick, C. G., 2004. Controlling iron availability to phytoplankton in iron-replete coastal waters. *Marine chemistry*. 86, 1-13.

Witter, A. E. & Luther, G. W. 1998. Variation in Fe-organic complexation with depth in the Northwestern Atlantic Ocean as determined using a kinetic approach. *Marine chemistry*. 62, 241-258.

Wu, J. & Luther, G. W. 1995. Complexation of Fe(III) by natural organic ligands in the Northwest Atlantic Ocean by a competitive ligand method and a kinetic approach. *Marine Chemistry*. 50, 159-177.

Wyman, M. & Bird, C. 2007. Lack of control of nitrite assimilation by ammonium in an oceanic picocyanobacterium, *Synechococcus* sp. Strain WH 8103. *Applied and Environmental Microbiology*. 73:9, 3028-3033.

Yeremenko, N., Kouril, R., Ihalainen, J.A., D'Haene, S., van Oosterwijk, N., Andrizhiyevskaya, E.G., Keegstra, W., Dekker, H.L., Hagemann, M., Boekema, E.J., Matthijs, H.C.P., Dekker, J.P. 2004. Supramolecular organisation and dual function of the IsiA chlorophyll binding protein in cyanobacteria. *Biochemistry*. 43 (32), 10308-10313.

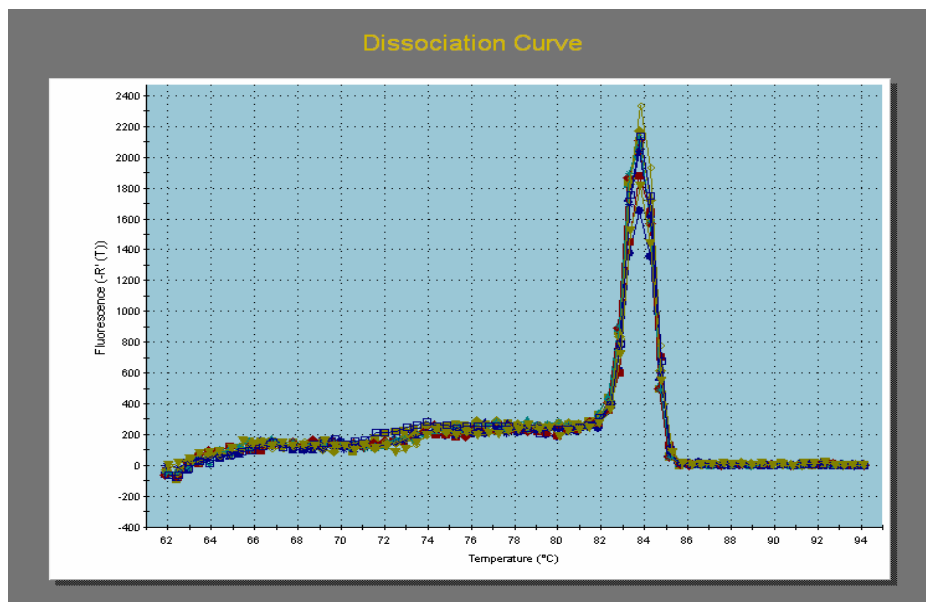
Young, J.R., Bown, P.R. & Burnett, J.A. 1994. Palaeontological perspectives. In the Haptophyte Algae (J.C. Green and B.S.C Leadbeater, eds). *The Systematics Association Special Volume*. 51, 379-392. Oxford: Clarendon Press.

- Yu, L., Zhao, J., Muhlenhoff, U., Bryant, D.A., & Golbeck, J.H. 1993. *Plant Physiology*. 103, 171-180.
- Zechel, K., & Weber, K. 1978. Actins from mammals, bird, fish and slime mould characterised by isoelectric focusing in polyacrylamide gels. *European Journal of Biochemistry*. 89, 105-112.
- Zhao, J., Snyder, W.B., Muhlenhoff, U., Rhiel, E., Warren, P.V., Golbeck, J.H., Bryant, D.A. 1993. Cloning and characterisation of the *psaE* gene of the cyanobacterium *Synechococcus* sp. PCC 7002: characterisation of a *psaE* mutant and overproduction of the protein in *Escherichia coli*. *Molecular Microbiology*. 9 (1), 183-194.
- Zondervan, I. 2007. The effect of light, macronutrients, trace metals and CO₂ on the production of calcium carbonate and organic carbon in coccolithophores – a review. *Deep Sea Research II*. 41, 521-537.

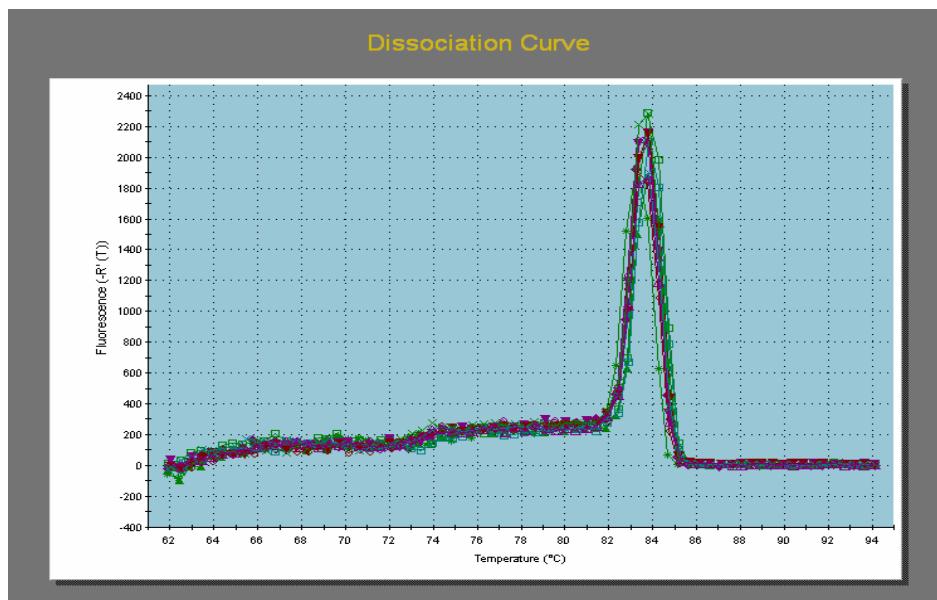
APPENDIX

RT real time PCR dissociation curves:

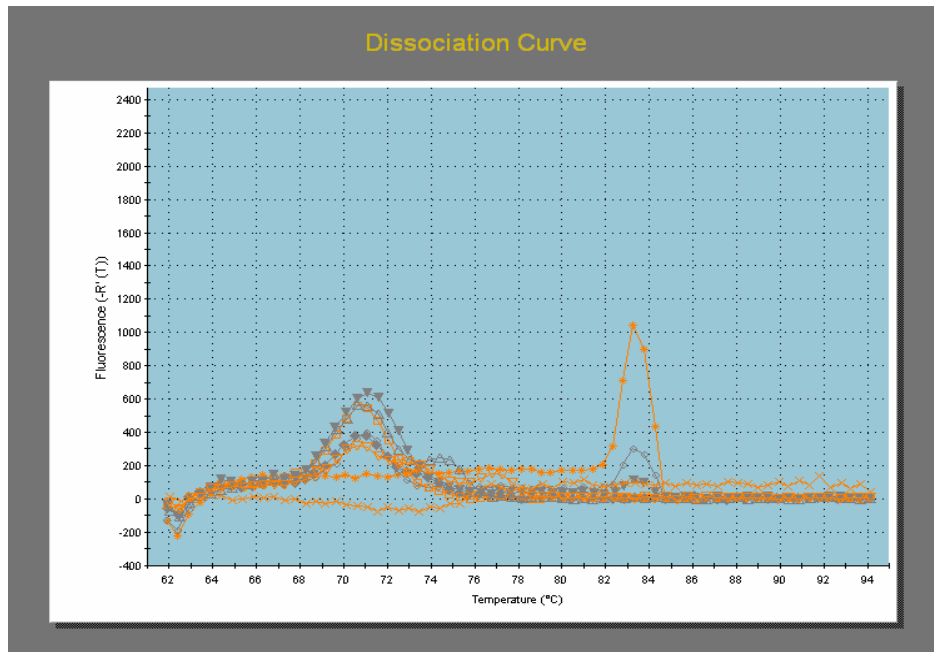
PMP iron replete cDNA



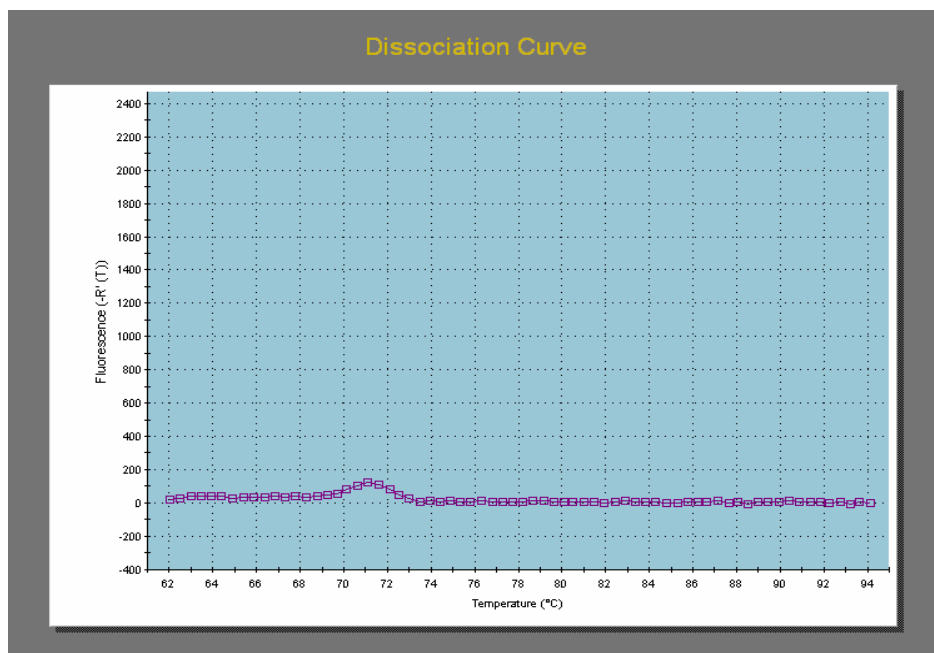
PMP iron limited cDNA



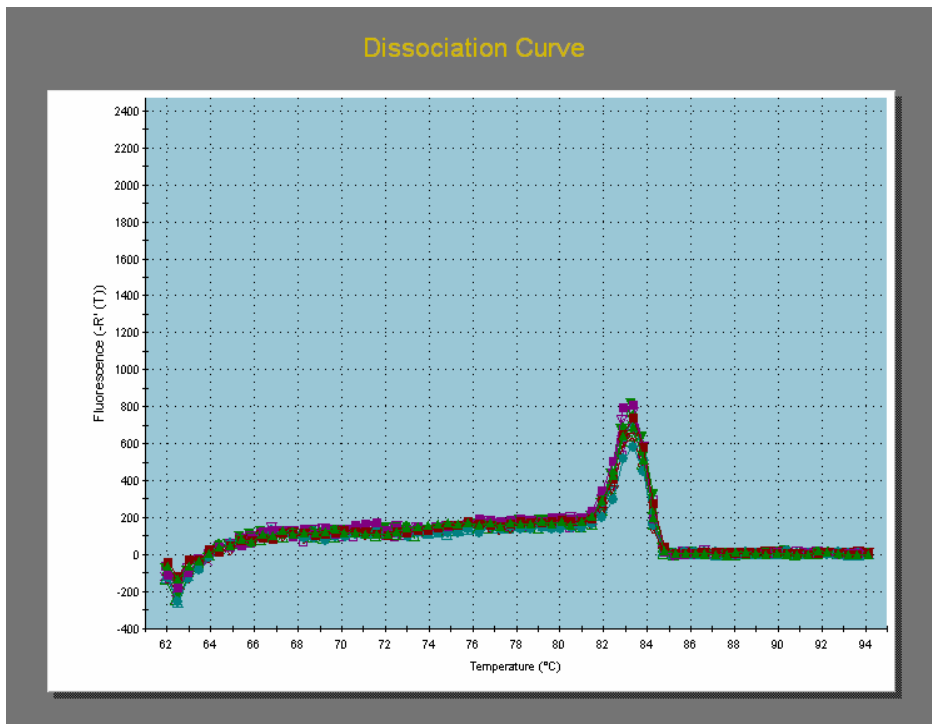
PMP -RT controls



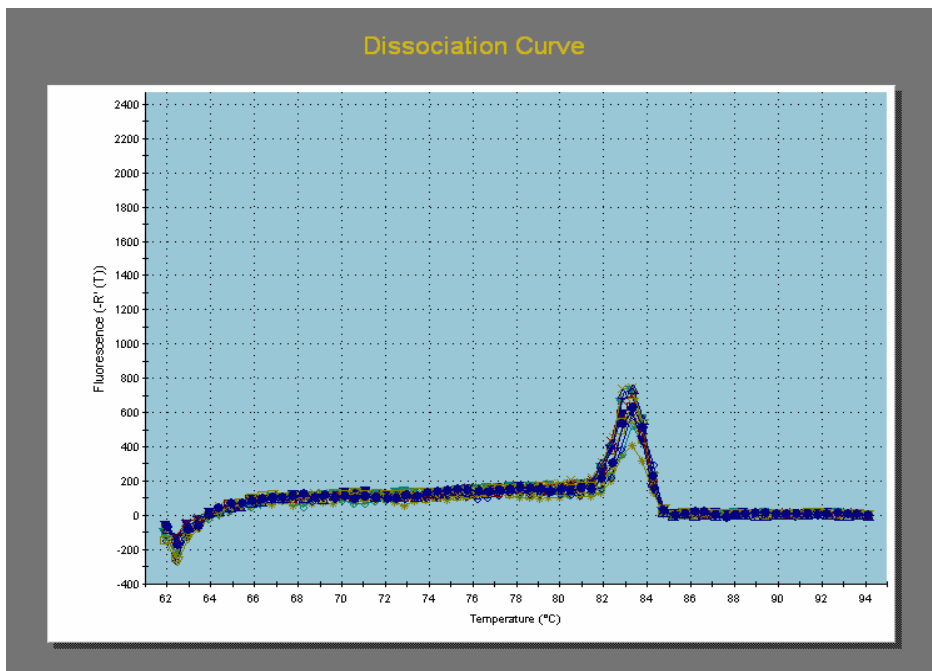
PMP Negative controls



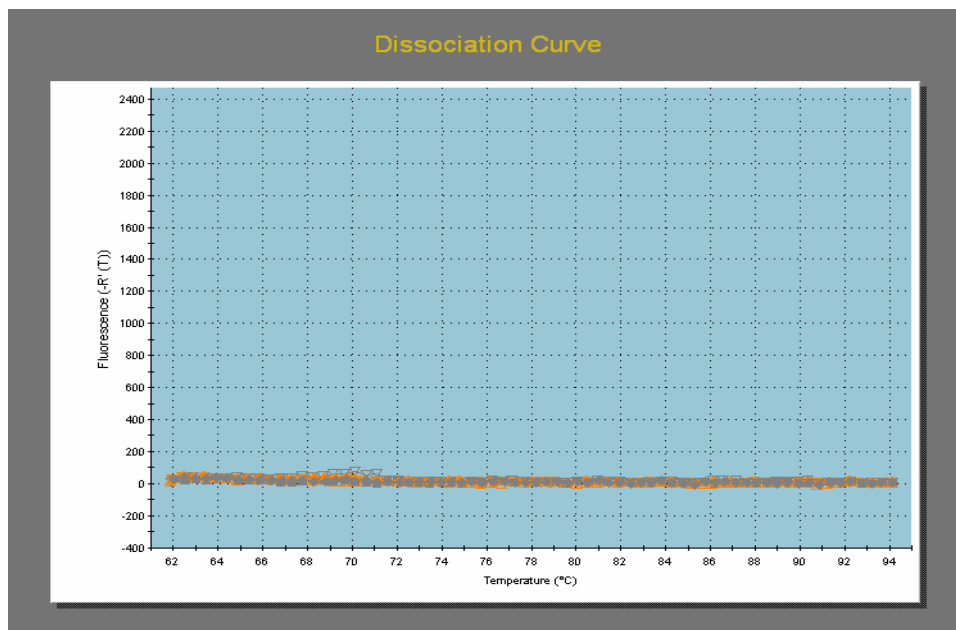
Fucoxanthin binding protein (6) iron replete cDNA



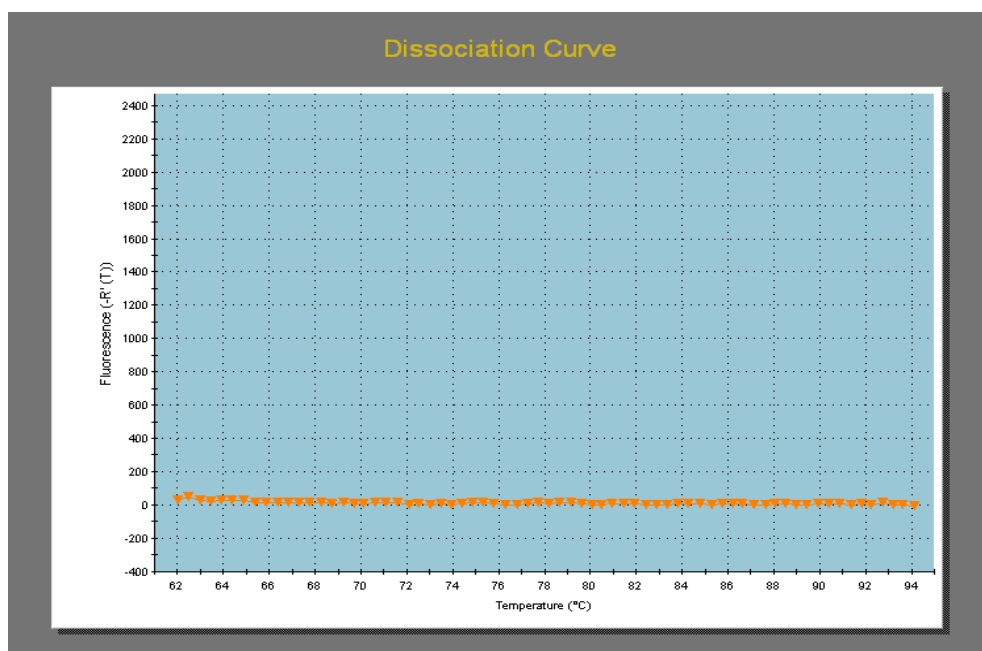
Fucoxanthin binding protein (6) iron limited cDNA



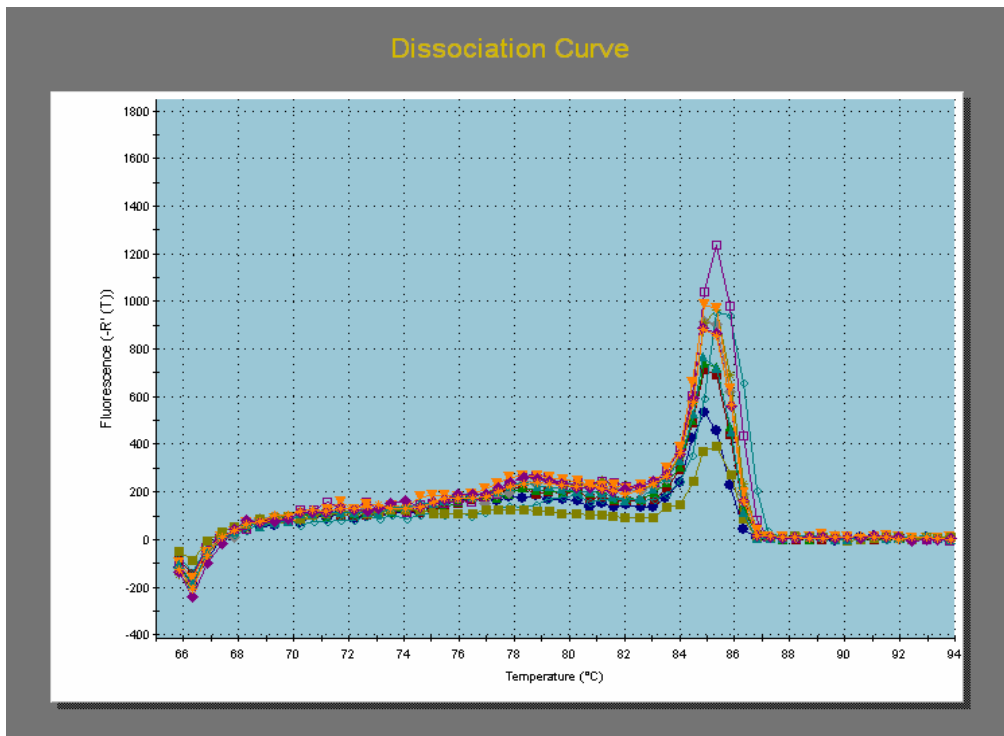
Fucoanthin binding protein (6) -RT controls



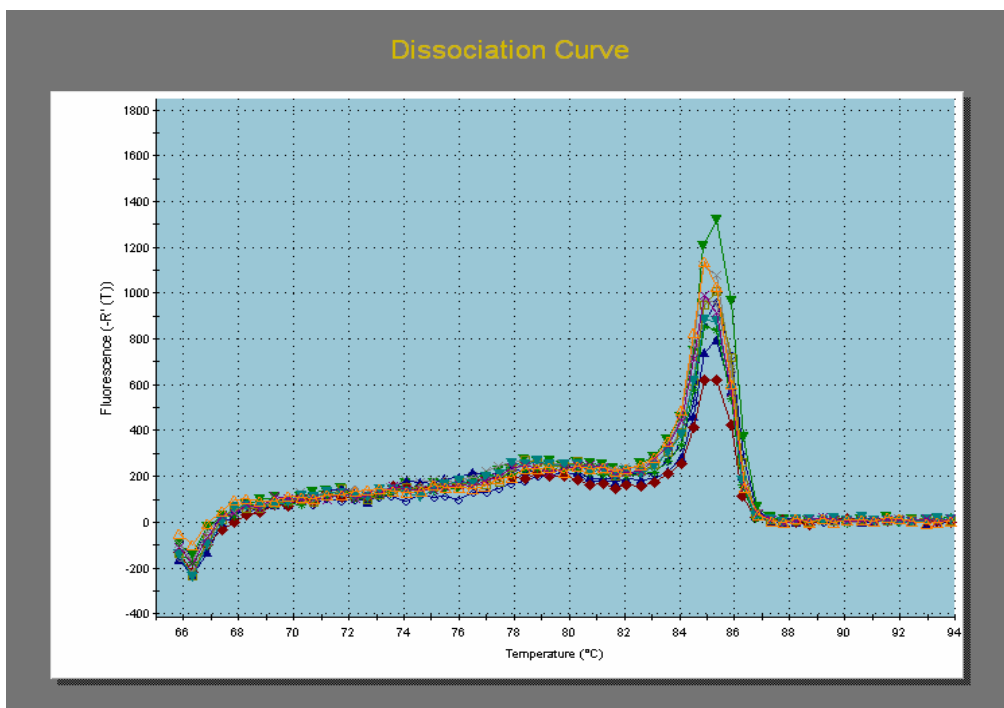
Fucoanthin binding protein (6) negative controls



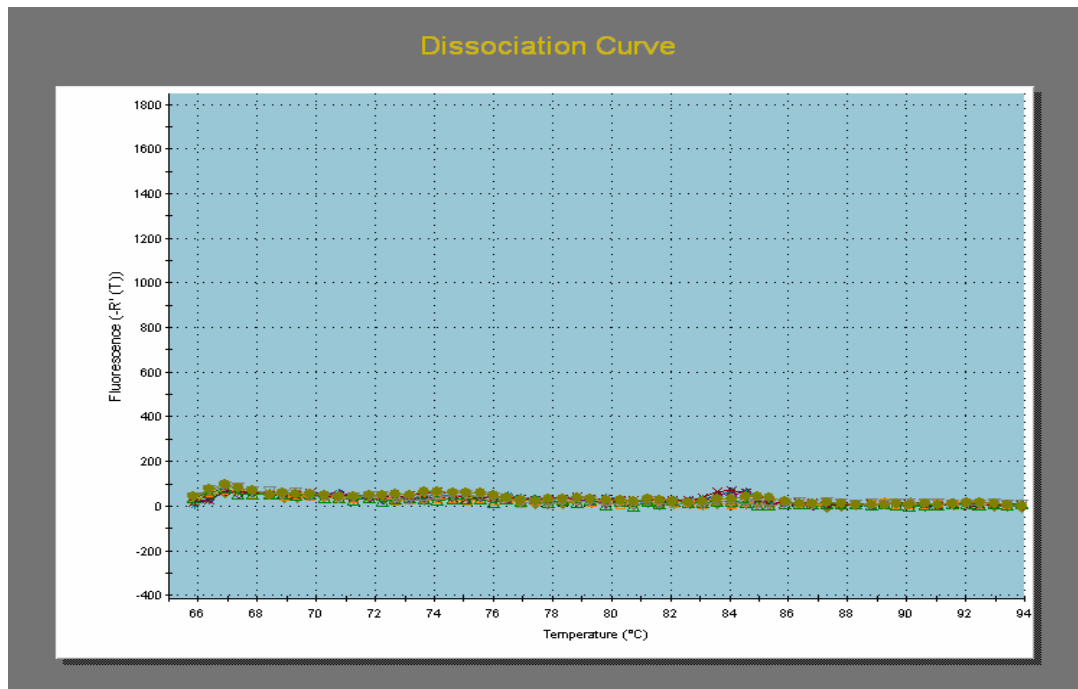
PsaE iron replete cDNA



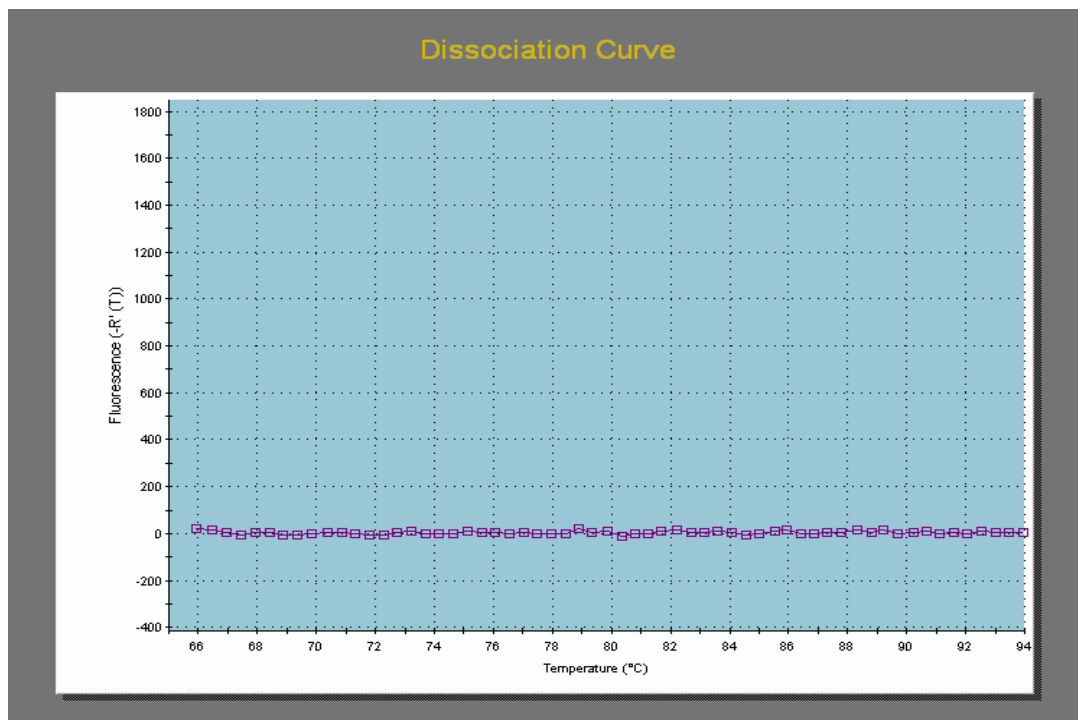
PsaE iron limited cDNA



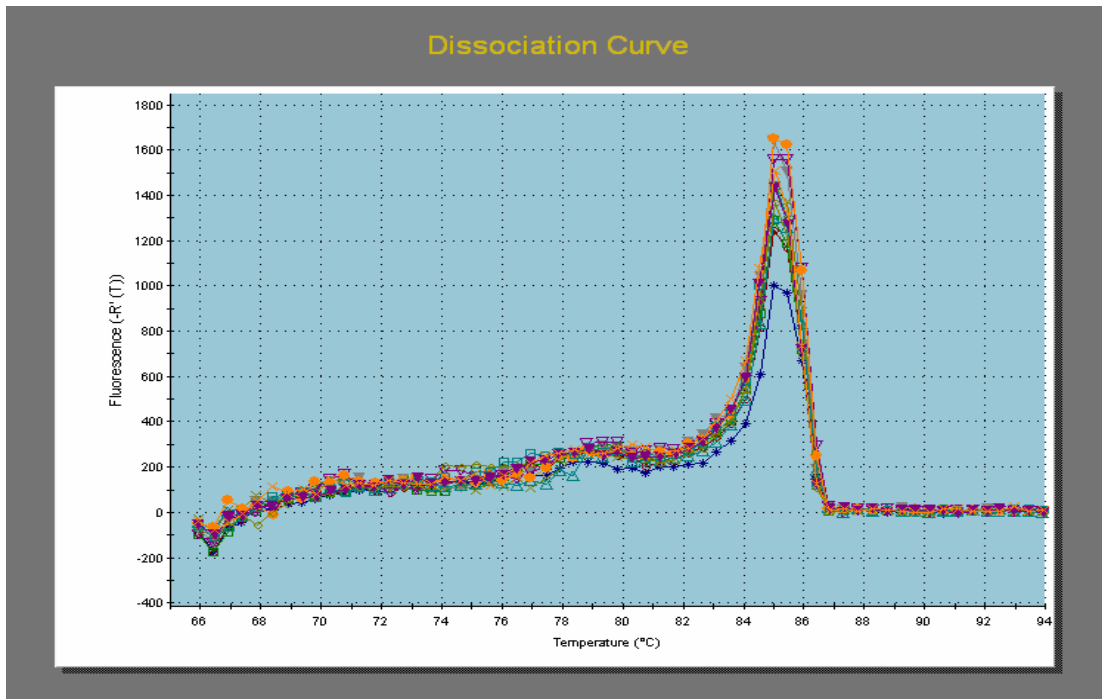
PsaE - RT controls



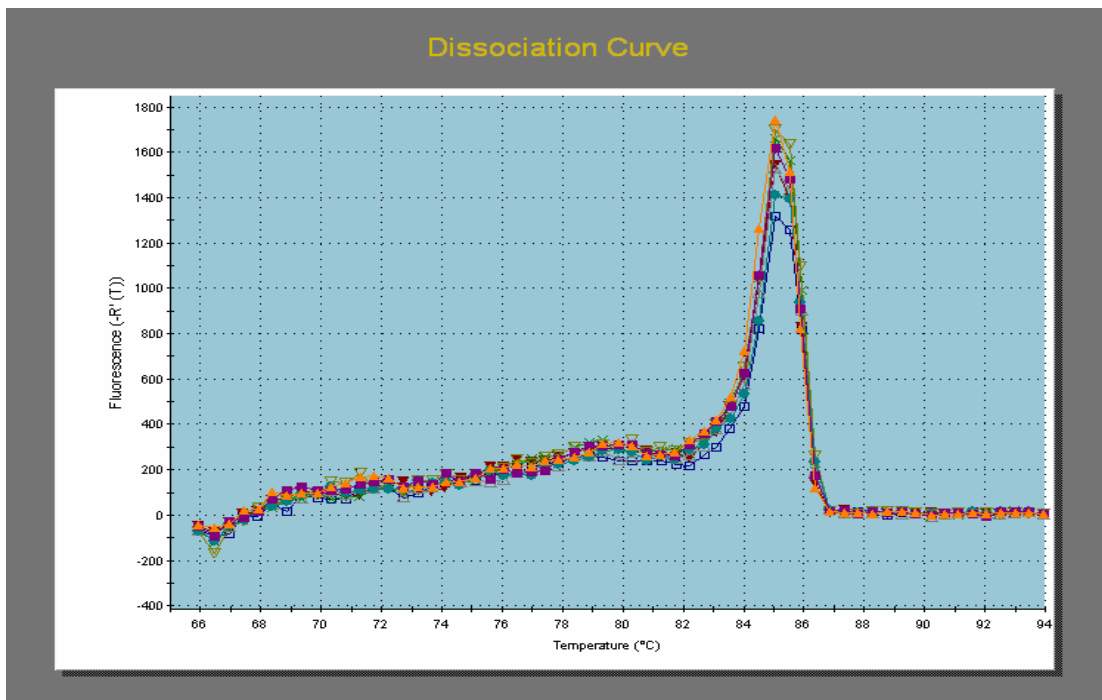
PsaE negative control



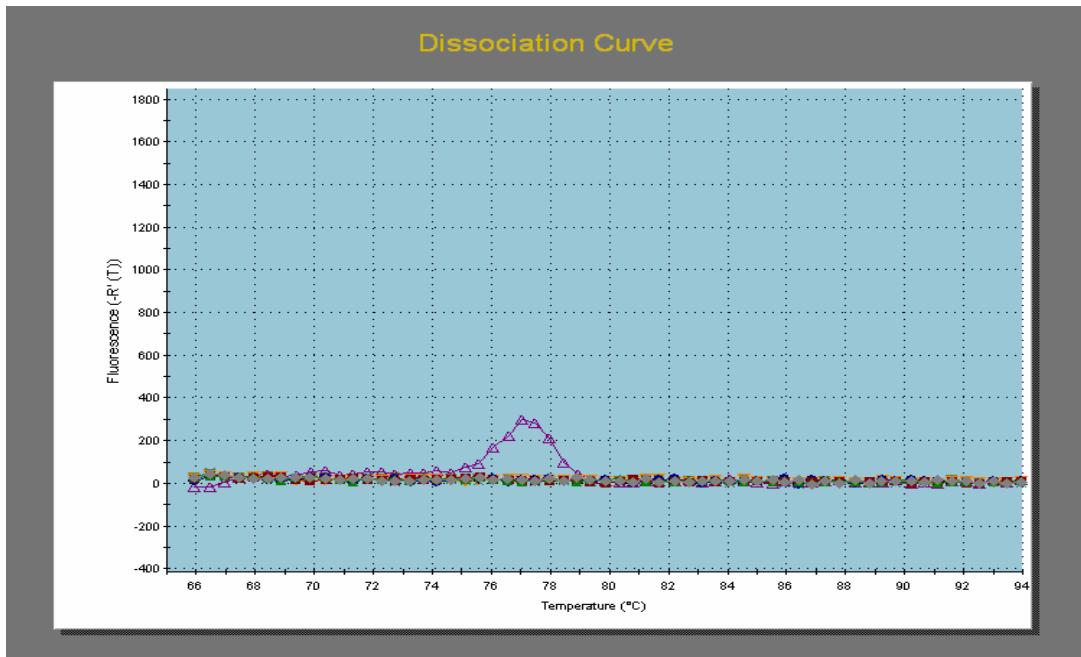
UCE iron replete cDNA



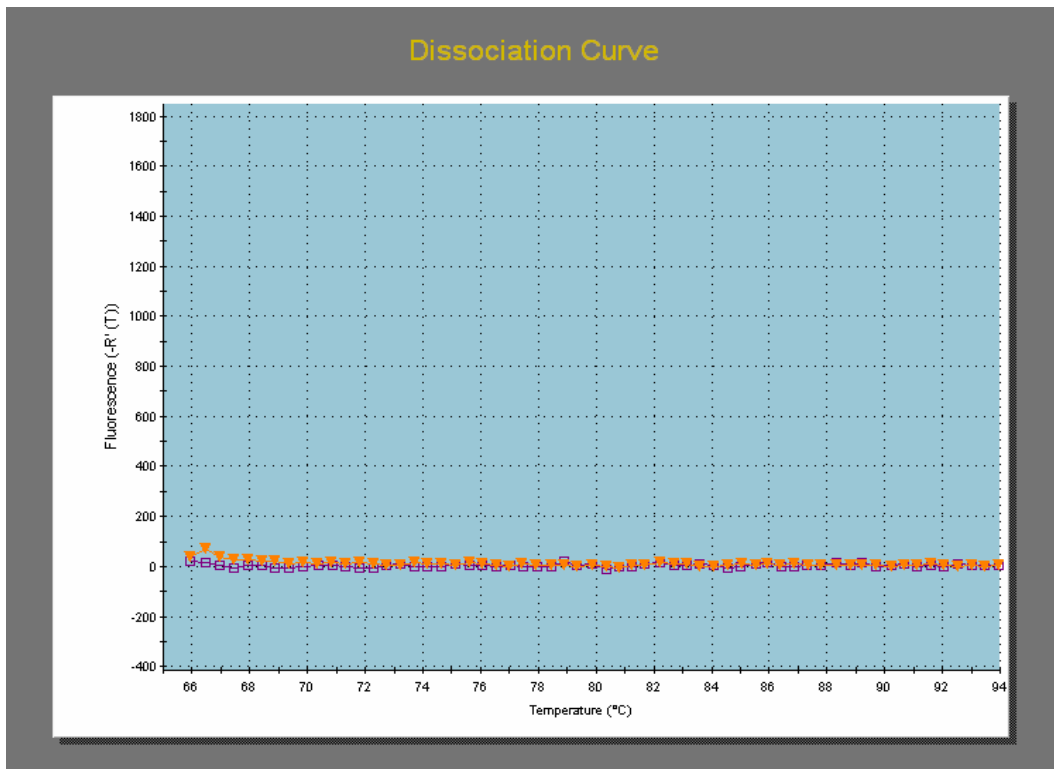
UCE iron limited cDNA



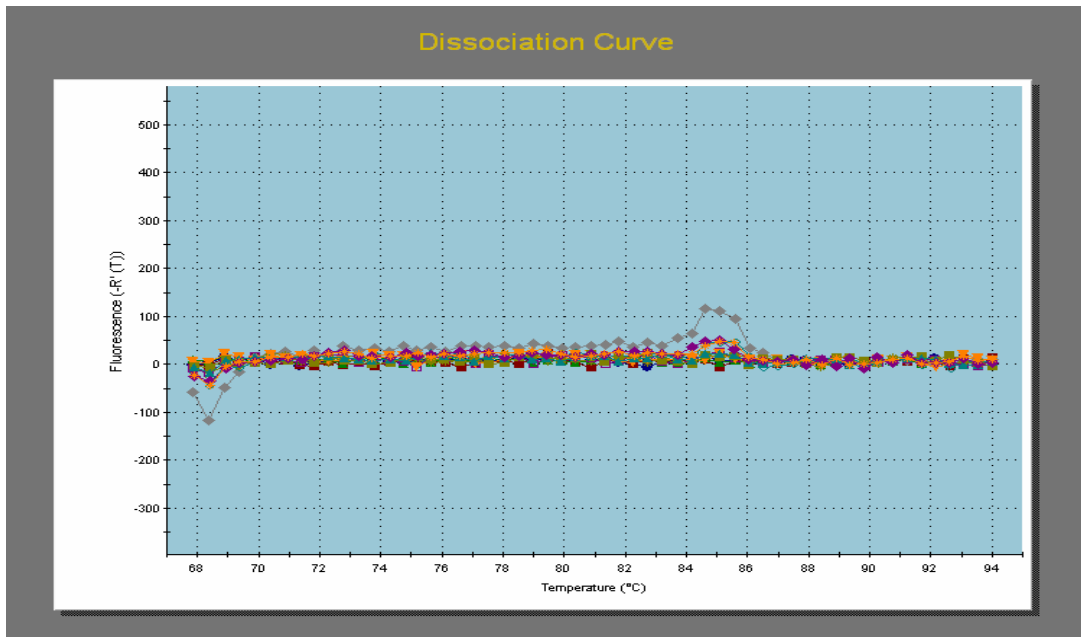
UCE -RT controls



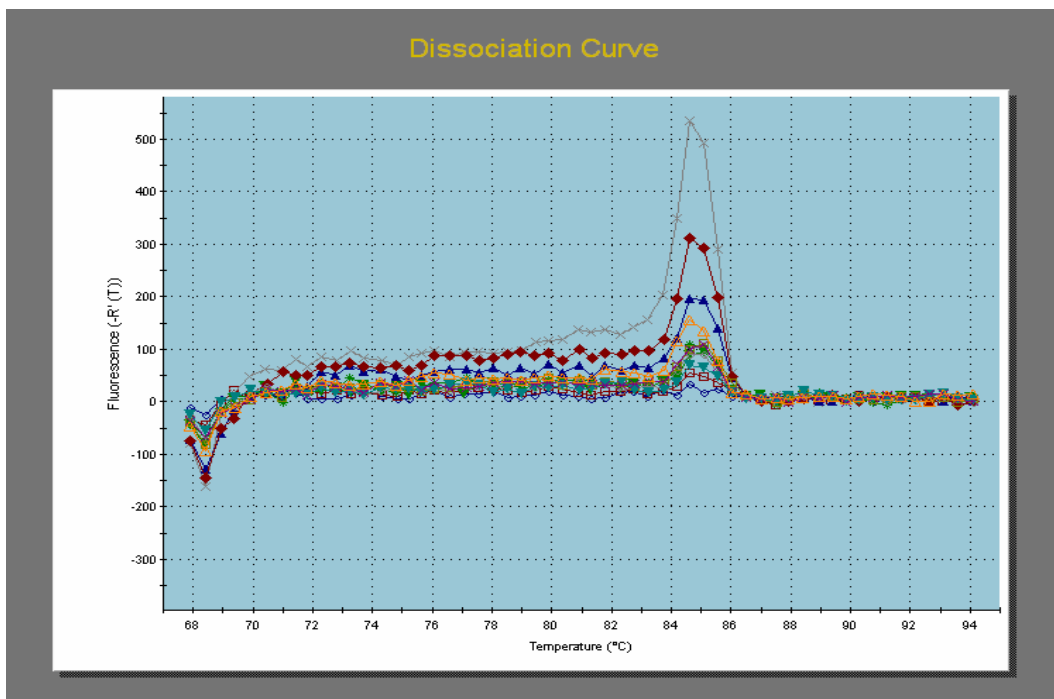
UCE negative controls



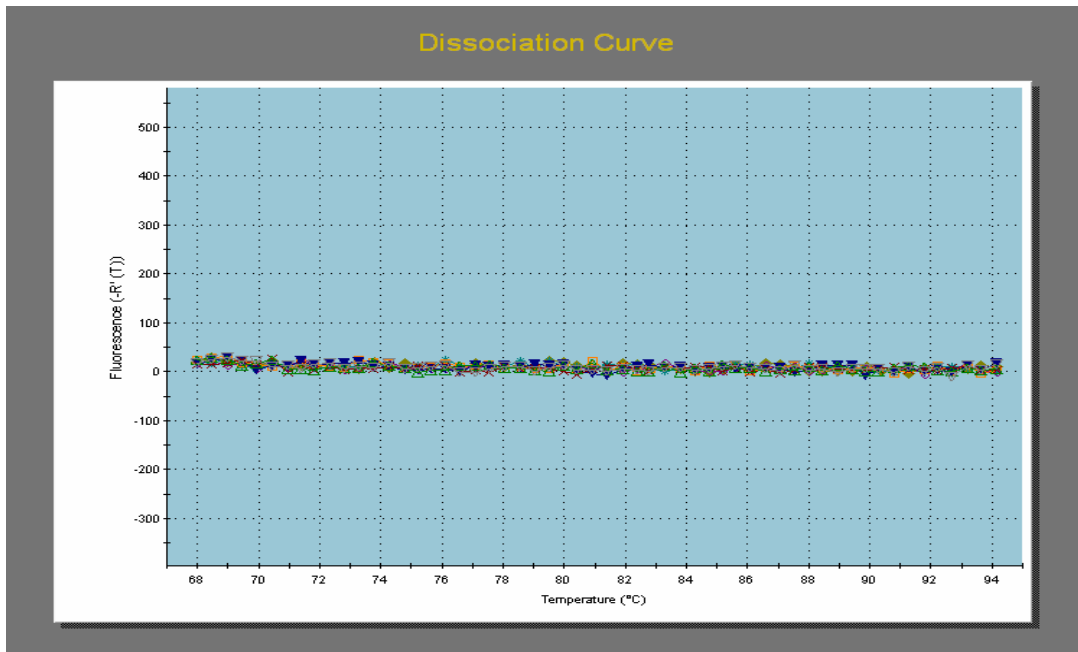
CM4E12 iron replete cDNA



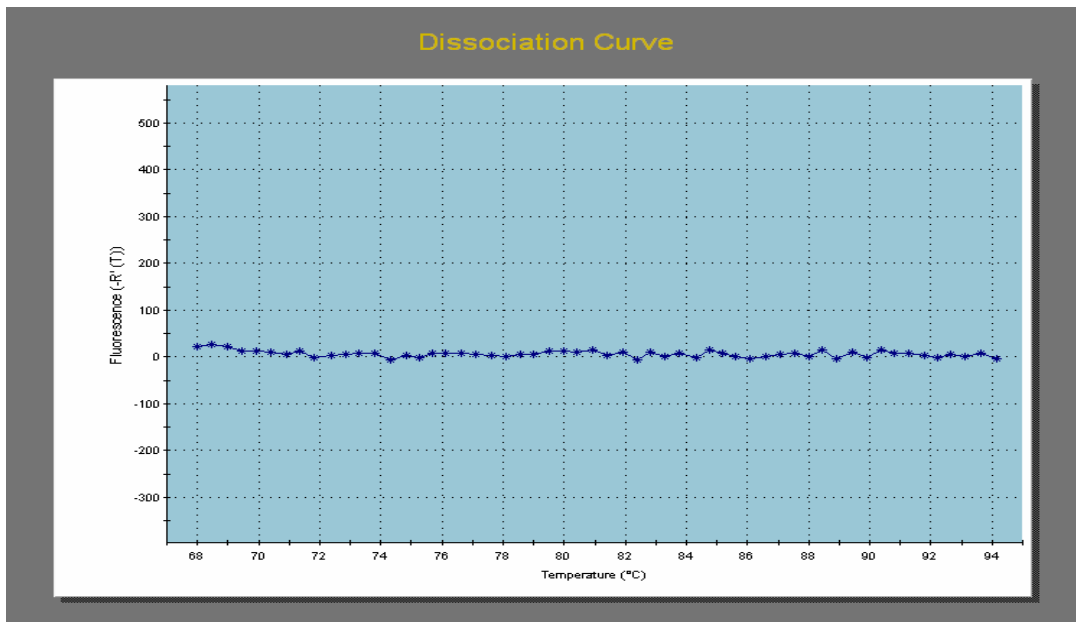
CM4E12 iron limited cDNA



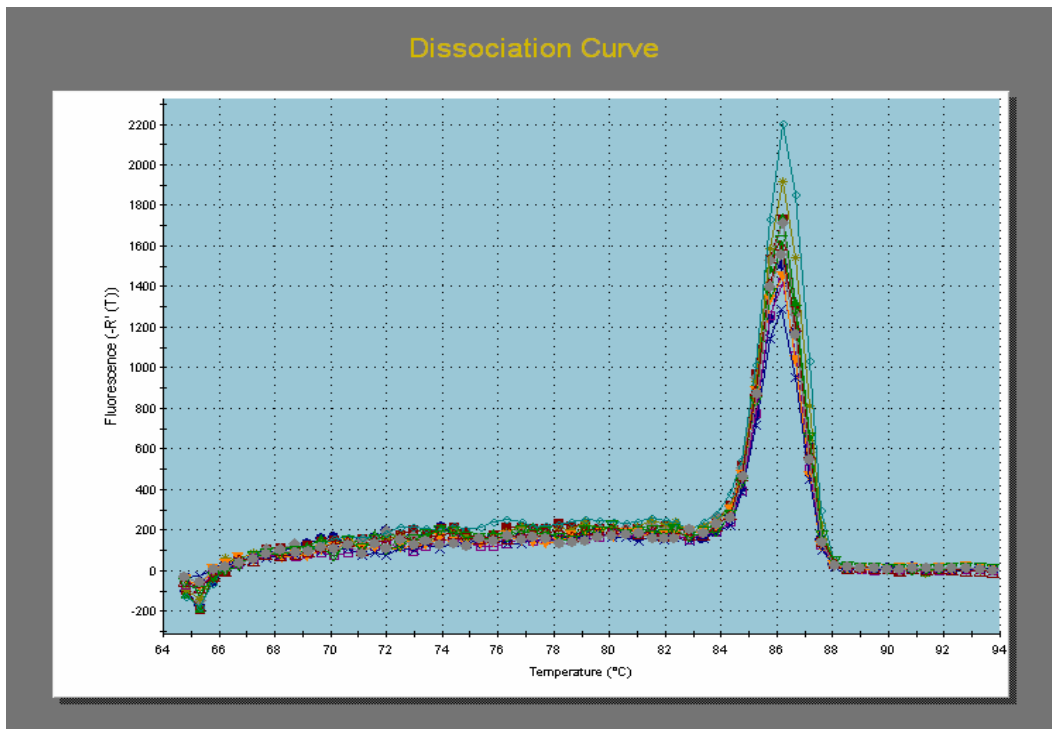
CM4E12 -RT controls



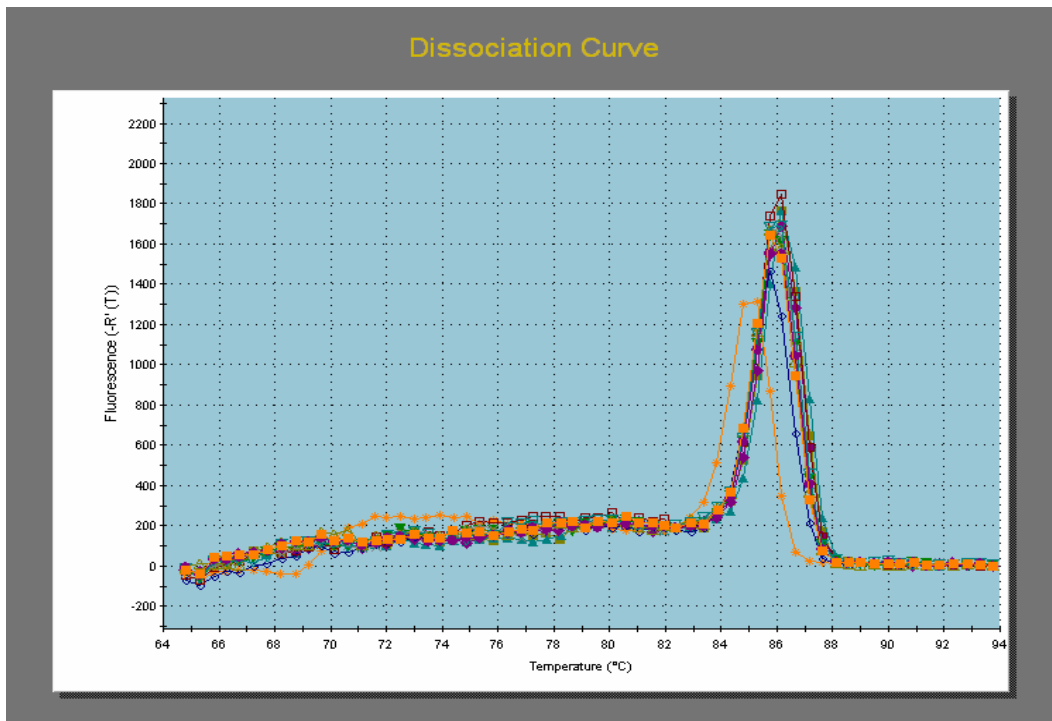
CM4E12 negative controls



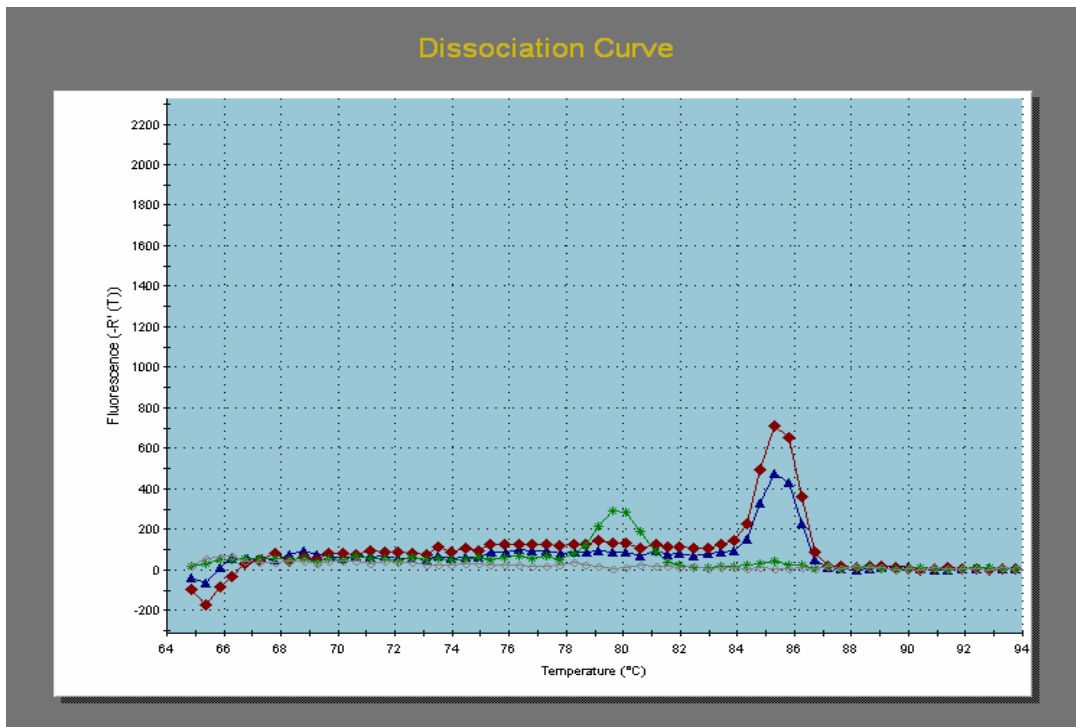
Ferredoxin iron replete cDNA



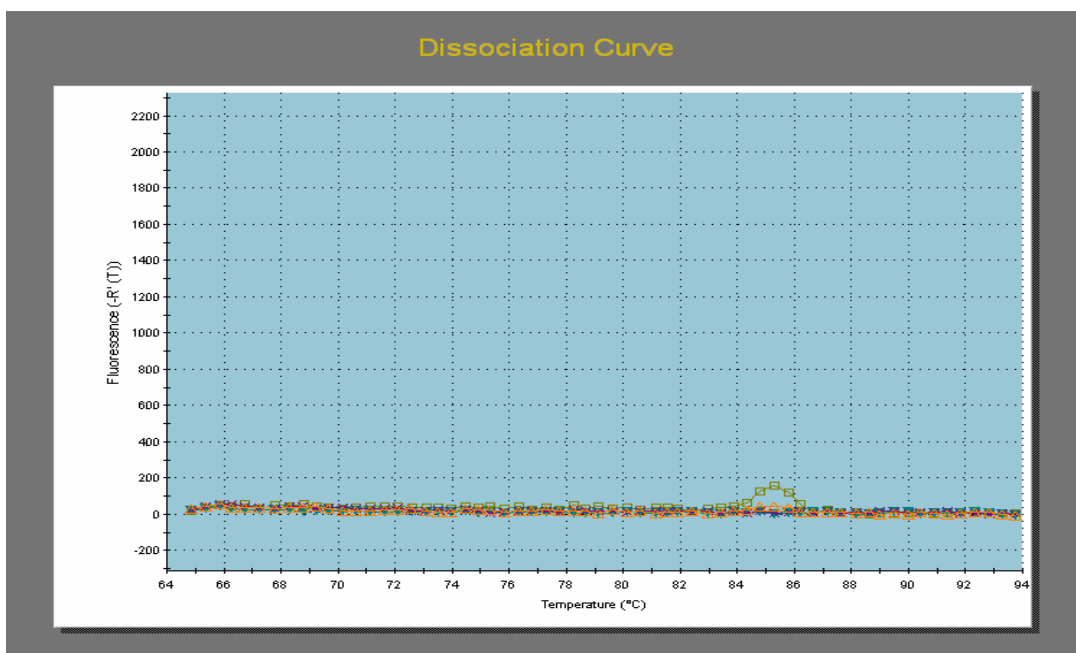
Ferredoxin iron limited cDNA



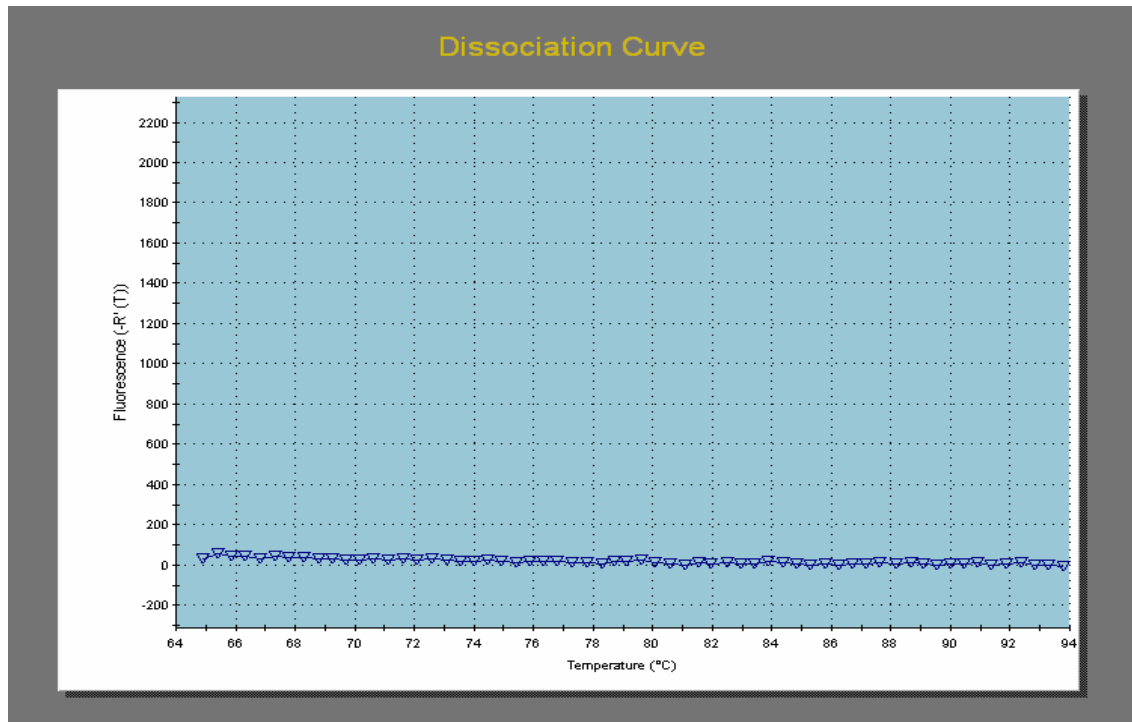
Ferredoxin iron limited -RT controls



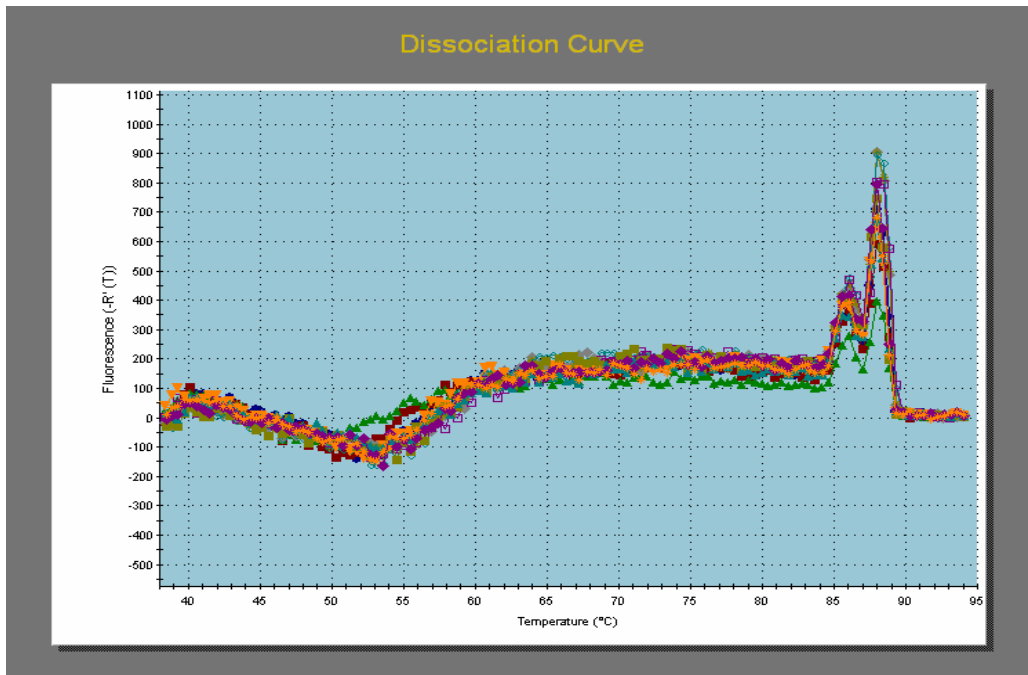
Ferredoxin iron limited -RT controls



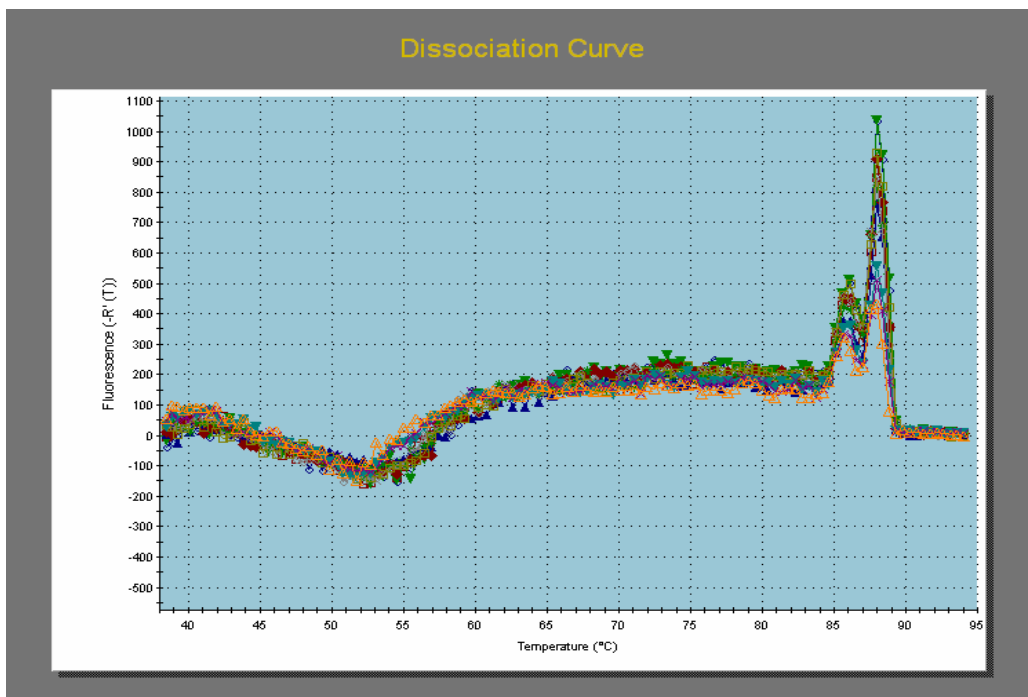
Ferredoxin negative control



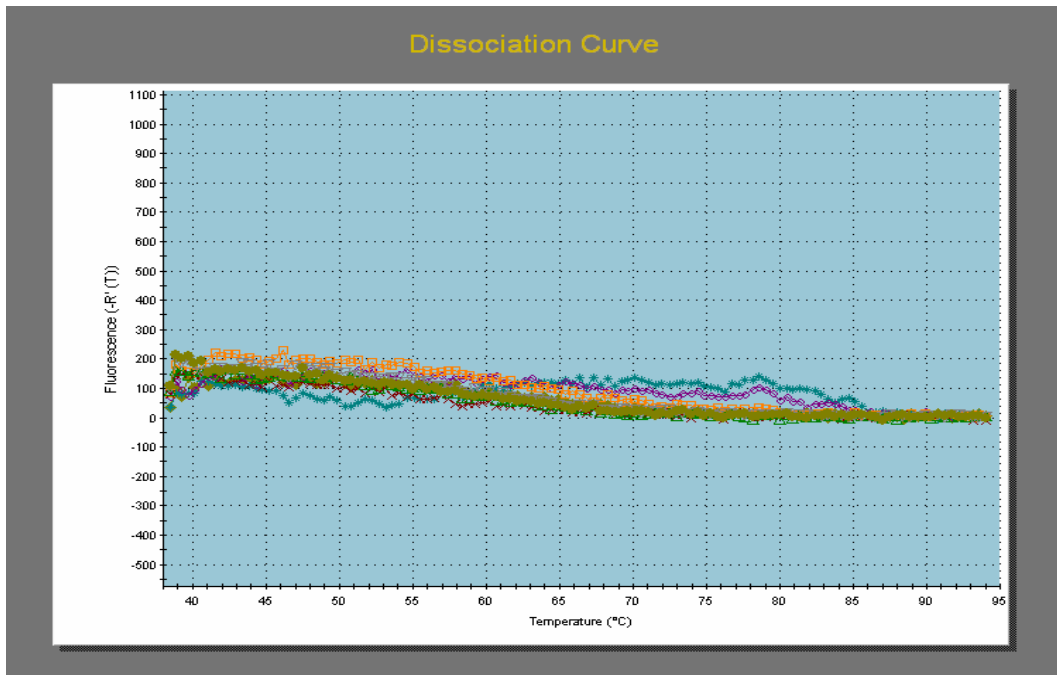
GAPDH iron replete cDNA



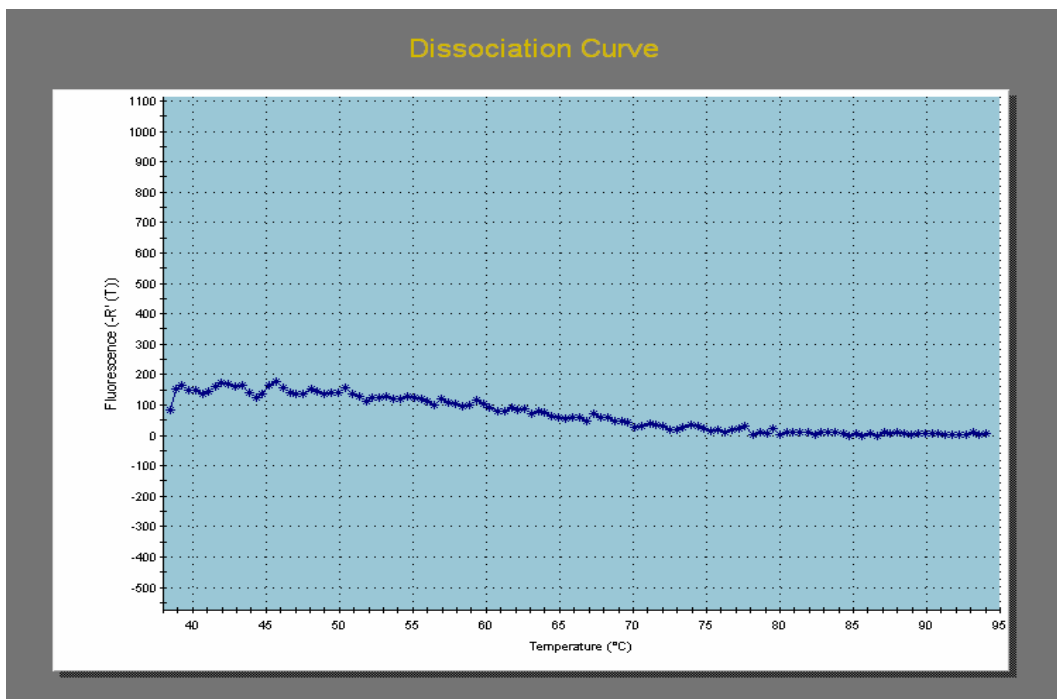
GAPDH iron limited cDNA



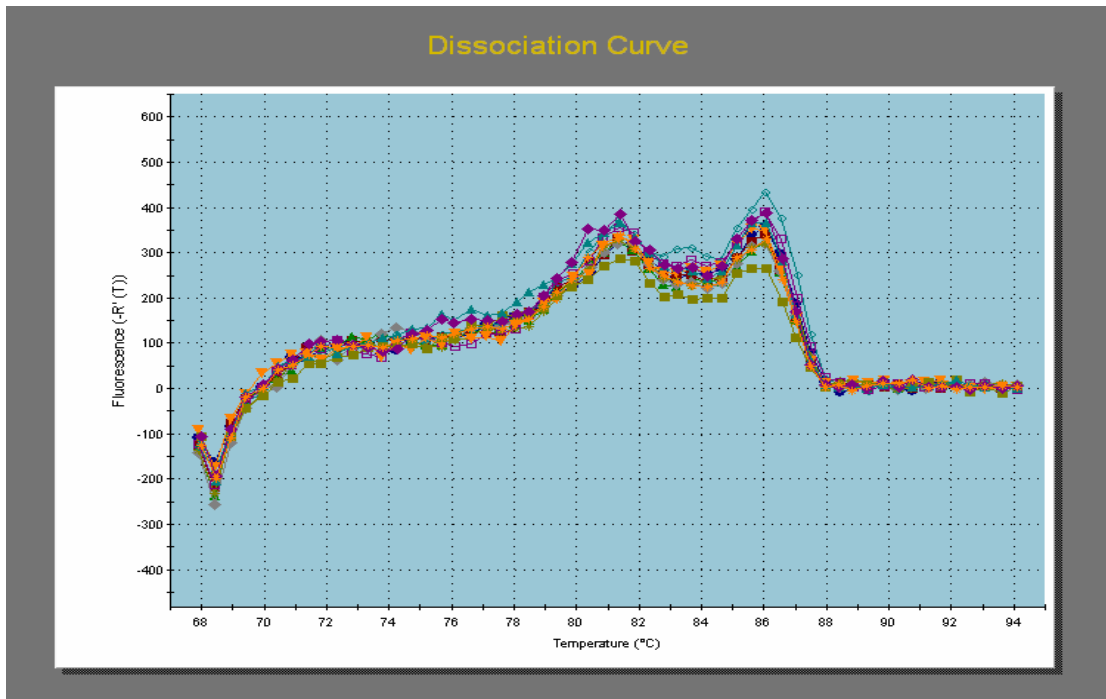
GAPDH -RT controls



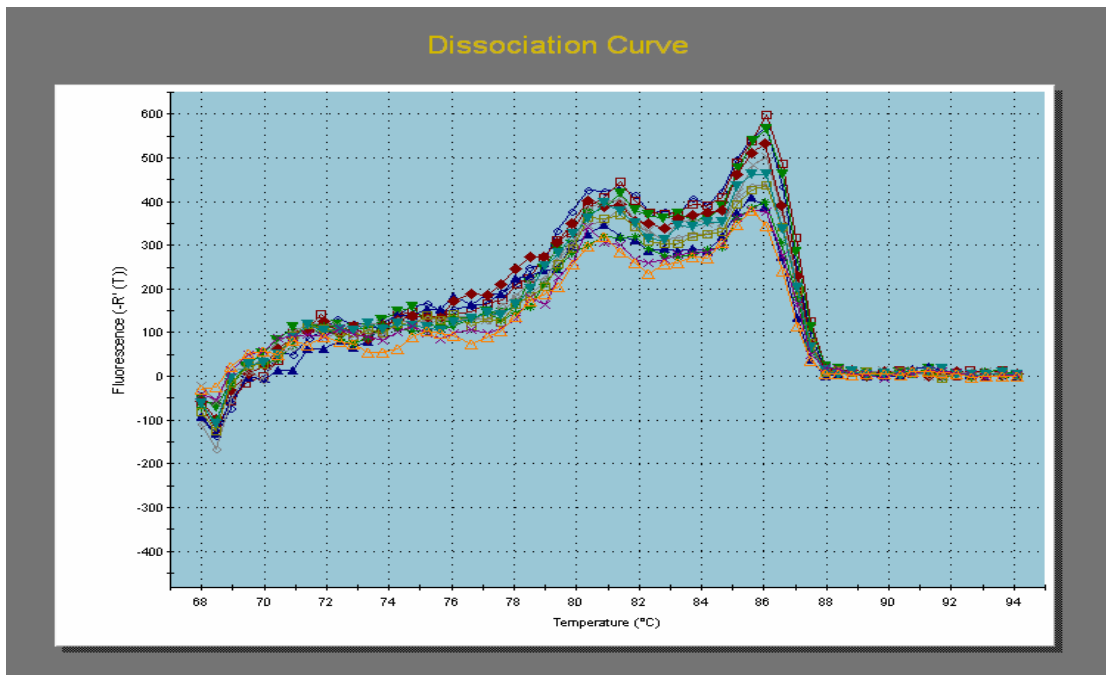
GAPDH negative control



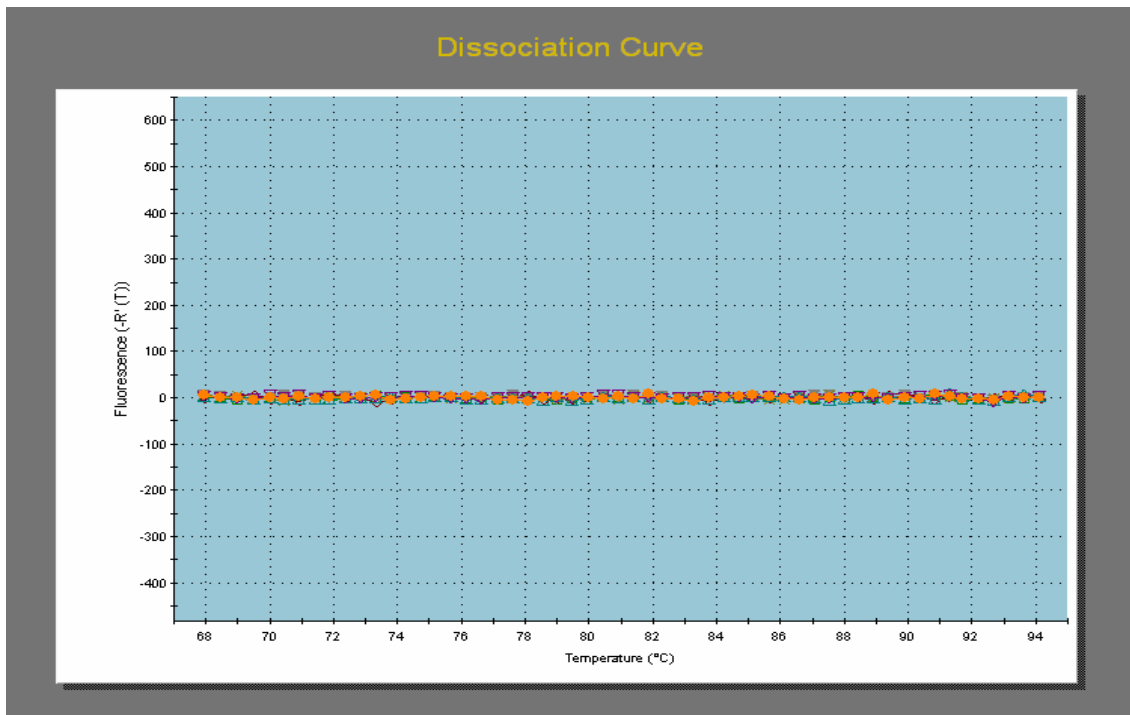
Chl LHP iron replete cDNA



Chl LHP iron limited cDNA



Chl LHP -RT controls



Chl LHP negative control

